

1990

Platinum(II) complexes as spectroscopic probes for biomolecules

Eva Marie Avanceña Ratilla
Iowa State University

Follow this and additional works at: <https://lib.dr.iastate.edu/rtd>

 Part of the [Inorganic Chemistry Commons](#)

Recommended Citation

Avanceña Ratilla, Eva Marie, "Platinum(II) complexes as spectroscopic probes for biomolecules " (1990). *Retrospective Theses and Dissertations*. 11216.
<https://lib.dr.iastate.edu/rtd/11216>

This Dissertation is brought to you for free and open access by the Iowa State University Capstones, Theses and Dissertations at Iowa State University Digital Repository. It has been accepted for inclusion in Retrospective Theses and Dissertations by an authorized administrator of Iowa State University Digital Repository. For more information, please contact digirep@iastate.edu.

INFORMATION TO USERS

The most advanced technology has been used to photograph and reproduce this manuscript from the microfilm master. UMI films the text directly from the original or copy submitted. Thus, some thesis and dissertation copies are in typewriter face, while others may be from any type of computer printer.

The quality of this reproduction is dependent upon the quality of the copy submitted. Broken or indistinct print, colored or poor quality illustrations and photographs, print bleedthrough, substandard margins, and improper alignment can adversely affect reproduction.

In the unlikely event that the author did not send UMI a complete manuscript and there are missing pages, these will be noted. Also, if unauthorized copyright material had to be removed, a note will indicate the deletion.

Oversize materials (e.g., maps, drawings, charts) are reproduced by sectioning the original, beginning at the upper left-hand corner and continuing from left to right in equal sections with small overlaps. Each original is also photographed in one exposure and is included in reduced form at the back of the book.

Photographs included in the original manuscript have been reproduced xerographically in this copy. Higher quality 6" x 9" black and white photographic prints are available for any photographs or illustrations appearing in this copy for an additional charge. Contact UMI directly to order.

U·M·I

University Microfilms International
A Bell & Howell Information Company
300 North Zeeb Road, Ann Arbor, MI 48106-1346 USA
313/761-4700 800/521-0600



Order Number 9035111

Platinum(II) complexes as spectroscopic probes for biomolecules

Ratilla, Eva Marie Avanceña, Ph.D.

Iowa State University, 1990

U·M·I
300 N. Zeeb Rd.
Ann Arbor, MI 48106

Platinum(II) complexes as spectroscopic probes for biomolecules

by

Eva Marie Avanceña Ratilla

**A Dissertation Submitted to the
Graduate Faculty in Partial Fulfillment of the
Requirements for the Degree of
DOCTOR OF PHILOSOPHY**

**Department: Chemistry
Major: Inorganic Chemistry**

Approved:

Signature was redacted for privacy.

In Charge of Major Work

Signature was redacted for privacy.

~~For the Major Department~~

Signature was redacted for privacy.

~~For the Graduate College~~

**Iowa State University
Ames, Iowa**

1990

TABLE OF CONTENTS

DEDICATION	vii
GENERAL INTRODUCTION	1
SECTION I.	
THE AQUEOUS CHEMISTRY OF PLATINUM(II) COMPLEXES	4
INTRODUCTION	5
SUBSTITUTION CHEMISTRY OF PLATINUM(II)	6
Kinetics and Mechanisms of Substitution	6
Incoming Ligand	6
Ancillary Ligand	7
Labile Ligand	7
Solvent	8
Aqueous Medium	8
PLATINUM(II) AND BIOMOLECULES	10
Amino Acids and Proteins	10
Nucleic Acids	14
DETECTION OF PLATINUM	17

SECTION II.	20
^{195}Pt NMR SPECTROSCOPY OF PLATINUM(II) THIOETHER COMPLEXES	
INTRODUCTION	21
EXPERIMENTAL SECTION	24
Chemicals	24
NMR Spectroscopy	24
RESULTS AND DISCUSSION	26
Complex Formation	26
Inversion at Sulfur	30
Chiral Discrimination	41
CONCLUSIONS AND PROSPECTS	45
SECTION III.	47
$\text{Pt}(\text{TRPY})\text{Cl}^+$ AS CHROMOPHORIC TAGS OF HISTIDINES IN CYTOCHROME C	
INTRODUCTION	48
EXPERIMENTAL SECTION	49
Materials and Methods	49
Synthesis and Preparation	51
RESULTS AND DISCUSSION	55
Complex Formation	55

Binding Sites on the Cytochromes	61
Structural and Redox Characterization	73
CONCLUSIONS AND PROSPECTS	81

SECTION IV. 83

GUANIDYL GROUPS: NEW METAL-BINDING LIGANDS IN BIOMOLECULES.

**REACTIONS OF $PT(TRPY)CL^+$ WITH ARGININE IN CYTOCHROMES
AND WITH OTHER GUANIDYL LIGANDS**

INTRODUCTION	84
EXPERIMENTAL SECTION	85
Chemicals	85
Methods	85
Protein Modification	85
Reactions with Potential Ligands	86
Reactions with Guanidyl-Containing Ligands	87
RESULTS AND DISCUSSION	88
The Binding Site	88
Rationale for Arg 91 Reactivity	94
Attempts at Direct Identification of Arg	
Binding Site in Cytochrome c	96

CONCLUSIONS AND PROSPECTS	99
----------------------------------	-----------

SECTION V.	100
-------------------	------------

**TERMINAL AND BRIDGING COORDINATION
OF GUANIDINE LIGANDS TO PLATINUM(II)**

INTRODUCTION	101
---------------------	------------

EXPERIMENTAL SECTION	103
-----------------------------	------------

Chemicals	103
------------------	------------

Methods	103
----------------	------------

Synthesis and Reactions	104
--------------------------------	------------

RESULTS AND DISCUSSION	112
-------------------------------	------------

Reactivity of Pt(trpy)Cl⁺ toward

Guanidine Ligands	112
--------------------------	------------

Characterization of the Guanidine Complexes	113
--	------------

Structures of the Complexes	133
------------------------------------	------------

CONCLUSIONS AND PROSPECTS	152
----------------------------------	------------

SECTION VI.	153
--------------------	------------

INTERACTIONS OF (PT(TRPY))₂CAN³⁺ WITH NUCLEIC ACIDS

INTRODUCTION	154
---------------------	------------

EXPERIMENTAL SECTION	157
Materials	157
Methods	158
RESULTS AND DISCUSSION	161
Spectroscopic Studies	161
Thermal Denaturation of DNA	165
Binding of $(\text{Pt}(\text{trpy}))_2\text{Ca}^{3+}$	168
Hydrodynamic Properties	173
Site-Specificity	177
CONCLUSIONS AND PROSPECTS	181
GENERAL SUMMARY	182
BIBLIOGRAPHY	184
APPENDIX: CRYSTALLOGRAPHIC STUDY OF $[\text{Pt}(\text{TRPY})\text{CL}]\text{CL}\cdot\text{H}_2\text{O}$	199
ACKNOWLEDGEMENTS	207

DEDICATION

**In loving memory of my father
who wished me the best possible education and
who finally accepted his sojourn that we may go on living
and
to Our Father
who is my strength,
my kind provider, and my consolation
walking in His ways has been a constant struggle
but the surprises I have witnessed
and the blessings in my follies and in my misery
have brought me closer to my quest
and for all of these I am most grateful**

GENERAL INTRODUCTION

The conjugation of compounds to biomolecules has been an area of interest for extrinsic probes are often necessary to detect and study the biomolecules.¹⁻⁴ The uses of ^3H , ^{14}C , and ^{32}P radioactive isotopes and of organic fluorophores and organic chromophores have been well-developed and have contributed much to the phenomenal growth in molecular biology and in modern biochemistry and biophysics.

The use of transition-metal complexes, in contrast, is not well-known although its importance in silver staining and in heavy atom labeling⁵ has long been recognized. The potential use of transition-metal conjugates in therapeutic chemistry has contributed to the growing interest in this area.

Various properties of transition metal complexes make them suitable probes for the study of biomolecules.⁶⁻⁸ Their high electron density make them good probes for X-ray diffraction and electron microscopy. With the choice of an NMR active metal, metal NMR spectroscopy could be another method of choice in the study of the biomolecule. The variety of radioisotopes that one can have extends the utility of autoradiography to a broader range of atoms or isotopes. The variety of ligands coordinated to the transition metal affords a versatility in the spectroscopic tools to use – from characteristic ^1H NMR signals to UV-visible spectroscopy, and perhaps, emission spectroscopy.

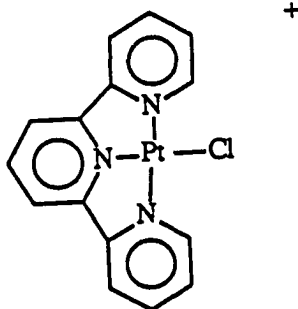
One advantage of using transition metal complexes is the mild condition for a covalent reaction to take place. The coordination chemistry involves simple nucleophilic displacement reactions, which can be made facile by the judicious choice of any combination of the following parameters: pH, metal, labile ligands, and ancillary ligands of the metal complex. Likewise, the potential for selectivity towards certain groups in the biomolecule can be achieved with the proper choice of the aforementioned parameters.

Yet another advantage is the recovery of the precious native biomolecule – use of a stronger nucleophile displaces the biomolecular ligand in the coordination sphere of the metal.

This dissertation focuses on the platinum(II) complexes for a number of reasons. The chemistry of platinum(II) is fairly well-known and simple.⁹⁻¹¹ Moreover, platinum has an abundant and receptive NMR active nucleus of spin = 1/2 whose chemical shift span some 15,000 ppm.¹²⁻¹³ From the X-ray crystal structure studies of cytochrome c, PtCl_4^{2-} , the heavy-atom label used, was found to preferentially bind sulfur of Met 65 and to some extent nitrogen of His 33.¹⁴ This result coupled with the known chemistry of platinum for sulfur and nitrogen ligating atoms afforded us a system for which selectivity towards certain residues in a protein during covalent modification can be achieved and tested. The first section thus begins with an introduction to the aqueous chemistry of platinum(II) complexes.

Section II of this dissertation then explores the use of ^{195}Pt NMR spectroscopy on the thioether complexes of PtCl_4^{2-} – these being the simplest models of a platinum(II) complex bound to a protein. The bulk of this work is part of two publications.^{15,16}

The rest of the dissertation focuses on another Pt(II) complex, $\text{Pt}(\text{trpy})\text{Cl}^+$. Its ancillary ligand, terpyridine (trpy), affords us a convenient spectroscopic tool – UV-



visible spectroscopy – to monitor its incorporation into the protein. Modification of histidine residues on the surface of cytochrome c is achieved at slightly acidic pH and is described in Section III. This part of the work has already been published.¹⁷

While trying to study the effect of higher pH on the yields of covalent modification of cytochrome c with $\text{Pt}(\text{trpy})\text{Cl}^+$, a new binding site, Arg 91, was observed and was communicated in a paper.¹⁸ This communication constitutes Section IV.

The unprecedented transition-metal complexes of guanidine containing compounds are further studied in Section V, and will be published in a forthcoming paper.¹⁹ This first crystallographic study of metal binding to guanidines and this first report of bridging coordination of guanidines to two metals constitute Section V.

Intercalation into double helical DNA by a sandwich compound was imminent from the crystal structure of the bridged complex, $[\{\text{Pt}(\text{trpy})\}_2\text{Can}](\text{ClO}_4)_3$. Interactions of this complex with nucleic acids are thus studied in Section VI.

For its proven utility the starting reagent, $[\text{Pt}(\text{trpy})\text{Cl}]\text{Cl}$, merits a structural study. The appendix thus contains the crystallographic study of this versatile reagent.

SECTION I
THE AQUEOUS CHEMISTRY OF PLATINUM(II) COMPLEXES

- 1

INTRODUCTION

Platinum(II) has the electronic configuration $[\text{Xe}]4f^{14}5d^9$. It generally exhibits a coordination number of four with a square planar geometry and is diamagnetic.^{9,11}

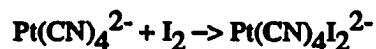
Platinum(II) forms stable compounds with both σ and π electron donors. Their thermodynamic and kinetic behavior are determined by the nature of the electron donation and by the ability of a ligand to accept metal π electron density.^{9,11}

Platinum(II) is classified as a b-type metal or a soft metal for its compounds formed with the heavier nonmetallic elements are generally more stable.^{9,11,20}

Ligand donor atoms with the appropriate orbital geometry and available electron density can bridge two or more platinum atoms forming dimeric or polymeric species.¹¹ In aqueous solutions of moderate or high pH the OH^- ion often serves as a bridging ligand.¹¹

Apart from ligand-bridged systems, square planar platinum(II) compounds form polymeric species in the solid state through axial metal-metal stacking interactions.^{21,22}

The stability of platinum(II) with respect to disproportionation to platinum(0) and platinum(IV) is also important.^{9,11} Oxidative addition reactions such as that shown below may occur even with the most stable of platinum(II)



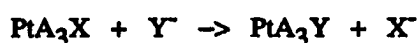
complexes.¹¹ Although, reduction to platinum(0) is usually difficult with the kinetically and thermodynamically stable platinum(II) complexes.

SUBSTITUTION CHEMISTRY OF PLATINUM(II)

Kinetics and Mechanisms of Substitution

Square planar platinum(II) complexes are relatively kinetically inert,^{9,11} which is a feature of considerable importance in their chemistry and in this dissertation. As a result of their slow reactions, they have been widely investigated^{10,23,24,25} and are thought to be fairly well-understood.^{9,11}

Substitution reactions occur with retention of configuration and generally follow a two-term rate law. The general rate expression⁹ for the substitution reaction



is $\text{rate} = \{k_1 + k_2 [\text{Y}^-]\} [\text{PtA}_3\text{X}]$.

This expression implies two parallel mechanisms, the first of which is solvent dependent while the second term corresponds to the solvent independent pathway.⁹ In general, $k_2 \gg k_1$.¹¹ Both paths are thought to be associative based on the following indirect evidences:^{9-11,23}

- (1) variation of charge has only slight effects on rates,
- (2) steric hindrances cause a sharp decrease,
- (3) rate of reaction depends on the incoming ligand, and
- (4) k_1 , the first order rate constant, depends on the solvent.

Incoming Ligand

Since the nature of the entering ligand has a profound effect on the rate of substitution,^{9,23} this effect can be utilized in determining target ligands for selective

labeling studies in biomolecules. In general, soft nucleophiles are most effective towards soft substrates like platinum(II).^{9,23} Factors such as polarizability of the nucleophile, π bonding between the nucleophile and platinum, as well as the ionic or covalent character of the nucleophile-metal bond are important.¹¹ Ligands reacting most rapidly have the capacity to form metal to ligand π bonds.^{9,11}

Ancillary Ligand

The nonlabile ligands⁹ or the ancillary ligands also affect the rate of substitution. A chelating ligand is stable towards displacement by another nucleophile, making the rest of the ligands in the platinum(II) complex more susceptible to substitution. This is also evident in the trans effect which is the effect of a coordinated group on the rate of substitution reaction of ligands opposite or trans to it in a metal complex. The trans influence effect wherein the ligand is found to weaken the bond trans to itself⁹ is another manifestation of the nonlabile ligand's effect. Lastly, steric effects causing hindered reactions^{9,17,25,26} are the most apparent of these effects.

Labile Ligand

The leaving group also affects the rate of substitution.⁹ Groups high in the trans effect order are replaced slowly, for usually those high in the trans effect series are bound strongly to platinum.^{9,23} However, ligands low in the trans effect series are not always easy to replace.⁸ In general, the more stable (weaker nucleophile) the leaving group as in the series $\text{Cl}^- > \text{Br}^- > \text{I}^-$, the easier it is to replace.⁹

Solvent

The solvent affects substitution in different ways. For coordinating solvents^{9,11} such as DMSO, water, nitromethane, and the alcohols, they can act as nucleophiles or solvate the compounds. Solvation of the leaving group is clearly an important kinetic consideration.⁹

Aqueous Medium

In aqueous media, water is present in highest concentration. Although water is a potential ligand, it is also an excellent leaving group and hydrolysis products can be suppressed in the presence of better nucleophiles in sufficiently high concentration.¹¹ Moreover, water is considered a poor ligand for platinum(II).⁹ There is a great deal of evidence for the platinum(II) aquo complexes as intermediates in the rapid reactions with incoming ligands.²⁷

Many buffer-salt systems contain potential ligands, the concentration of which can affect the platinum(II) chemistry in aqueous solution.¹¹

The chloride ion is especially effective in inhibiting hydrolysis reactions. Water is ca. 70 times faster a leaving group than Cl^- in some amine complexes and ca. 40 times faster in a DMSO complex.¹¹ Acetate ion is a poorer nucleophile toward platinum than is chloride^{9,11} and thus is a poorer entering group.¹¹ On the otherhand, ammonia is a slightly better nucleophile than chloride.^{11,23} Phosphate ion usually coordinates but its propensity for platinum(II) is low. Moreover, it is a better leaving group than water.¹¹

Perchlorate and sulfate ions are considered to be noncoordinating for platinum(II).¹¹ Sulphato complexes are rare and must be prepared under forcing

conditions.⁹ Nitrate is a better leaving group than water.¹¹ The nitrate ligand is readily liberated with heating and preparation of the nitrate complexes requires concentrated nitric acid and platinum(0).⁹

The OH^- ion in alkaline conditions is a strong candidate in nucleophilic substitution. Although being a hard base, it is not expected to react rapidly.⁹ It is, however, a good bridging ligand.¹¹ Hence, dimeric and polymeric hydroxo-bridged platinum compounds may form in moderate to high pH conditions.¹¹

PLATINUM(II) AND BIOMOLECULES

As discussed earlier, platinum being a class b metal and a soft substrate is expected to form stable complexes with biomolecules containing sulfur. Complexation with nitrogen may also occur. Metal binding will be kinetically controlled, and the nucleophilicity of the potential ligand together with its leaving group ability will be important. The degree of exposure or accessibility of the potential ligand and its relative concentration will also be important considerations.

Amino Acids and Proteins

Amino acids, the building blocks of proteins, bind platinum(II) through their terminal amino and carboxyl groups, to form chelates.^{11,27-29} In the presence of a potential donor atom in the side chain, chelate rings form using the amino terminal and the donor atom of the side chain.^{11,27-29} Under acidic conditions, the proton competes successfully for the carboxyl and amino groups, giving a monodentate complex.^{11,28} Under basic conditions and sufficiently high amino acid concentrations the greater affinity of the amine group becomes evident.¹¹

Dipeptides containing no potential ligands in their side chains bind to platinum(II) readily under basic conditions. In this case, both peptide bond and terminal groups serve as ligands.¹¹

In general, the reaction of platinum(II) complexes containing a labile ligand with methionine sulfur is rapid.^{11,27,28} The trans labilizing effect of the bound sulfur often aids the addition of a second methionine wherein the sulfur atoms are trans to one

another.¹¹ This preponderance has been aptly used in the development of PtCl_4^{2-} as an inorganic cross-linking agent of proteins in our laboratory.⁶

Less work^{6,11} has been reported involving cysteine and platinum(II), although the metallointercalation reagent $\text{Pt}(\text{trpy})\text{Cys}^+$ has been synthesized.³⁰

Histidine reacts very slowly with PtCl_4^{2-} under basic conditions to form a bis-chelated complex.^{11,27} Coordination is reported to be through the imidazole and α -amino nitrogen atoms.¹¹

Information on platinum binding to other amino acids is scarce.^{11,27} The complexes of platinum(II) with amino acids do not really model those complexes with the protein as seen by the preponderance of chelate formation with the free amino acids. This is due to the accessibility of the terminal amino and carboxyl groups in contrast to their rigidity and non-availability within the proteins. It is apparent that any consideration of platinum complex formation with proteins must take the functional groups of the side chains into consideration.

Of the 21 common amino acids (shown in Table I-1), the amino acids cysteine, cystine, and methionine are potential sulfur donors. Those with potential nitrogen ligands are the imidazole – histidine, the indole – tryptophan, the guanidine – arginine, the amines – lysine and proline, and the amides – glutamine and asparagine. Those with potential oxygen donors include the alcohols – tyrosine, serine and threonine, as well as the carboxylates – aspartic acid and glutamic acid.

Many platinum(II)-protein binding sites have been determined by X-ray crystallography for platinum(II) is heavily employed in isomorphous replacement studies.^{5,14,27} The extent and type of binding depends on the nature of the platinum complex, the composition and tertiary structure of the protein, the ionic strength of the

Table I-1. Amino Acids and their Side Chains



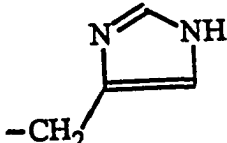
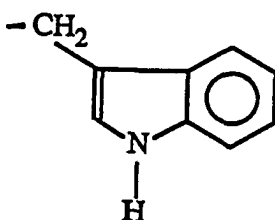
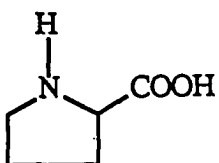

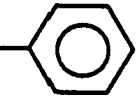
Amino Acids		pK_3 of R	- R
Sulfur-Containing			
Methionine	Met	-	$-(\text{CH}_2)_2 - \text{S} - \text{CH}_3$
Cysteine	Cys	8.3	$-\text{CH}_2 - \text{S} - \text{H}$
Cystine	Cys-Cys	-	$-\text{CH}_2 - \text{S} - \text{S} - \text{CH}_2 -$
Nitrogen-Containing			
Histidine	His	6.0	
Tryptophan	Trp	-	
Arginine	Arg	12.5	$-(\text{CH}_2)_3 - \text{NH} - \text{C}(=\text{NH}) - \text{NH}_2$
Lysine	Lys	10.5	$-(\text{CH}_2)_4 - \text{NH}_2$
Proline	Pro	-	

Table I-1 (Continued)

Amino Acids		pK ₃ of R	- R
Glutamine	Gln	-	$-(\text{CH}_2)_2 - \text{C}(=\text{O}) - \text{NH}_2$
Asparagine	Asn	-	$-\text{CH}_2 - \text{C}(=\text{O}) - \text{NH}_2$
Oxygen-Containing			
Tyrosine	Tyr	10.1	$-\text{CH}_2 - $ 
Serine	Ser	-	$-\text{CH}_2 - \text{OH}$
Threonine	Thr	-	$-\text{CH}(\text{OH}) - \text{CH}_3$
Glutamic Acid	Glu	4.2	$-(\text{CH}_2)_2 - \text{COOH}$
Aspartic Acid	Asp	3.9	$-\text{CH}_2 - \text{COOH}$
No Heteroatoms			
Glycine	Gly	-	$-\text{H}$
Alanine	Ala	-	$-\text{CH}_3$
Valine	Val	-	$-\text{CH}(\text{CH}_3) - \text{CH}_3$
Leucine	Leu	-	$-\text{CH}_2 - \text{CH}(\text{CH}_3) - \text{CH}_3$
Isoleucine	Ile	-	$-\text{CH}(\text{CH}_3) - \text{CH}_2 - \text{CH}_3$
Phenylalanine	Phe	-	$-\text{CH}_2 - $ 

medium, and the time allowed for incubation.^{5,11} Complexes such as $\text{Pt}(\text{CN})_4^{2-}$ with no labile ligands bind proteins electrostatically, associating externally with Glu, Lys, and Ser residues in a nonspecific manner.⁵ Complexes such as PtCl_4^{2-} generally form covalent linkages.^{14,27} PtCl_4^{2-} was found to preferentially bind to methionine, occasionally to disulfide, and to a much lesser extent, histidine.¹⁴ Charged complexes are less likely to penetrate the hydrophobic interior of proteins than are neutral species.

Investigations on inhibition of enzymes such as malate dehydrogenase and liver alcohol dehydrogenase run parallel with the substitution chemistry of PtX_4^{2-} .²⁷ Indeed, inhibition is 6 to 8 x faster with PtBr_4^{2-} than with PtCl_4^{2-} .³¹ No indication of the nature of the binding site amino acid in the enzyme was given, but the inhibition has been proven to be due to some specific binding and not merely due to dissociation of the enzyme into subunits.^{27,31} Furthermore, recovery of the enzyme to 38 % of its activity could be achieved with addition of methionine to the platinum(II)-enzyme conjugate.³¹

Nucleic Acids

Nucleic acids consist of polynucleotides whose monomer units have a phosphate diester, a pentose ring, and an organic base. The negative charge of the phosphate moiety can attract electrostatically a positive platinum(II) ion. The phosphate oxygen is expected to be about as good a leaving group as nitrate oxygen, which has been shown to be a better leaving group than water.¹¹ The ether oxygens in the pentose ring are known to be poor donor atoms and in particular have no affinity for platinum(II).^{9,11} These atoms are thus unlikely to bind strongly to platinum both for steric and electronic reasons.¹¹

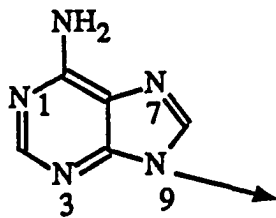
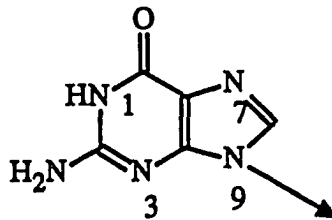
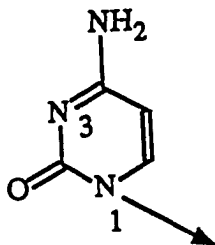
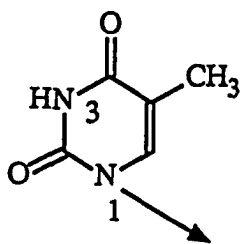
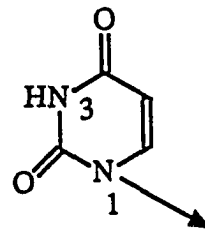
Purines**Adenine****Guanine****Pyrimidines****Cytosine****Thymine****Uracil**

Figure I-1. Nucleic Acid Bases. The bases are joined to the pentose ring as shown by the arrow

The organic bases of the nucleotides (shown in Figure I-1), the purines – adenine and guanine, and the pyrimidines – uracil, cytosine, and thymine, offer the best potential donor atoms for platinum(II) coordination.¹¹ The recent crystal structure of the cis-diammine platinum(II) adduct shows the N7 atom of guanosine is a favored site.³² The relative order of nucleophilicity of the ribonucleotides toward the anticancer agent cis-diammine platinum(II) was determined to be GMP > AMP >> CMP >> UMP at 25 °C and pH of 7.³³

Whether the interaction of the platinum(II) complex with proteins plays a role in the antitumor therapy of platinum drugs is still unknown.²⁷ Speculations that platinum(II)-protein complexes may be important in either drug delivery to target cells or in its removal from the cell may have some bearing. Strong binding to proteins as in the inhibition of enzymes contribute to the increased toxicity of the drug,²⁷ while weak binding to the cytoplasm may be beneficial. The delicate balance in the competitive binding of platinum(II) complexes with nucleic acids and proteins may be a key role in the design of better platinum drugs.

DETECTION OF PLATINUM

With the potential use of platinum(II) complexes in chemotherapy as well as with its utility as probes for anion binding sites in biopolymers,²⁷ metallointercalation probes³⁰ in nucleic acids and its role in reversible inhibition of enzymes,²⁷ the detection of platinum(II)-conjugates becomes an important task.

The effects of platinum on the properties of a biopolymer – such as hydrodynamic properties, enzyme activity, and spectroscopic properties – have been used.^{11,30,34} It is also desirable to detect the platinum complex directly to ascertain how much and where it is bound on the biomolecule.

Fortunately, there are several properties and methods that are applicable for platinum. Some methods are destructive while some are nondestructive. Obviously, the latter procedure may be necessary due to the nature of the sample or because of the cost of the biomolecules.

The destructive methods – atomic absorption and mass spectrometry – have already been applied to platinum-bound biomolecules.¹¹ Colorimetric measurements which are performed after subjecting the biomaterial to strong and harsh redox reagents have also been used.¹¹

The use of spectroscopic properties of the platinum(II) complex is clearly the way for nondestructive procedures. The metastable isotope, ^{195m}Pt , can be used over a wide range of concentration. However, its limited availability and short half-life of 4.1 days limits the use of this approach.¹¹

The most stable isotope, ^{195}Pt is 33.8 % abundant and has a nuclear spin of $1/2$.^{12,13} The use of ^{195}Pt NMR as a means of detection is possible although applications to biomolecules have not been well-established. To date, the ^{195}Pt NMR

has been studied in our laboratory, as will be discussed in Section II with a tripeptide, and recently its application to a platinum-bound dinucleotide has been achieved.³⁵ The concentration in which this technique is applicable is in the millimolar regime.

Enrichment will only lower the concentration requirements by a factor of three. Concentration range is not the only difficulty, the chemical shift anisotropy (CSA) of the ^{195}Pt nucleus apparently presents potential problems. CSA effects cause broadening in platinum resonances^{12,13} and make detection in undissolved³⁶ and rigid biomolecules such as membranes close to impossible for platinum(II) complexes. The additional quadrupolar interactions with ^{14}N ligands^{12,13} presents another potential hurdle for this method. The success of the ^{195}Pt NMR method will depend on the nature of the platinum complex. As such our exploratory approach to this method as described in Section II begins with the PtCl_4^{2-} complex instead of the $\text{Pt}(\text{trpy})\text{Cl}^+$. The use of ^{15}N enriched samples have recently increased for the sharpened ^{195}Pt NMR resonances and the coupling of the two nuclei are very informative.¹³

^{13}C NMR, ^1H NMR, and ^{31}P NMR of the ancillary ligands in the Pt complex can also be studied. Coupling between platinum and these nuclei can surely be evidence for platinum in the biomolecule. Theoretically, these techniques may be used to show where the platinum is bound in the biomolecule.

The use of chromophoric platinum(II) complexes may be the convenient and practical means to its detection. The metal-to ligand charge-transfer (MLCT) bands are strong enough to permit quantitation in the micromolar regime. Specific interactions with the biomolecule may result in new spectral bands which can be easily followed. The starting material, $\text{Pt}(\text{trpy})\text{Cl}^+$, was initially thought to probe for thiophosphates in DNA since strong MLCT bands characteristic of a platinum-sulfur bond results.^{34,37} Its derivative, the effective metallointercalation reagent $\text{Pt}(\text{trpy})\text{HET}^+$, had strong

absorption bands which were useful in obtaining binding isotherms with DNA. Its strong electron density had also been useful in determining sites of intercalation in DNA by X-ray fiber diffraction. These useful precedents of the terpyridine platinum(II) complexes, set the stage for developing the reagent $\text{Pt}(\text{trpy})\text{Cl}^+$ as spectroscopic probes for proteins in our laboratory, as will also be discussed in Sections III to V.

SECTION II.

^{195}Pt NMR SPECTROSCOPY OF PLATINUM(II) THIOETHER COMPLEXES

INTRODUCTION

To explore the utility of ^{195}Pt NMR spectroscopy as a tool for studying biomolecules with platinum (II) complexes tagged on them necessitates the use of the simplest and well-studied complex, PtCl_4^{2-} . The complex has been widely used as a reference signal for ^{195}Pt NMR. The absence of ligating atoms in this complex which contributes to the broadening of signals makes initial ^{195}Pt NMR studies in the presence of biomolecules simpler and feasible.

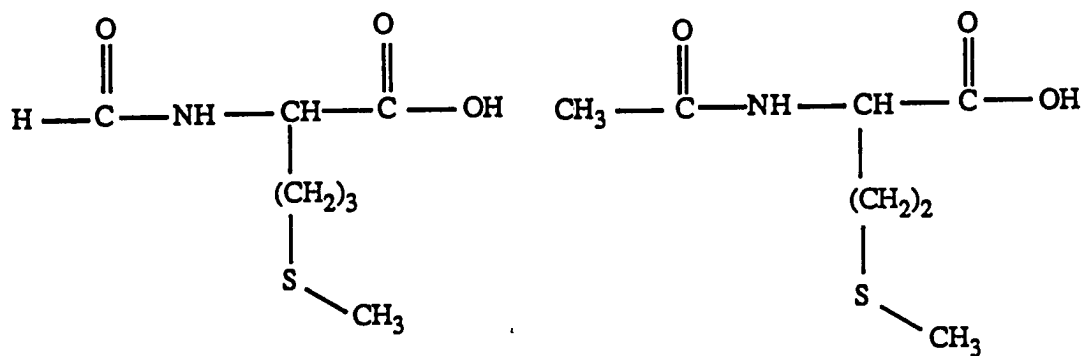
This complex has been widely used as a heavy atom label for X-ray studies of protein structure.⁵ This work was prompted in particular by the discovery that PtCl_4^{2-} binds covalently to the exposed methionine residue, Met 65, in cytochrome c.¹⁴ Using N-acetyl-L-methionine (AcMetH) as a monodentate thioether ligand, the complex $\text{PtCl}_3(\text{AcMetH})^-$ serves to model the binding of PtCl_3^- label to the side chains of methionine residues in proteins.

Inversion of the pyramidal configuration at the coordinated S atom in various metal complexes have been studied using ^1H NMR spectroscopy.³⁸ Reliance on ^1H NMR restricted previous studies to complexes of simple ligands of the types $(\text{RCH}_2)_2\text{S}$ and $\text{RCH}_2\text{SCHR}'$ and to the corresponding bidentates, for which the collapse of the methylene quartet upon heating is easily observed.

Stereodynamic studies of metal complexes with biological ligands such as in $\text{PtCl}_3(\text{AcMetH})^-$ clearly require a different technique. ^{195}Pt NMR fortuitly proves to be suited to this task for the ^{195}Pt chemical shifts depend on the ligand atoms and on the more distant environment.^{12,13}

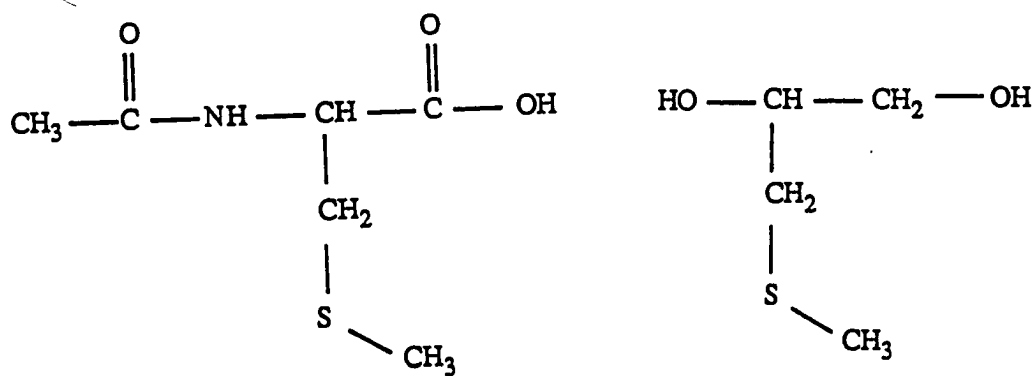
To examine the factors governing the stereodynamics in metal complexes with thioether ligands, various monodentate ligands (shown below): N-formyl-DL-

homomethionine (FHMeth), AcMetH, DL-3-(methylthio)-1,2-propanediol (MTPD), N-acetyl-S-methyl-DL-cysteine (AcMeCysH), and DL-3-(methylthio)-2-butanone (MTB) and a bidentate ligand methyl-DL-cysteine (MeCysH) were used. To extend the applicability of ^{195}Pt NMR to complexes of larger biomolecules, the complex with the thioether peptide, S-methylglutathione (SMG) or N-(N-L- γ -glutamyl-L-methylcysteinyl)glycine was also studied.



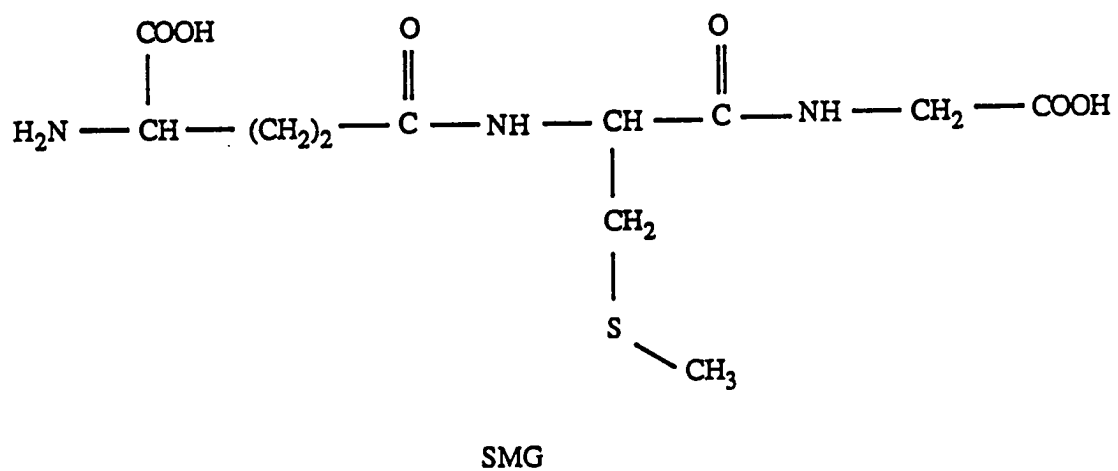
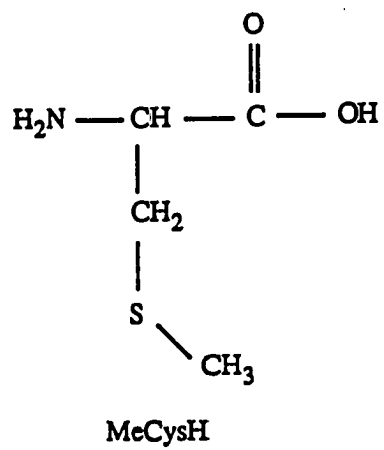
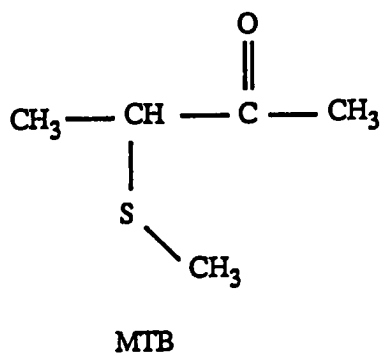
FHMeth

AcMetH



AcMeCysH

MTPD



EXPERIMENTAL SECTION

Chemicals

The ligands, AcMetH, MTPD, SMG, MTB, and deuteriated solvents were obtained from Aldrich Chemical Co. while the ligand MeCysH was from Sigma Chemical Co. K_2PtCl_4 was obtained from Aldrich Chemical Co. or borrowed from Johnson Matthey, Inc. The ligands, FHMtH³⁹ and AcMeCysH⁴⁰ and the various thioether complexes of platinum(II) were prepared as outlined in the published articles.^{15,16}

NMR Spectroscopy

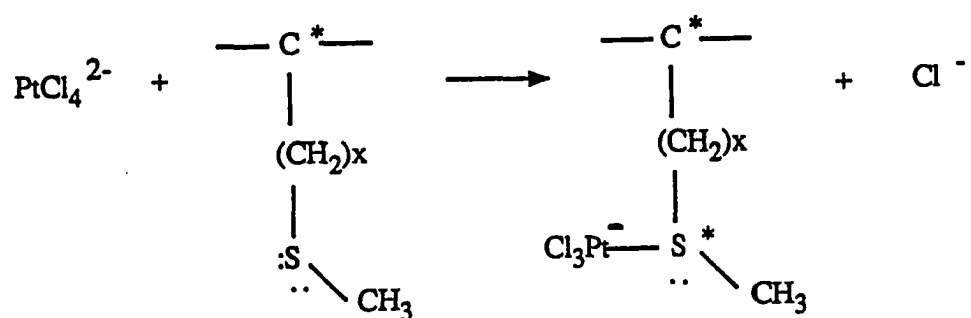
The 1H (at 90 MHz and 300 MHz) and ^{13}C (at 74.5 MHz) NMR spectra were recorded with JEOL FX 90 Q and Nicolet NT 300 spectrometer using residual H_2O , acetone, and dioxane as internal standards. The ^{195}Pt NMR spectra of the samples were recorded with a Bruker WM 300 spectrometer at 64.4 MHz, using 10- and 20- mm probes. Solvents contained ca. 25% of the deuterium isotopomer for lock and were made 0.5 M in HCl in order to prevent decomposition of the complexes. Each spectrum was acquired in 8K data points, with two sets of parameters, and delay time. With the 10-mm probe, they were as follows: 100 kHz, 10 μs , 90 $^\circ$, 3300 ms. With the 20-mm probe, they were as follows: 20 kHz, 100 μs , 90 $^\circ$, 500 ms; 50 kHz, 50 μs , 45 $^\circ$, 200 ms. The sample temperature was maintained with the Bruker variable-temperature controller. A solution of K_2PtCl_4 in aqueous NaCl, kept in a coaxial inset tube, was used as an external reference at room temperature. The ^{195}Pt chemical shift at 294 K with respect to the

PtCl_6^{2-} reference is -1614 ppm.¹² Signals occurring at stronger fields than the reference signal have negative chemical shifts. The chemical shifts of PtCl_4^{2-} and PtCl_6^{2-} ions with similar compositions and identical charges, depend similarly on temperature.^{12,13,41} Since these temperature effects are small, and the range of ^{195}Pt shifts is extremely wide, the use of the same correction factor at other temperatures would have little, if any effect on the discussion and conclusions.

RESULTS AND DISCUSSION

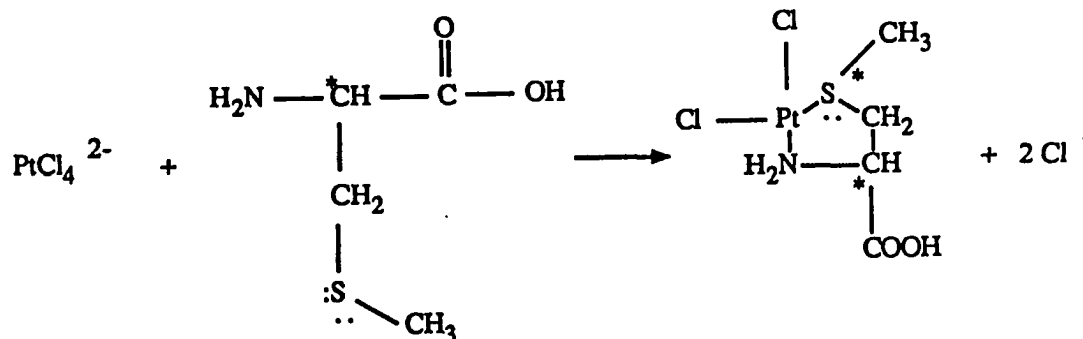
Complex Formation

FHMetH, AcMetH, MTPD, AcMeCysH, SMG, and MTB displace one Cl^- ligand and coordinate to the platinum(II) atom as a monodentate thioether, as shown below.

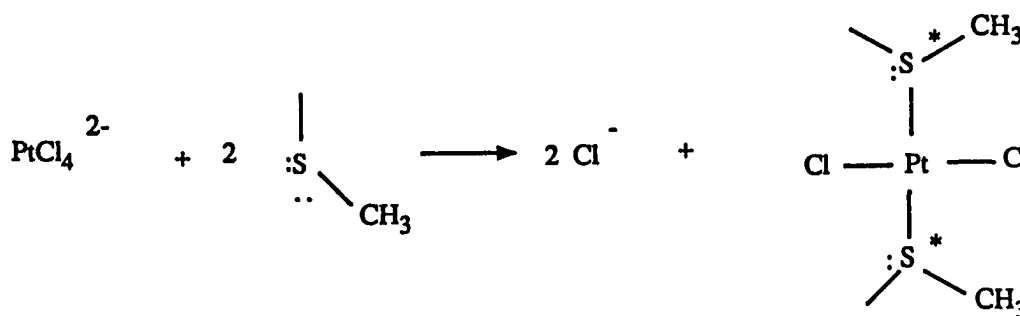


ligand	x
FHMetH	3
AcMetH	2
MTPD	1
AcMeCysH	1
SMG	1
MTB	0

MeCysH forms a chelate complex^{42,43} as shown below.



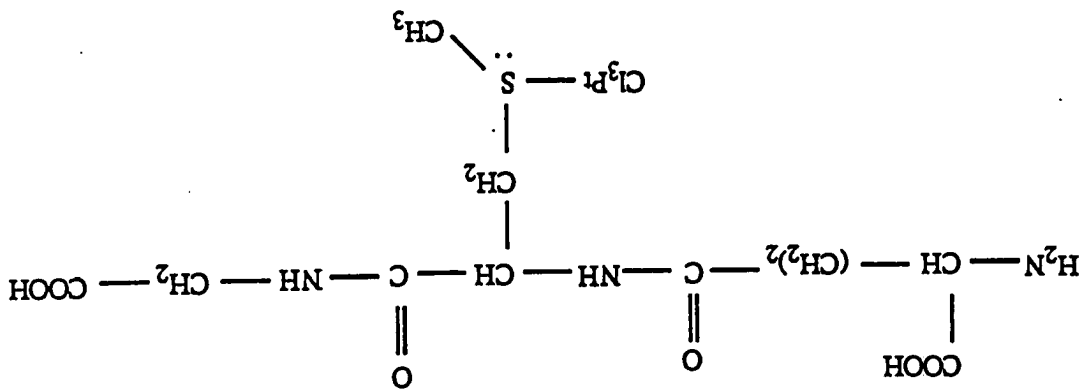
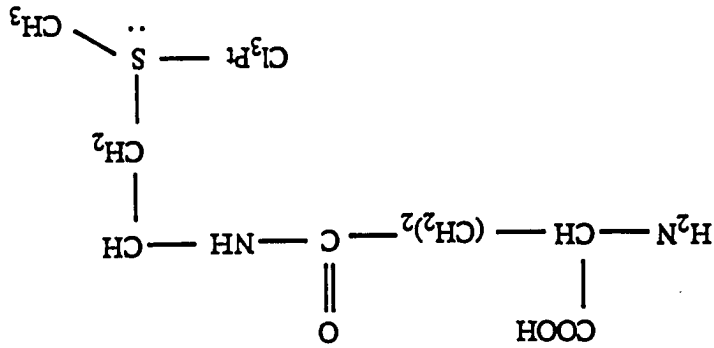
When two equivalents of AceMetH are mixed with one equivalent of PtCl_4^{2-} , the disubstituted complex is obtained, as shown below.



This preponderance for disubstitution necessitates the order in mixing reagents. The ligand is thus added to PtCl_4^{2-} to ensure only the formation of the monodentate thioether complex.

The complexes are virtually stable in solution and as solid salts in the absence of light. However, the complex $\text{K}[\text{PtCl}_3(\text{SMG})]$ interestingly decomposes to give glycine and presumably the remaining part of the thioether peptide still complexed to platinum as shown below and in Figure II-1 perhaps by a platinum-mediated hydrolysis.

Gly



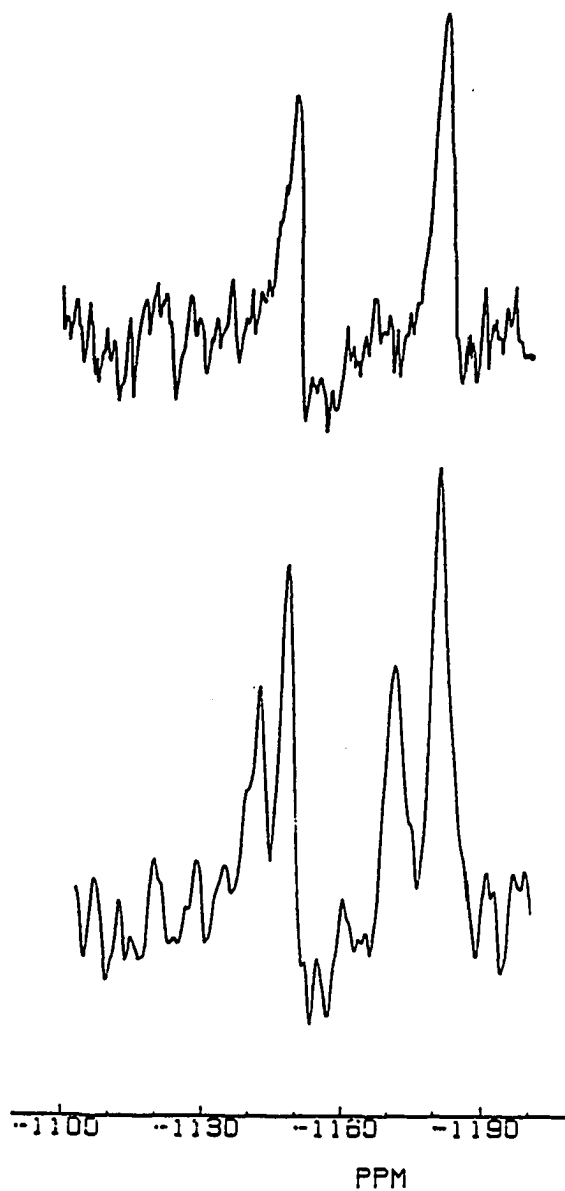


Figure II-1. The ^{195}Pt NMR Spectra of $\text{PtCl}_3(\text{SMG})^-$ Dissolved in 0.5 M DCl at 294 K. The upper spectrum is obtained before hydrolysis while the lower spectrum is obtained after hydrolysis

^1H NMR The ^1H NMR spectra of the complexes reveal the expected effects of coordination.^{15,16} There is a downfield shift in the ligand resonances due to the deshielding effect of platinum. Particularly informative of platinum coordination is the triplet with relative intensities 1:4:1 which arises from the three-bond coupling ^{195}Pt - ^1H in PtSCH_3 , the fragment present in all of the monodentate thioether complexes. The spectroscopic data^{15,16} agree fully with the corresponding values for simpler complexes containing the $\text{trans ClPt(II)S(CH}_3)_2$ fragment.⁴⁴⁻⁴⁶

^{195}Pt NMR The ^{195}Pt chemical shifts of all the unidentate complexes, listed in Table II-1, fall near the value of -1143 ppm (vs. PtCl_4^{2-}), found for the simple thioether complex $\text{PtCl}_3(\text{SMe}_2)^-$. This agreement indicates again that all the ligands except MeCysH are coordinated to Pt(II) as unidentate thioethers.

Inversion at Sulfur

Diastereomerism The chirality of the sulfur atom gives rise to the two diastereomers shown below since the chiral carbon atom in each of the ligands is stable toward racemization under the experimental conditions.

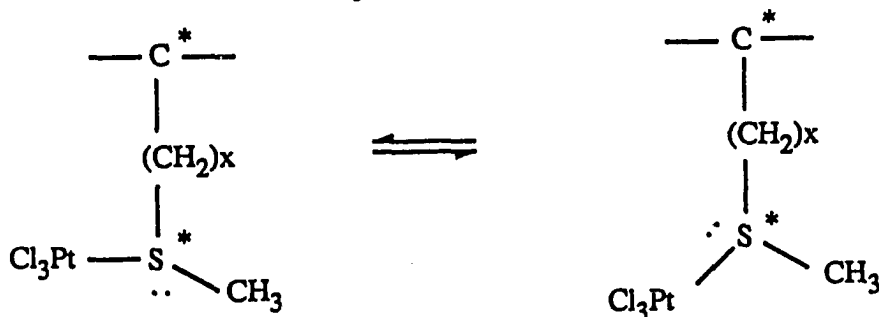


Table II-1. Platinum-195 NMR Spectra of Unidentate $\text{PtCl}_3(\text{thioether})^-$ Complexes and of the Bidentate $\text{cis-}[\text{PtCl}_2(\text{MeCysH})]$ Complex

thioether ligand	x in $-(\text{CH}_2)_x\text{S}^*$	solvent	chem shifts, ν , ppm ^a	$\Delta\nu$, ppm (temp, K)	intensity ratio
FHMetH	3	acetone	-1147, -1152	5 (200)	1.0:1.0
AcMetH	2	6:1 0.5 M HCl:diglyme	-1168, -1174	6 (278)	1.0:1.0
MTPD	1	0.5 M HCl	-1152, -1171	19 (294)	1.0:1.2
AcMeCysH	1	0.5 M HCl	-1145, -1179	34 (294)	1.0:1.2
SMG	1	0.5 M HCl	-1147, -1179	32 (294)	1.0:1.4
MTB	0	0.5 M HCl	-1124, -1138	14 (294)	1.0:1.0
MeCysH ^b	1	DMF	-1381, -1414	33 (294)	2.6:1.0

^aReferenced to PtCl_4^{2-} .

^bCoordinated as S,N-bidentate ligand.

The ^1H and ^{13}C nuclei are not quite sensitive to the small differences in the molecular environment of the two diastereomers because of the narrow range of chemical shifts these nuclei span. The superposition of ^{195}Pt - ^1H coupling, ^1H - ^1H coupling, and diastereoisomerism obscures the spectroscopic information of diastereomerism.

Although the ^1H and ^{13}C spectra proved somewhat useful in the case of the MTB complex (for which $x = 0$), the NMR methods based on these two nuclei are neither generally applicable nor convenient.

The larger the frequency difference between the NMR signals of the isomers, the higher the temperature (designated T_c) at which the signals will coalesce as the isomers interconvert.⁴⁷⁻⁵⁰ Unlike the ^1H or ^{13}C resonances of the two diastereomers, which are already coalesced below 273 K, the ^{195}Pt resonances are well-separated (by 6-35 ppm, depending on the thioether ligand) at room temperature. In all the unidentate complexes except that of AcMeCysH, the resonances coalesce in the accessible temperature region, as shown in Table II-2 and in typical sets of spectra shown by Figures II-2 through II-4.

All the temperature-related changes are reversible. The barriers to inversion, i.e., the ΔG^\ddagger values at the respective coalescence temperatures were determined by the following equation in which $\delta\nu$ is the separation in hz of the two resonances when no interconversion has yet occurred.⁴⁷⁻⁵⁰ The results are presented in Table II-3.

$$\Delta G^\ddagger = 19.14 T_c (9.97 + \log T_c / \delta\nu) \text{ j-mol}^{-1}$$

Table II-2. Barriers to Inversion of Sulfur Configuration in Unidentate Thioether Complexes

thioether ligand	x in $-(CH_2)_xS^+$	solvent 0.5 M HCl: diglyme	coalescence temp, T_C , K	ΔG^\ddagger at T_C kJ- mol ⁻¹
FHMetH	3	^a	-250	
AcMetH	2	6:1	335	66.7
MTPD	1	1:0	>376	
		1:2	353	66.4
AcMeCysH	1	1:0	>376	
		4:1	>376	
		2:1	>376	
		1:1	>376	
		1:2	>376	
MTB	0	1:0	370	70.6
		6:1	367	70.1
		4:1	363	69.3
		1:1	338	64.5
		2:3	300	57.3
		1:2	<290	

^aThe solvent is acetone for the FHMetH complex.

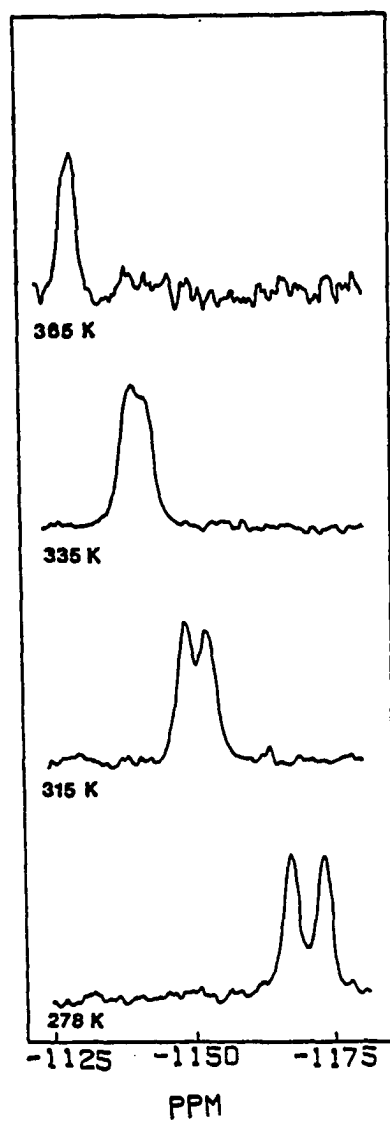


Figure II-2. Variable-temperature ^{195}Pt NMR Spectra of $\text{PtCl}_3(\text{AceMetH})^-$
Dissolved in 0.5 M DCl

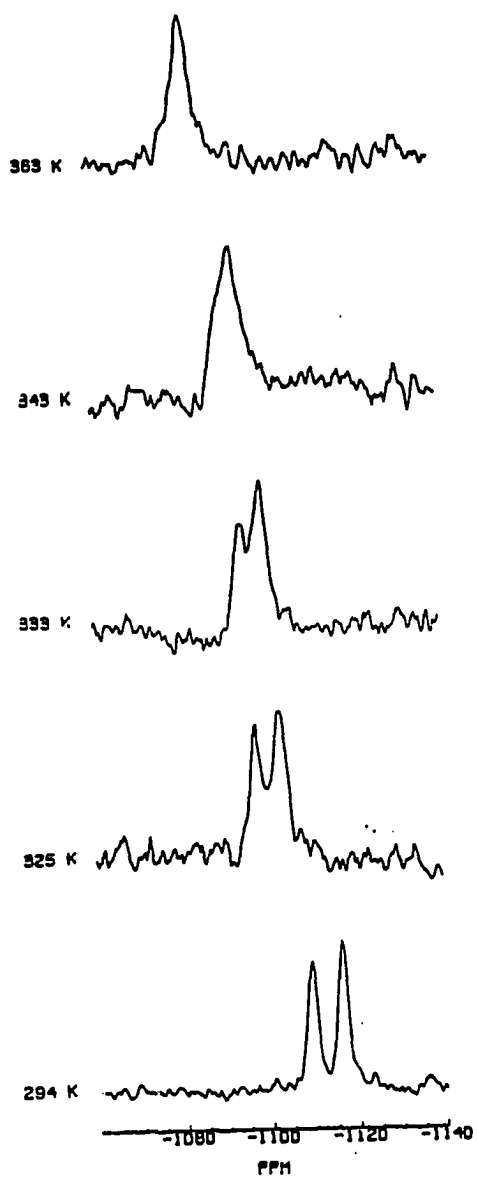


Figure II-3. Variable-temperature ^{195}Pt NMR Spectra of $\text{PtCl}_3(\text{MTB})^-$ in a Solution Containing 0.5 M DCl and Diglyme in the Ratio of 1:1

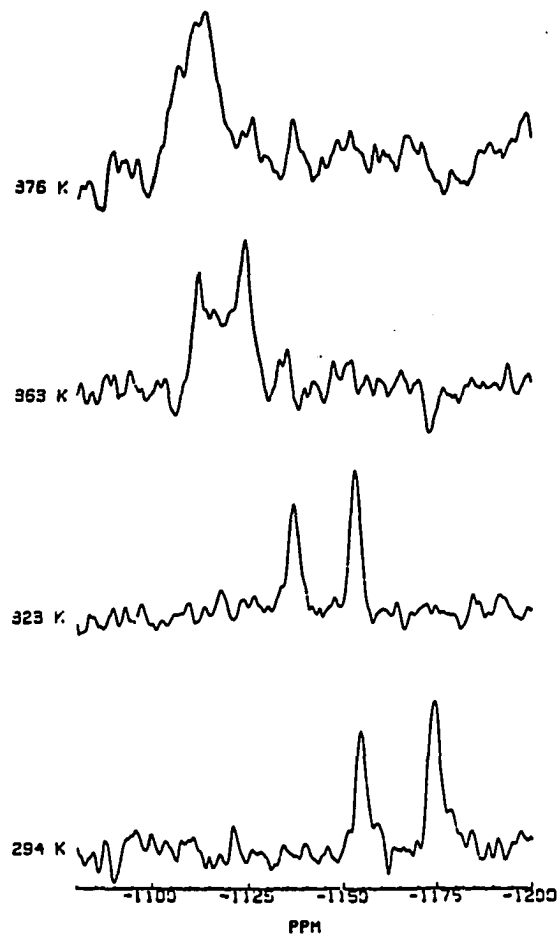


Figure II-4. Variable-temperature ^{195}Pt NMR Spectra of $\text{PtCl}_3(\text{MTPD})^-$ Dissolved in 0.5 M DCl

Table II-3. Effect of Solvent Composition on the ^{195}Pt NMR Spectrum of $\text{PtCl}_3(\text{MTB})^-$ at 294 K

0.5 M HCl:diglyme	chem shift, δ, ppm^a	$\Delta\nu$, ppm
1:0	-1123, -1138	15
6:1	-1126, -1140	14
4:1	-1119, -1132	13
2:1	-1111, -1120	9
1:1	-1109, -1116	7
2:3	-1107, -1109	2
1:2	-1110	0

^aReferenced to PtCl_4^{2-} .

Mechanisms The coalescence of the ^{195}Pt peaks is caused by the intramolecular inversion of configuration at sulfur. Indeed, the ΔG^\ddagger values fall in the middle of the rather narrow range of such data obtained for platinum(II) complexes with common thioether ligands.³⁸ Other mechanisms such as nuclear tunneling and dissociation with subsequent recombination are ruled out because the range of ΔG^\ddagger values for such processes are relatively large.³⁸ The latter mechanism is further ruled out by the observed sharpening of the ^{195}Pt signal above the coalescence temperature. Moreover, other Pt(II)-thioether complexes were shown to maintain the ^1H - ^{195}Pt coupling above the coalescence temperature^{38,51} and not to exchange the thioether ligands.^{38,52}

Although the ^{195}Pt chemical shifts of the two diastereomers depend on temperature, the coalescence of the corresponding NMR signals is not due simply to their merger upon heating. The temperature coefficients of both signals in Figure II-3 at lower temperatures, while they are still separate, is 0.4 ppm K^{-1} , consistent with the known values for similar complexes.^{12,41,53} Since the temperature coefficient depends mainly on charge and is insensitive even to the geometric isomerism, it is understandable that the two diastereomers, which have the same composition and charge should have the same temperature coefficient of the ^{195}Pt chemical shift. In the absence of the inversion, therefore, the separation between the two peaks, $\Delta\nu$, should remain constant upon heating.

The spectra in Figure II-2 through II-3 clearly demonstrate the broadening of the signals around the coalescence temperature and the sharpening of the signal above this

temperature. The line widths (in Hz) of the five spectra for Figure II-3, in order of increasing temperature, are as follows: 123 and 113, 225 and 266, 256 and 276, 429, and 272. This pattern of line widths is fully consistent with intramolecular inversion as the cause of the coalescence. The spectra of the $\text{PtCl}_3(\text{MTPD})^-$ complex, shown in Figure II-4, exhibit even larger broadening near T_c because the $\Delta\nu$ value for this complex is greater than that for the MTB complex.

The FHMeth complex, which has the longest side chain ($x = 3$), already exhibits a single ^{195}Pt NMR signal at 294 and 273 K. Upon cooling, however, this signal splits into two, which move apart as the temperature decreases; their separation is 2 ppm at 235 K and 5 ppm at 200 K, the lowest temperature accessible. Since the process of interchange could not be frozen to obtain the limiting value of $\Delta\nu$ value, which is necessary for calculation of the ΔG^\ddagger barrier, there was no need for an accurate value of the coalescence temperature, either.

The ^{195}Pt signals due to the diastereomers of the AcMeCysH complex were 34 ppm apart when pure aqueous solvent was used and 25 ppm apart when the solvent was two-thirds diglyme; intermediate separations were obtained with solvents of intermediate compositions. In no case were the signals close enough to permit coalescence in the accessible range of temperatures.

Dependence of Inversion Barrier on Solvent In order to extend the temperature range in which ^{195}Pt NMR spectra could be measured, diglyme, which has a high boiling point and a low freezing point, was added to the solutions of complexes in 0.5 M

HCl. The temperature range did expand as expected, but some unexpected phenomena occurred as well. These interesting additional effects are best examined in the case of the MTB and MTPD complex, on the basis of the data in Tables II-2 and II-3.

Addition of diglyme causes small changes in the signal positions, an effect not unusual in view of the general dependence of ^{195}Pt chemical shift on solvent properties. As long as diglyme remains the minor constituent (less than ca. 10 %) of the solvent, it merely raises the boiling point, the original purpose for its use. When more abundant, but still the minor constituent (up to ca. 20 %), it reduces the separation between the diastereomer signals and thus lowers the coalescence temperature; the inversion process itself appears to remain virtually unaffected, however, because the ΔG^\ddagger value changes only slightly. Further increase in the fraction of diglyme brings about a significant decrease in the barrier to inversion, an indication that the process itself has been affected. When the excess of diglyme over the aqueous component becomes approximately twofold, the signals of the two diastereomers already become coalesced below room temperature. All the solvent-related changes are reversed when the solvent is restored to its original composition.

This lowering of the coalescence temperature for the given stereodynamic process would otherwise require use of an NMR spectrometer with a weaker magnet. Our findings indicate that the same can perhaps be achieved with the proper choice of the solvent. In the MTB case the decrease in $\Delta\nu$ is large (see Table II-3) and T_c is insufficient to render it accessible with the strong magnetic field (64.4 MHz for ^{195}Pt).

The solvent effect is evident in both cases. The difference in degree between the MTB and MTPD complexes may be related to the difference between the ligands: whereas the former is hydrophobic, the latter contains two hydroxyl groups and is hydrophilic. The exact cause of the difference is not clear.

This interesting solvent effect is not limited to diglyme; acetone and perhaps N,N-dimethylformamide (DMF) behave similarly. Since the MTB complex, the simplest one used in this study, gives rise to a tractable ^1H spectrum, the ^1H NMR spectra of $\text{PtCl}_3(\text{MTB})^-$ in solutions in which the ratio $\text{D}_2\text{O}:\text{acetone-d}_6$ was 1:0, 2:1, 1:2, and 0:1 were compared. Addition of acetone causes the CH_3S and the CH_3CH peaks of the two diastereomers, which were distinct in the D_2O solution, to gradually merge and coalesce at room temperature. Although DMF reduces $\Delta\nu$ in a desired way, as a coordinating solvent its use is limited.

Chiral Discrimination

Stereoselectivity in chemical reactions often results from small details of molecular structure, which the ^{195}Pt nucleus evidently can sense. The potential of ^{195}Pt NMR spectroscopy in the study of diastereoisomerism went virtually unrecognized^{54,55} prior to our work.^{15,16} The present study seems to be the first one devoted to a systematic examination of chiral (in)discrimination in a series of homologous Pt complexes by means of ^{195}Pt NMR spectroscopy.

Unidentate Complexes Each of the unidentate thioether complexes of the diastereomers have nearly equal abundance as indicated by the relative intensities of the resonances in Table II-1. The chiral carbon atom apparently provides virtually no discrimination between the two configurations of the chiral sulfur atom regardless of the length of the methylene chain between these two atoms. The difference between the ^{195}Pt chemical shifts of the two diastereomers probably is a consequence of long-range, noncovalent interactions of the Pt atom with the different substituents at the chiral carbon atom. Since the difference is evidently small, these interactions probably are weak or similar in the diastereomers, or both. Since the diastereomers evidently are very similar in properties and in stability, an attempt to assign the ^{195}Pt NMR peaks to them, i.e., to assign absolute configuration would be unwarranted.

Salts of the $\text{PtCl}_3(\text{MTB})^-$ complex with the cations K^+ and AsPh_4^+ give virtually identical ^{195}Pt NMR spectra. Properties of the counterion evidently have no significant effect on the relative abundance of the two diastereomers.

Chelate Complexes In search of the thioether complex that would exhibit chiral discrimination, the compound $\text{cis-}[\text{PtCl}_2(\text{MeCysH})]$, in which S-methyl-L-cysteine acts a bidentate ligand shown earlier was investigated. Previous studies of diastereoisomerism in these chelate complexes⁵⁶⁻⁵⁹ and in related α -amino acid chelates^{56,60-62} were impeded by the complexity of the ^1H NMR patterns due to the superposed effects of ^1H - ^1H coupling, ^{195}Pt - ^1H coupling, and diastereomerism.

Although ^{13}C NMR spectra of the chelates can be assigned with more certainty, their acquisition requires concentrated solutions and relatively long time.

As in the studies of the unidentate complexes (see above), ^{195}Pt NMR spectroscopy proved to be well-suited to the task. The spectrum obtained is extremely simple and is easily recorded. The complex $\text{cis-}[\text{PtCl}_2(\text{MeCysH})]$ in DMF-d_6 solution at 294 K gives rise to just two ^{195}Pt NMR signals, at -1381 and -1414 ppm relative to the PtCl_4^{2-} standard. These peaks occur at higher magnetic field than those of the unidentate complexes (see Table II-2) mainly because of the ring effect and partly because the donor set SNCl_2 creates a stronger ligand field than the set SCl_3 .¹²⁻¹³

The intensity ratio of the two signals is 2.6:1.0. The chelate complex apparently exhibits greater chiral discrimination than do the unidentate complexes. The difference between the ^{195}Pt chemical shifts of the diastereomer resonances reflects the dissimilarity between the Pt environments, but this difference alone cannot be taken as a measure of chiral discrimination. Although the shift difference in the unidentate AcMeCysH complex (34 ppm) is virtually the same as that in the chelate MeCysH complex (33 ppm), the intensity ratio is 1.0:1.2 in the former complex and 2.6:1.0 in the latter one. Chiral discrimination evidently is absent from the former complex and present in the latter one.

Molecular structures are known for the two chelate complexes homologous to the one under consideration: $\text{cis-}[\text{PtCl}_2(\text{EtCysH})]$ ⁵⁸ and $\text{cis-}[\text{PdCl}_2(\text{MeCysH})]$.⁶³ Both diastereomers are present in the crystal of each complex. In each case, the chelate ring of

the L-amino acid adopts the λ conformation with an equatorial COOH group and axial alkyl (Et or Me) group. The opposite configurations at the S atom keep the alkyl group on the different sides of the average ring plane, trans or cis with respect to the α -H atom. Although the environments of the metal atom in the diastereomers are only slightly different, the corresponding ^{195}Pt NMR signals are far apart.

Comparison between the unidentate and chelate complexes reveal the structural characteristics associated with the occurrence of chiral discrimination. Unidentate thioethers do not exhibit it probably because they are too flexible. A greater constraint, such as that provided by bidentate coordination, seems to be a prerequisite for chiral discrimination.

CONCLUSIONS AND PROSPECTS

This work has demonstrated the use of variable-temperature ^{195}Pt NMR spectroscopy on the stereodynamics of biologically relevant thioether complexes of platinum. This method is well-suited to monitoring exchange processes involving relatively complex molecules specially those which are not readily tractable by the common ^1H and ^{13}C NMR methods.

Future studies will tell whether solvent effects can be used profitably in stereodynamic studies. A suitable liquid must be miscible with the principal solvent and compatible with the solute and should raise the boiling point, lower the freezing point, or both. A simple method for lowering the coalescence temperature would be highly desirable in the work with biomolecules, many of which have limited thermal stability.

The applicability of ^{195}Pt NMR spectroscopy to larger biologically relevant molecules and ultimately to proteins and chromosomal components is an attractive goal to realize. We have not yet been successful in applying this technique to proteins. In our attempts to achieve this goal, we began to study the thioether peptide complex, $\text{PtCl}_3(\text{SMG})^-$. The sensitivity of the ^{195}Pt nucleus enabled us to observe the unexpected platinum-mediated hydrolysis of the tripeptide, which is now being further studied in our laboratory⁶⁴ for the development of PtCl_4^{2-} as a selective, inorganic mediator of peptide hydrolysis at cysteines and methylated cysteines. Studies along the lines of using longer thioether peptide complexes of platinum for the potential success of using ^{195}Pt NMR

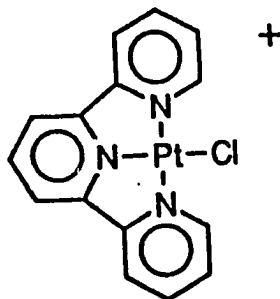
will no longer be simple since peptide hydrolysis at methylated cysteine- as well as methionine- containing peptides will have to be considered in addition to the problems of increased viscosity and relaxation in high molecular weight samples.

SECTION III.

PT(TRPY)Cl⁺ AS CHROMOPHORIC TAGS OF HISTIDINES IN CYTOCHROME C

INTRODUCTION

Few inorganic labeling reagents have been developed for the purpose of covalent modification of amino acid side chains in proteins.⁶ A main objective in labeling studies is to achieve selectivity of a reagent toward various potential binding sites in the protein. Reconstitution of apoproteins is usually specific as the metal ion occupies the active site. Binding of solvated metal ions to holoproteins may however be nonspecific. Selectivity towards particular functional groups on the proteins can be achieved by exploiting the coordination preferences of metals and ligands for each other. In one elegant method, a side chain is converted into a chelating agent and a metal ion introduced into the chelate.^{4,65-78} In another, a substitution reaction is effected between a protein and a preformed labile metal complex. This work involves the use of the preformed reagent, $\text{Pt}(\text{trpy})\text{Cl}^+$ with the well-studied protein, cytochrome c.



Its selectivity toward proteins, as established here with cytochromes c, is opposite from that of the commonly used PtCl_4^{2-} (as discussed in the previous Section).

EXPERIMENTAL SECTION

Materials and Methods

Chemicals The proteins, trypsin treated with TPCK, amino acids and peptides were obtained from Sigma Chemical Co. Horse-heart cytochrome c (of types VI and III) was oxidized with $K_3Fe(CN)_6$ and then purified by cation-exchange chromatography on CM 52 cellulose.⁷⁹ Tuna-heart cytochrome c (of Type XI) was used as received. Chloro(2,2':6',2"-terpyridine)platinum(II) dihydrate, $[Pt(trpy)Cl]Cl \cdot 2H_2O$, was purchased from Strem Chemicals or Aldrich Chemicals.⁸⁰ Compound $[Co(phen)_3](ClO_4)_3$ was prepared according to the published method.⁸¹ Deuteriated chemicals were from Aldrich Chemicals.

Spectrometers The 1H NMR spectra were recorded with Nicolet NT 300 and Bruker WM 300 spectrometers. The ^{195}Pt NMR spectra were recorded with the Bruker instrument at 64.4 MHz, using a 20-mm broad-band probe. Absorption spectra were recorded with an IBM 9430 UV-vis spectrophotometer, equipped with a two-grating monochromator. The X-band EPR spectra at 6 K were obtained with a Bruker ER 200D instrument, using a rectangular cavity with a nominal frequency of 9.6 GHz and an Oxford Instruments ESR 900 cryostat.

NMR Measurements The 1H Spectra were recorded in D_2O solutions. The proteins were dialyzed into D_2O by ultrafiltration and then lyophilized repeatedly with D_2O . The N-H resonances were removed either by deuteration at room temperature for 24 hours or at elevated temperatures.⁸²⁻⁸⁴ The resolution was enhanced by standard techniques: a broadened spectrum was subtracted from a normal one and a convolution difference spectrum obtained according to the published method.⁸⁵

The ^{195}Pt NMR spectra of 15-30 mM solutions of $\text{Pt}(\text{trpy})\text{L}^{2+}$ complexes were recorded with a 20-mm broad-band probe. The spectra were obtained from 1000 transients in 8K data points with a 90° pulse or from 10,000-20,000 transients in 2K data points with a 10° pulse. The chemical shifts are expressed with respect to PtCl_4^{2-} . 12,13,86

Peptide Mapping Tryptic hydrolysis and the separation of the resulting peptides by HPLC were performed according to the published procedures^{87,88} with minor modifications. To a sample containing 2-4 mg of cytochrome in 1-2 mL of water was added 4.5 mg of NH_4HCO_3 while keeping the pH at 7.5. Trypsin was added at the beginning and again after five hours, and the reaction mixture maintained at 37°C for a total of ten hours. Digestion was terminated by lyophilization. The lyophilized material was dissolved in 0.1-0.2 mL of phosphate buffer (49 mM KH_2PO_4 and 5.4 mM H_3PO_4) at pH 2.85 and filtered through a $0.2\ \mu\text{m}$ nylon membrane. A 100- μL aliquot of the solution was then injected onto a C_{18} reverse-phase (Sepalyte) column sized 4.6 mm x 25 cm. The peptides were eluted for 120 min at a flow rate of 1 mL/min, while acetonitrile gradient was run linearly from 0 to 45 % by an Axxiom HPLC gradient controller. The absorbance at 220 nm, due to peptide bonds and at 342 nm, due to $\text{Pt}(\text{trpy})\text{His}^{2+}$ chromophore were recorded with an ISCO V-4 absorbance detector and a Shimadzu CR-3A Chromatopac data processor. Fractions of 0.5 mL were collected with an ISCO Foxy Collector. Those to be examined spectrophotometrically were dried and redissolved in water. The retention times and chromatographic behavior of the $\text{Pt}(\text{trpy})\text{L}^{n+}$ complexes, wherein L is Cl^- , His, Im His-Lys, Gly-His-Gly, and Ala-Pro-Gly-Asp-Arg-Ile-Tyr-Val-His-Pro-Phe, were studied under the same conditions that were used for the tryptic peptides.

Voltammetry Three voltammetric techniques were used. Differential-pulse, constant-potential differential-pulse, and cyclic voltammograms were obtained with an IBM EC 225 Voltammetric analyzer and Houston Instruments Omnigraph 200 X-Y recorder. A BAS cell assembly consisted of a Ag/AgCl couple as reference, a platinum wire as auxiliary, and a 1.6-mm gold disc as a working electrode. The composition of the sample solutions was as follows: 0.1-0.4 mM in cytochrome, 10 mM in 4,4'-dipyridyl (from Sigma) as a mediator⁸⁹, 100 mM in NaClO₄, and 85 mM in phosphate buffer at pH 7.0. The temperature was maintained at 25^o C with a Forma Scientific 2067 circulatory bath. Solutions were deoxygenated before the measurements by gentle bubbling of argon and kept under this gas.

Molecular orbital Calculations An approximation to the Hartree-Fock-Roothaan technique, the Fenske-Hall method,⁹⁰ described elsewhere, was performed by an associate, Mr. Longgen Zhu. Since this iterative SCF method is devoid of empirical or adjustable parameters, the results of a calculation – eigenvalues, eigenvectors, and the derived quantities – are determined fully by the molecular geometry and basis functions. The dimensions of the Pt(trpy)²⁺ fragment⁹¹ and of the Pt-S(CH₃)₂^{92,93} and Pt-imidazole^{94,95} units were taken from the actual structures. The standard basis sets were used.

Synthesis and Preparation

Protein Modification Ferricytochrome c was incubated with an equimolar amount of [Pt(trpy)Cl]Cl at room temperature in 0.1 M acetate buffer at pH 5.0 for 24 hours. The concentration of each was 2 mM. Procedures involving 5.0 or 25 mg of the protein and 0.20 or 1.0 mg of the platinum complex, respectively, proved particularly convenient

although equal yields were obtained with larger and smaller quantities of the reactants. The incubation was terminated by ultrafiltration of the reaction mixture into the acetate buffer at pH 5.0 and subsequently into 85 mM phosphate buffer at pH 7.0. The components of the reaction mixture were separated on a CM 52 column, previously equilibrated with the same phosphate buffer at 4^o C. About 1 mg of cytochrome was applied per 1 mL of the resin bed. The modification of the horse cytochrome yielded the following derivatives, in their elution order: native (N), 38 %; major singly-labeled (S_A), 42 %; minor, singly-labeled (S_B), 2 %; and doubly-labeled (D), 7 %. The first three fractions were eluted with 85 mM phosphate buffer, whereas fraction D required a gradient to 125 mM buffer. The modification of tuna cytochrome gave two fractions, eluted in the same order: N (90 %) and derivative S_B (7 %). Incubation of either cytochrome with a ten-fold molar excess of [Pt(trpy)Cl]Cl did not yield any new derivatives. The separated protein derivatives were oxidized with [Co(phen)₃](ClO₄)₃ and dialyzed exhaustively before spectroscopic and electrochemical studies.

Survey of Amino Acids Every amino acid containing a heteroatom in the side chain was incubated with [Pt(trpy)Cl]Cl under the general conditions of the protein modification. The aqueous solutions, 5 mM in the amino acid and in the platinum reagent, were left at room temperature for several days and examined periodically by UV-vis spectrophotometry. The following amino acids showed no sign of reaction: Lys, Trp, Arg, Asp, Asn, Glu, Gln, Pro, Thr, Ser, Tyr, and Met. With cysteine (Cys) and reduced glutathione the color changed immediately upon mixing, as expected. With histidine (His), the color change developed over an hour.

[Pt(trpy)His](BPh₄)₂·2H₂O A solution containing 15.5 mg (0.1 mmol) of free base L-histidine in 1.0 mL of water was added dropwise to a stirred solution containing 53.2 mg (0.1 mmol) of [Pt(trpy)Cl]Cl·2H₂O in 4.0 mL of water. The mixture, 20 mM in

each compound, was kept at 50^o C. Although the color changed from dark orange to pale yellow in less than an hour and the quotient of absorbances at 342 and 328 nm (A_{342}/A_{328}) became constant, heating was continued for one day. A concentrated aqueous solution containing 68.4 mg (0.2 mmol) of NaBPh₄ was added dropwise to the stirred reaction mixture. Upon cooling, the yellow precipitate was filtered off, washed with cold water, and dried overnight in air at room temperature. Yield: 82 mg or 65 %. percentages calculated for C₄₅H₅₉N₆O₂PtB₂·2H₂O and found: C, 65.87 (65.25); H, 5.13 (4.91); and N, 6.68 (6.53).

Complexes [Pt(trpy)L]Cl₂ Ligands imidazole (Im), N α -acetyl-L-histidine (AcHis), L-histidyl-L-histidine (His-His), L-histidyl-L-lysine (His-Lys), and glycyl-L-histidyl-glycine (Gly-His-Gly) were similarly treated with [Pt(trpy)Cl]Cl. After the reactions were completed and the quotient A_{342}/A_{328} became constant, the complexes in solution were characterized by UV-vis and ¹H NMR spectroscopy. The Job's plot showed that Gly-His-Gly and Pt(trpy)Cl⁺ react in the ratio of 1:1.

Unreactivity of Thioether and Disulfide Ligands Compound

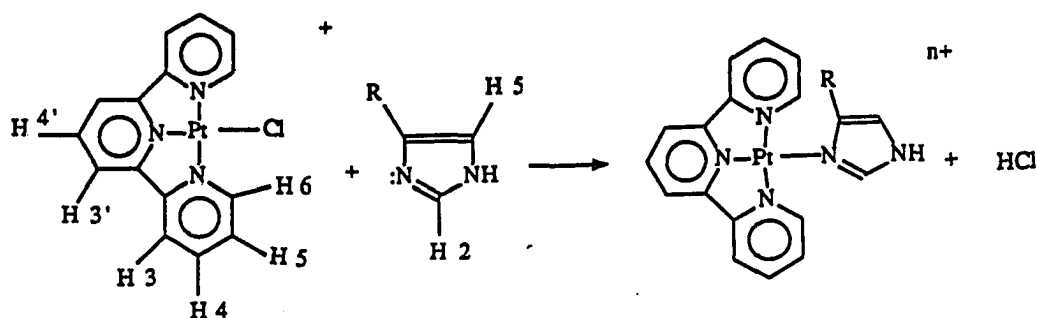
[Pt(trpy)Cl]Cl was treated with methionine, its derivatives, and a methionine containing peptide under various conditions. The following potential ligands were used: DL-methionine, N-acetyl-DL-methionine amide, l-methionine methyl ester hydrochloride, S-methyl-L-cysteine, tetrapeptide Trp-Met-Asp-Phe hydrochloride, cystine, and oxidized glutathione. First, [Pt(trpy)Cl]Cl was incubated with an equimolar amount of each ligand at the concentrations of 0.5, 1, 2, 5, 10, or 20 mM and the mixtures were heated at 50, 60, 80, 90 or 100^o C for ten hours. Next were incubations with tenfold excess of N-acetylmethionine for several hours at 90^o C and with hundredfold excess of methionine at room temperature for 75 days. Finally, compound [Pt(trpy)Cl]Cl was treated with AgNO₃, AgCl removed, and an equivalent amount of the ligands added. None of the

experiments caused a significant change in the UV-vis and the ^1H NMR spectra of the starting complex and added ligands. Cation-exchange chromatography of the mixtures permitted virtually full (ca. 95 %) recovery of $[\text{Pt}(\text{trpy})\text{Cl}]\text{Cl}$.

RESULTS AND DISCUSSION

Complex Formation

Histidine and its Derivatives Imidazole, histidine, and their homologs displace the Cl^- ligand from $\text{Pt}(\text{trpy})\text{Cl}^+$ to yield complexes of the type $\text{Pt}(\text{trpy})\text{L}^{2+}$, as shown below.



Since all of the complexes exhibit virtually identical UV-vis and ^1H NMR spectra (see Tables III-1 and III-2), all of the ligands must be bonded through the imidazole ring. Since the pyrrole-type nitrogen atom is highly basic ($\text{pK}_a = 14.5$ in imidazole),⁹⁶ it remains protonated under the conditions used in the experiments. Evidently, the ligating atom is the pyridine-type nitrogen, whose pK_a value is 6.0-6.5 in histidine and its derivatives.⁹⁶ Since the complexes with N-acetylhistidine and with histidine have identical positions of the absorption bands, both of these ligands must be coordinated solely through the imidazole ring; this finding rules out chelation of histidine via the amino and imidazole groups.

As Table III-3 shows, all of the ^{195}Pt chemical shifts fall in the region characteristic of $\text{Pt}^{\text{II}}\text{N}_4$ complexes.⁹⁷ The signals appear about 70 ppm upfield from that of the starting chloro complex, as expected upon displacement of the Cl^- ligand by nitrogen donors.^{12,13}

Table III-1. Extinction Coefficients of UV-visible bands of Pt(trpy)Lⁿ⁺ Complexes

L	n	$\epsilon, \text{ }^a \text{ M}^{-1} \text{ cm}^{-1}$				$\epsilon_{342}/\epsilon_{328}$
		342	328	270	242	
Cl ⁻	1	13 300		24 300	27 800	
Im	2	16 000	10 400	21 200	31 800	1.54
His	2	14 600	9 400	19 600	28 700	1.53
AcHis	1	15 800	11 500	23 100	33 500	1.37
His-Lys ^b	3	13 900	8 700	18 300	27 400	1.60
Gly-His-Gly	2	13 700	10 400	22 000	30 800	1.32

^aFor 10 μM solutions in water; the wavelengths are in nm.

^bThe uncoordinated side chain is assumed to be protonated.

Table III-2. ^1H NMR Chemical Shifts of $\text{Pt}(\text{trpy})\text{L}^{n+}$ Complexes and of Free Imidazole Containing Ligands L

L	^1H NMR chemical shift in ppm ^a								
	Pt(trpy)		Im		aliphatic				
	H4,4'	H3,3'	H6	H5	H2	H5	H7	H8	H9
Cl ⁻	8.08 m,3H	7.88 d,4H	7.82 m,2H	7.37 m,2H					
Im	8.33 m,3H	7.85 m,4H	8.45 m,2H	7.67 m,2H	8.50 s,1H	7.58 s,1H			
AcHis	8.32 m,3H	7.82 m,4H	8.45 m,2H	7.66 m,2H	8.50 s,1H	7.58 s,1H	4.55 T,1H	3.18 D,2H	1.96 S,3H
Free Ligand									
Im					7.73 s,1H	7.09 s,1H			
AcHis					8.52 s,1H	7.55 s,1H	4.40 t,1H	3.00 D,2H	1.94 S,3H

^aFor solutions in D₂O at 22 °C. Atoms are numbered as in the text. The chemical shifts are with respect to the residual water as an internal reference (4.79 ppm vs. DSS as a standard).

Table III-3. ^{195}Pt NMR Chemical Shifts of $\text{Pt}(\text{trpy})\text{L}^{\text{n}+}$ Complexes

L	n	δ^{a}, ppm
Cl⁻	1	-1080
Im	2	-1150
His	2	-1146

^aFor 15-30 mM solutions in 25 % D₂O, 75 % H₂O, with respect to K₂PtCl₄, as an external standard.

The ^1H NMR signals were assigned on the basis of NMR titrations of $\text{Pt}(\text{trpy})\text{Cl}^+$ with the ligands and of pH titrations of formed complexes. These assignments agree with previous analyses of $\text{Pt}(\text{trpy})\text{L}^{n+}$ complexes⁹¹ and of the free amino acids and peptides.⁹⁸⁻¹⁰⁰ In each case, coordination is accompanied by a large movement downfield of the H6 signal and by slight movements, in the same direction of the other trpy signals. Changes of similar magnitude, observed in $\text{Pt}(\text{trpy})\text{SR}^+$ complexes, were attributed to the magnetic anisotropy of the Pt-S bond⁹¹ and it is possible that a similar effect may operate when the new Pt-N bond is formed. The pronounced movement downfield of the imidazole signals is a consequence of the electron-attracting power of the platinum(II) complex.^{101,102} Because of their distance from the donor atom, the aliphatic H atoms in the main chain are not affected significantly by coordination.

The electronic absorption spectra of the $\text{Pt}(\text{trpy})\text{L}^{2+}$ complexes, presented in Table III-1 are particularly interesting. The ultraviolet bands at 242 and 270 nm correspond to transitions in the aromatic trpy ligand. The bands at 328 and 342 nm can be attributed to metal-to-ligand charge-transfer transitions on account of their intensity, dependence on the fourth ligand, and sensitivity to the exogenous species in solution.⁸⁰ All the measurements were made with 10 μM samples, a concentration at which Beer's law applies rigorously. Although all the complexes contain imidazole as the fourth ligand, their $\epsilon_{342}/\epsilon_{328}$ quotients differ. The main chain, attached to the imidazole ring, evidently affects the chromophore: directly, by approaching it, or indirectly, by altering the solvation of the complex. Although it would be difficult to explain this small effect, the relative band intensities did prove useful as diagnostic features of the labels differently located on the protein, as will be discussed below.

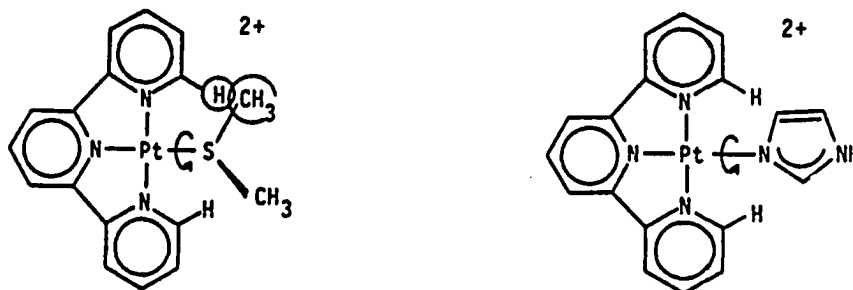
Unreactivity of Thioethers Six thioether and two disulfide compounds failed to displace the Cl^- ligand from $\text{Pt}(\text{trpy})\text{Cl}^+$ even under forcing conditions. Their

unreactivity is surprising in view of the affinity of the soft, nucleophilic thioether ligands toward the soft, electrophilic Pt(II) atom,¹⁰³⁻¹⁰⁵ especially since the trpy ligand is known to facilitate the displacement of the fourth ligand; for example, Pt(trpy)Cl⁺ is approximately 10³-10⁴ times more reactive than its aliphatic homolog, Pt(dien)Cl⁺, with respect to the Cl⁻ displacement by several small nucleophiles.¹⁰⁶

Whereas the thioethers methionine, S-methyl cysteine, and oxidized glutathione are unreactive, their thiol counterparts, homocysteine, cysteine, and reduced glutathione displace the Cl⁻ ligand from Pt(trpy)Cl⁺ fast.³⁷ The thiols react rapidly even in the neutral and weakly acidic solutions, in which the SH group (pK_a = 8.3) is protonated. Although the anionic thiolate is more nucleophilic than the neutral thioether or disulfide, the contrast between the facile reactivity and the complete inertness cannot be ascribed solely to the difference in nucleophilicity. The unreactivity of the biological thioethers and disulfides must be attributed to the bulkiness of their respective RSCH₃ and RSSR functional groups.¹⁰⁷ Although the square-planar complexes of Pt(II) are uncongested, the rate of substitution can depend markedly on the size of the entering ligand. Indeed, evidence for steric effects on the rate of such reactions has begun to appear.^{107,108} The quantum-mechanical study supporting this claim is presented next.

Electronic Structure and Bonding Molecular orbital calculations of Pt(trpy)SMe₂²⁺ were performed with the Pt-S torsion angle of 0, 22.5, 45, 67.5, and 90°. The orbital interactions in each case allow for a total overlap population of 0.44 to 0.47 e⁻ between the Pt and S atoms, a value corresponding to a normal metal-ligand bond. Regardless of the torsion angle, however, there exist prohibitively short contacts between a CH₃ group of the thioether ligand and an ortho CH group of the pyridine ring cis to this ligand as shown below. These contacts, far shorter than the sums of the van der Waals radii of C and H atoms, bring about considerable repulsions between the filled

C-H orbitals. These interactions between the closed electron shells, a quantum-mechanical equivalent of steric crowding of the ligands, outweigh the Pt-S attraction and cause net repulsion between $\text{Pt}(\text{trpy})^{2+}$ and the thioether.



Complex $\text{Pt}(\text{trpy})\text{Im}^{2+}$ exhibits some repulsive interactions when the imidazole and trpy ligands are coplanar, but this crowding is relieved already at the Pt-N torsion angle of 22.5° . Net attraction seems to exist between the $\text{Pt}(\text{trpy})^{2+}$ and Im fragments in all conformations, even in the planar one.

Similar molecular orbital calculations of $\text{PtCl}_3(\text{SMe}_2)^-$ and PtCl_3Im^- , complexes reveal an absence of steric interactions because the Cl^- ligands are sufficiently small that the H atoms in the thioether and imidazole ligands never approach their cis neighbors too closely. The difference between trpy and Cl^- will be invoked below to explain how ancillary ligands may alter the selectivity of transition metal complexes toward numerous potential binding sites in proteins.

Binding Sites on the Cytochromes

Absorption Spectra Of all the amino acids that contain heteroatoms in their side chain, only cysteine and histidine proved reactive toward $\text{Pt}(\text{trpy})\text{Cl}^+$ under the

conditions of protein labeling. Since cytochromes c from horse and tuna lack free cysteine, the most likely binding sites in these proteins are imidazole rings.

The electronic absorption spectra of the native (N), major singly-modified (S_A), and doubly-modified (D) cytochromes from horse are shown in Figure III-1. The characteristic absorption bands of the $Pt(trpy)Im^{2+}$ chromophore at 328 and 342 nm are clearly evident. In this region, fortunately, the absorbance of the protein itself is low. Comparison between the difference spectra in Figure III-2a with the spectrum in Figure III-2b of an equimolar solution of $Pt(trpy)(Gly-His-Gly)^{2+}$ confirms that both sites A and B are histidine residues. The spectrum in Figure III-2c shows how markedly the fourth ligand affects the $Pt(trpy)^{2+}$ chromophore. The spectra confirm, moreover, that the S and D derivatives contain one and two labels per protein molecule, respectively. The difference D-N is exactly the sum of the differences S_A-N and S_B-N , i.e., the two labels in the doubly-modified derivative are the same two that are found in the singly-modified derivatives. The chromophores at histidine residues designated A and B exhibit the same band positions, characteristic of the imidazole ligand, but different intensities: the $\epsilon_{342}/\epsilon_{328}$ quotient is 1.58 and 1.15 in S_A and in S_B , respectively. This dependence of the band intensities on the details of the ligand structure, already evident among the model $Pt(trpy)L^{2+}$ complexes (Table III-1), may render the $Pt(trpy)^{2+}$ tag applicable as a probe of its environment in biomolecules.

The horse protein contains histidine in positions 18, 26, and 33. The axial ligand to the heme, His 18, can be ruled out as a binding site. The ferriheme absorption bands at 410 and 530 nm^{87,88} are unperturbed by the protein labeling. The band at 695 nm depends in part on the interactions between the Fe atom and the axial ligands (Met 80 and His 18)¹⁰⁹⁻¹¹¹ is retained in all of the modified proteins. The reduction potential, EPR g-values, and hyperfine ¹H NMR shifts all retain their native values.

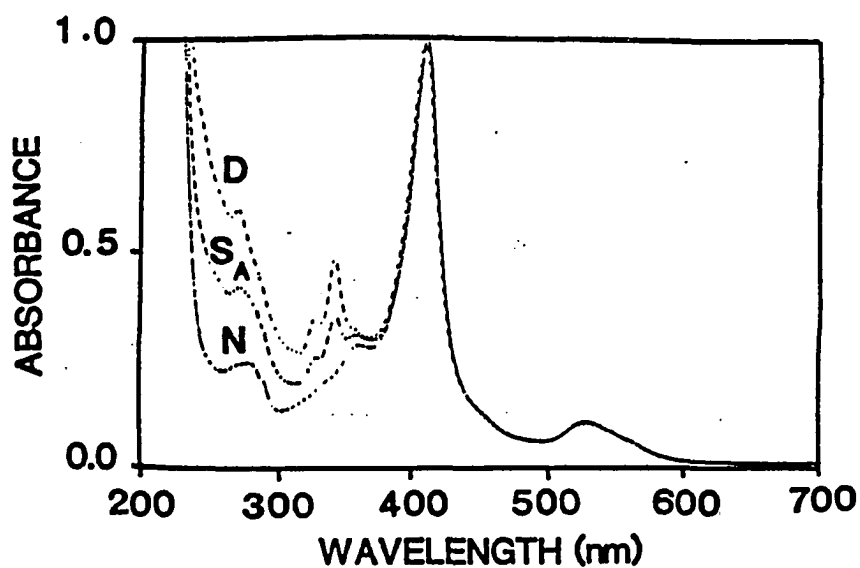
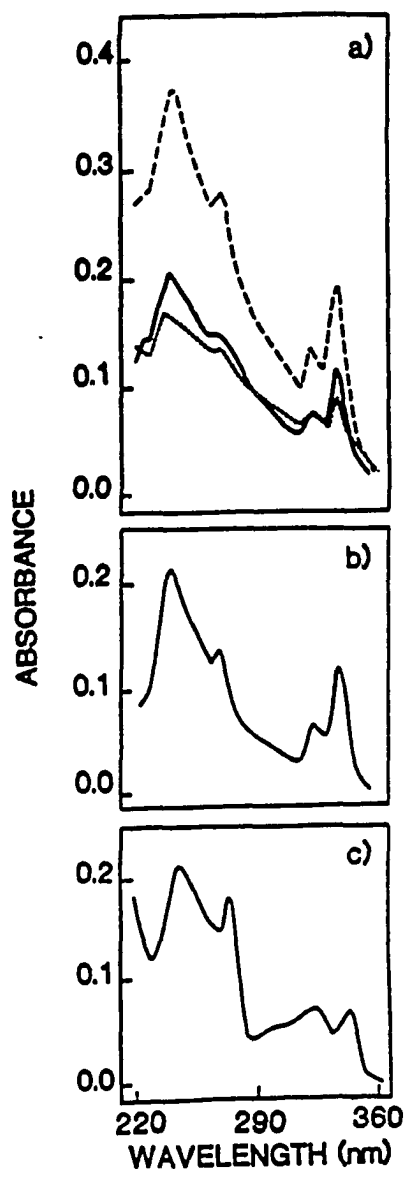


Figure III-1. Absorption Spectra of the Native (N) Horse-heart Cytochrome c and of its Derivatives Designated S_A and D. The former is singly-labeled with a Pt(trpy)²⁺ chromophore at the site marked A (His 33), whereas the latter is doubly-labeled at sites marked A (His 33) and B (His 26)

Figure III-2. Difference Absorption Spectra of Pt(trpy)²⁺-Labeled Cytochromes c and Absorption Spectra of Pt(trpy)Lⁿ⁺ Complexes. (a) Difference absorption spectra obtained by subtraction of the spectrum of the native (N) horse-heart cytochrome c from the spectra of the respective protein derivatives designated S_A (—), S_B (…), and D (---), which are tagged with Pt(trpy)²⁺ chromophore: singly at His 33, singly at His 26, and doubly at both His 33 and His 26, respectively. (b) Absorption spectrum of Pt(trpy)(Gly-His-Gly)²⁺, a complex wherein the tripeptide is coordinated to platinum through the imidazole ring in the side chain. (c) Absorption spectrum of Pt(trpy)Cl⁺. All the spectra were obtained with 10 μM solutions of the respective proteins and Pt(trpy)Lⁿ⁺ complexes in 85 mM phosphate buffer of pH 7.0



Both residues His 33 and His 26 are located on the protein surface, but in different environments.¹¹²⁻¹¹⁵ The former lies in a hydrophilic region and is exposed to the exterior, whereas the latter is hydrogen-bonded, located in a hydrophobic pocket,¹¹⁶ and unreactive.¹¹⁶⁻¹²¹ Since these two sites evidently differ from each other in accessibility to external reagents, the major one (A) can tentatively be identified as His 33 and the minor one (B), as His 26. The difference between the $\epsilon_{342}/\epsilon_{328}$ quotients for the respective $\text{Pt}(\text{trpy})^{2+}$ chromophores probably reflects the difference between the environments of the sites.

This assignment is confirmed by the experiments with tuna cytochrome c, which has His 26 but lacks His 33 and has tryptophan, an amino acid unreactive toward $\text{Pt}(\text{trpy})\text{Cl}^+$, in its place. Since the tuna protein does not yield the major derivative, corresponding to S_A , the site A in the horse protein clearly is His 33. The minor derivative, which is obtained, closely resembles the S_B derivative of the horse protein by the $\epsilon_{342}/\epsilon_{328}$ quotient and by its elution behavior on the CM 52 column. The site B in both cytochromes must then be His 26.

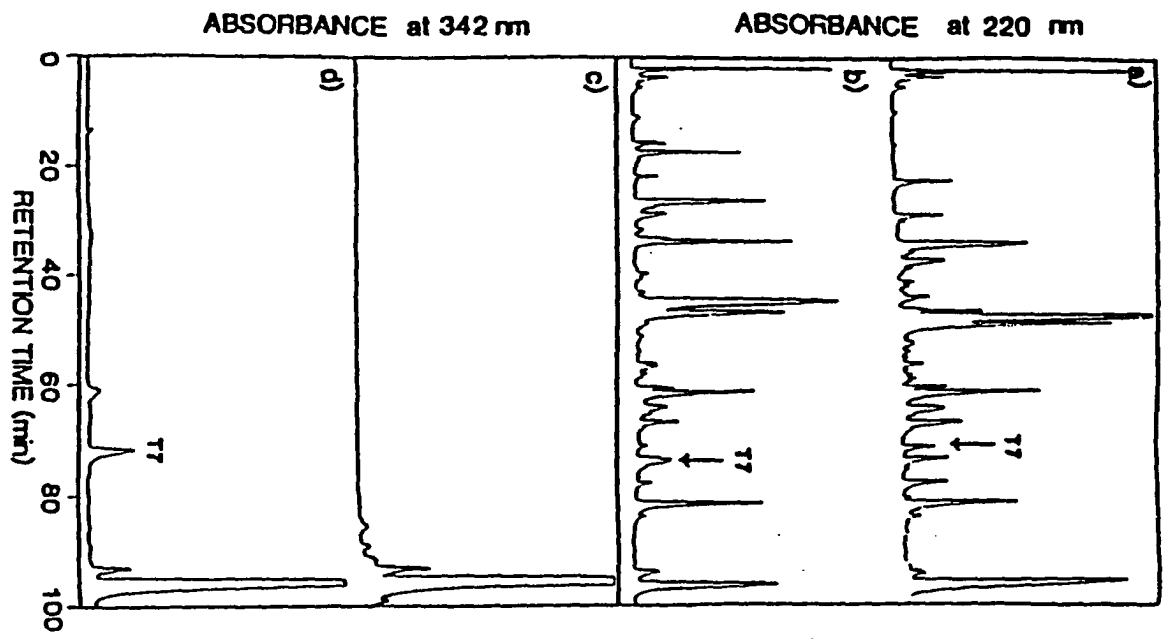
Elution Behavior The order of elution of the native and modified proteins from the cation exchanger confirms the assignment of the binding sites. As the number of the cationic $\text{Pt}(\text{trpy})^{2+}$ tags increases from none (in N) to one (in S_A and S_B) to two (in D), the protein becomes more retained. Although the S_A and S_B derivatives have the same overall charge, they separate completely on a short column because different locations of the cationic tag cause different charge distributions^{79,122} in the two derivatives. The

positive patches on the protein surface known to interact with the CM 52 resin^{79,122,123} are remote from His 33 whereas one lies close to His 26. This is why the derivative S_B , labeled at His 26, is retained more than S_A , labeled at His 33.

Peptide Mapping Although the labels are otherwise stable in acid, neutral, and weakly basic solutions, they undergo partial dissociation in the course of tryptic digestion. To simplify the comparison between the chromatograms of the digests from the native and modified proteins, the histidine containing dipeptide His-Lys and undecapeptide Ala-Pro-Gly-Asp-Arg-Ile-Tyr-Val-His-Pro-Phe and the corresponding $Pt(trpy)(peptide)^{2+}$ were also chromatographed under the conditions used for the protein digests. The dipeptide is identical to the tryptic fragment T6 of the horse cytochrome c, which contains His 26.⁸⁷ The undecapeptide is similar by composition and by the degree of hydrophobicity to the tryptic fragment T7 of the protein, Thr-Gly-Pro-Asn-Leu-His-Gly-Leu-Phe-Gly-Arg, which contains His 33.⁸⁷

The undecapeptide T7, which contains His 33, is eluted after 70 min from the native digest (see Figure III-3a). A small retardation, to 75 min, of the corresponding peptide from the digest of the derivative S_A (see Figures III-3a, III-3b, and III-3d) can be attributed to the presence of a platinum label. This explanation has been confirmed by demonstrating that the model undecapeptide becomes similarly retarded upon labeling. The difference is small (several minutes) because only one out of eleven residues is modified. The absorption spectrum shows that the peptide T7 from the major derivative

Figure III-3. HPL Chromatograms of Tryptic Digests. Reversed-phase chromatograms of tryptic digests of the following: (a) and (c), the native horse-heart cytochrome c; and (b) and (d), its derivative designated S_A , which is singly labeled with $Pt(trpy)^{2+}$ at His 33. Note the wavelengths at which the absorbances are recorded



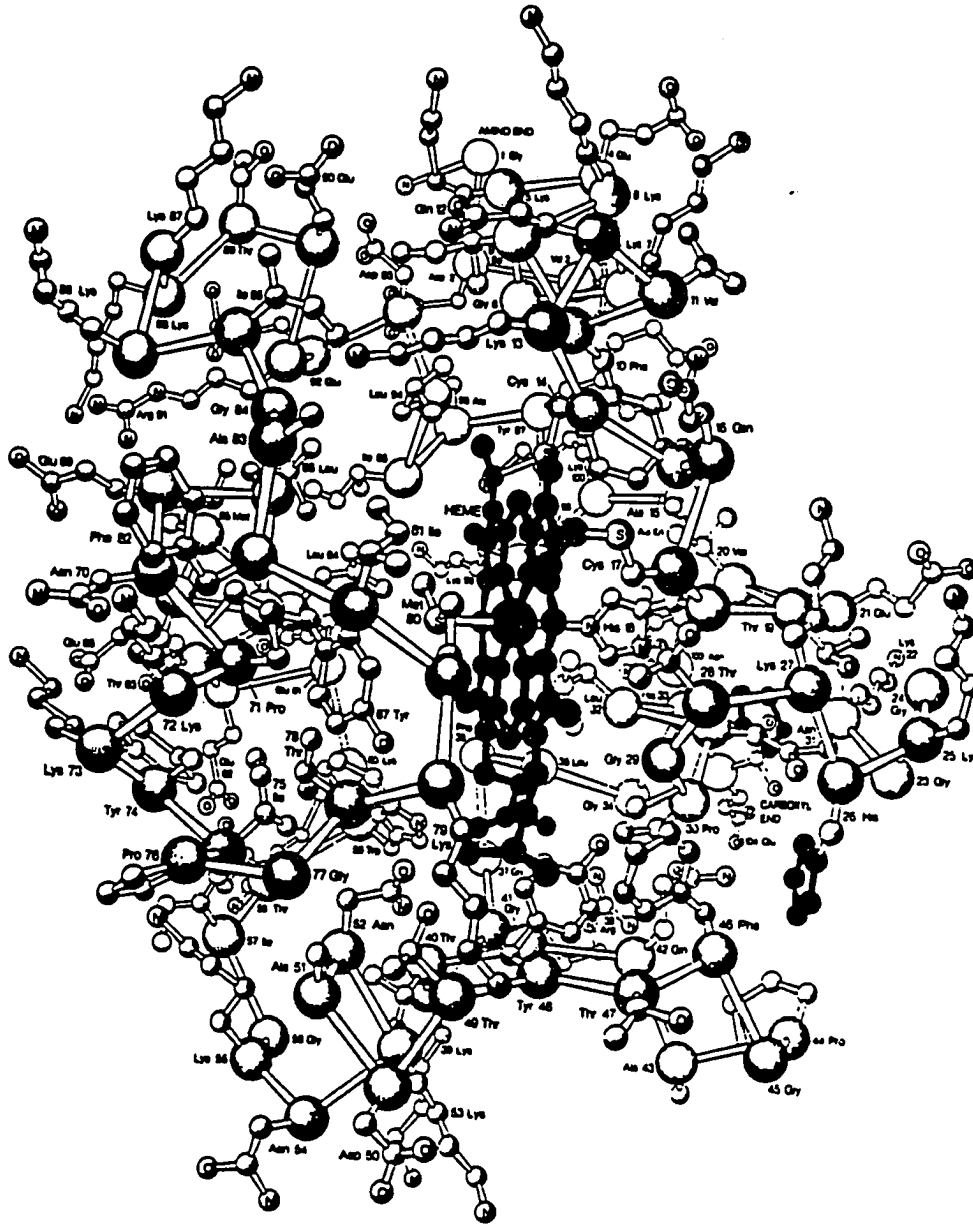
S_A , indeed contains a $Pt(trpy)His^{2+}$ chromophore. Clearly, His 33 is the major binding site in the horse cytochrome c.

The dipeptide T6 is eluted at 2 min from the native digest, but at 18 min from the digest of the minor derivative, S_B . The small peak at 18 min (a doublet) in the chromatograms of S_A (see Figures III-3b and III-3d) is due to the partial dissociation of the label from the major site and its subsequent attachment to the minor site during digestion. A similar large retardation occurs between the authentic dipeptide His-Lys, which elutes at 2.3 min, and its labeled derivative, which gives rise to a close doublet of peaks at 18.3 and 20.5 min. The general agreement between the retention times confirms His 26 as the minor binding site in the cytochrome c. The two binding sites are shown in Figure III-4.

Selectivity in Binding Compound $Pt(trpy)Cl^+$ reacts with proteins under mild conditions – in equimolar ratio at room temperature. Its specificity (at pH 5) toward histidine was confirmed by thorough studies of model reactions with amino acids, their derivatives, and peptides. Even with tenfold molar excess of the reagent at pH 5, the same protein derivatives are produced in somewhat higher yields. No new sites are however, modified.

Substitution reactivity of $Pt(trpy)Cl^+$ is opposite from that of another platinum(II) chloro complex, the common $PtCl_4^{2-}$. Whereas the latter is highly reactive toward methionine and barely so toward histidine,^{11,14,124} the former proved totally unreactive toward methionine and very reactive toward histidine.

Figure III-4. Horse-heart Cytochrome c Structure. In this picture, based on ref 112, the heme plane is viewed obliquely from the left side, that of Met 80 axial ligand to iron. Both positions 26 and 33 are occupied by histidine residues, their respective imidazole chains are shown in black: that of His 26 to the right and that of His 33 in the back right



The interesting and unusual selectivity of $\text{Pt}(\text{trpy})\text{Cl}^+$ can be attributed to the properties of the trpy ligand. By its steric demands, it prevents reactions with the thioether ligand, which is otherwise highly nucleophilic toward platinum(II) complexes. By its electronic properties, at the same time, the trpy ligand facilitates the displacement of Cl^- by imidazole which is otherwise comparatively unreactive toward these complexes. The specificity of a transition-metal reagent toward a multifunctional biomolecule evidently can be controlled by the judicious choice of the ancillary ligands.

Structural and Redox Characterization

The platinated derivatives of the horse cytochrome c were compared with one another and with the native protein by various physical methods in order to determine whether labeling with the novel reagent alters the protein structure or its redox activity. The absorption spectra indicate that the electronic structure of the heme is not noticeably perturbed.

Reduction Potentials The results of differential-pulse voltammetry, listed in Table III-4, demonstrate that modification has no detectable effect on the redox ability of the horse cytochrome c. Cyclic voltammetry showed the redox process to be quasi-reversible with peak separations of 75 mV. The peak current in each case increased linearly with the square root of the scan rate, an indication of a diffusion-controlled one-electron process.⁸⁹

Table III-4. Reduction Potentials of Horse-heart Cytochrome and of its Derivatives Labeled with Pt(trpy)²⁺

Proteins	E⁰, in mV vs. NHE^a
Native	256 ± 3
Labeled at	
His 33	255 ± 7
His 26	245 ± 6
His 33 and His 26	247 ± 6

^aDifferential-pulse and cyclic voltammetry at 0.1-0.4 mM solutions of the respective proteins, also 10 mM in 4,4'-dipyridyl and 100 mM in NaClO₄, in 85 mM phosphate buffer at pH 7.0 and 25 °C.

Concerned over the possibility that the platinum labels might be displaced from the proteins by 4,4'-dipyridyl, the mediator, the samples were dialyzed after electrochemical measurements and the UV-vis spectra proved that the tags remained intact on the proteins.

EPR Spectroscopy The EPR g-values of all the derivatives presented in Table III-5 agree with the literature value for the native cytochrome c from horse.^{125,126,127} These clearly rule out His 18, an axial ligand to Fe, as a binding site. Even in the derivative D, which is doubly modified at His 33 and His 26, the coordination sphere of the Fe atom evidently remains unperturbed by the Pt(trpy)²⁺ labels.

¹H NMR Spectroscopy The proton NMR spectrum of the paramagnetic ferriheme in cytochromes and myoglobins depend markedly on the interactions between the iron atom and its axial ligands and between the heme periphery and the side chains of neighboring amino-acid residues.¹²⁸⁻¹³⁷ Particularly sensitive to these interactions are the hyperfine ¹H shifts.⁸⁸ As Table III-6 shows, labeling causes virtually no perturbation.

Only the shifts of the CH₃ group in the pyrrole ring II and of the β-CH₂ group in the propionate chain attached to the ring IV are altered by more than ± 0.25 ppm.¹³² The ring II is connected with the protein by a thioether linkage involving Cys 17; attachment of a Pt(trpy)²⁺ label to His 33 perhaps causes a slight movement in the polypeptide backbone,

Table III-5. EPR g Values of Horse-heart Cytochrome C and of its Derivatives

Protein^a	g_x	g_y	g_z
Native	1.3	2.24	3.00
Labeled at			
His 33	1.3	2.22	3.04
His 26	1.2	2.27	3.03
His 33 and 26	1.3	2.27	3.00

^aMeasured with 0.1-1.0 mM solutions of the respective proteins in 85 mM phosphate buffer of pH 7.0 and 6 K.

Table III-6. Hyperfine-Shifted ^1H NMR Signals of Horse-heart Cytochrome c and of its Derivative Labeled with $\text{Pt}(\text{trpy})^{2+}$ at His 33

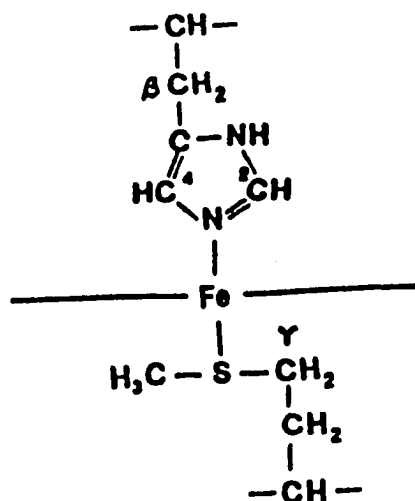
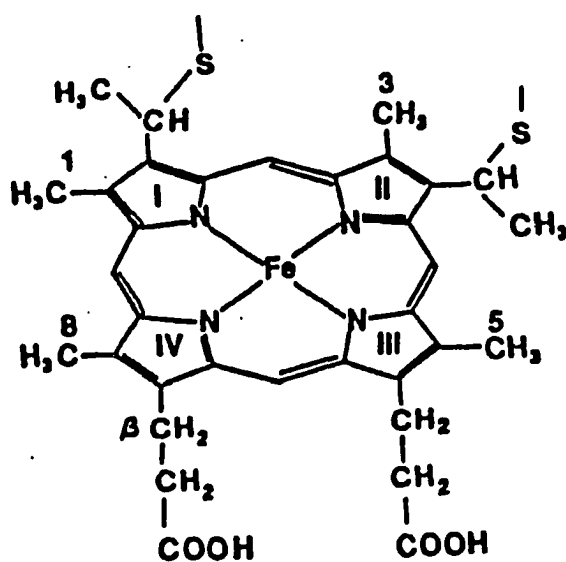


Table III-6 (Continued)

<u>chemical shift,^a ppm</u>			<u>perturbation,^b</u>	
native	labeled	assignment	ppm	references
35.73	35.73	CH ₃ (8)	0	131,134-137
32.69	33.03	CH ₃ (3)	+0.34	131,134-137
24.2	24.2	S-CH-CH ₃ in II; or CH (2) and CH (4) of His 18	0	134,135
19.22	18.71	βCH ₂ of propionate in IV	-0.51	134-137
14.64	14.46	βCH ₂ of His 18	-0.18	135
12.81	12.81	unassigned	0	135
11.47	11.71	βCH ₂ of propionate in IV	+0.24	135
9.89	9.89	CH ₃ (5)	0	134-137
6.81	6.81	CH ₃ (1)	0	134-137

^aMeasured with 2- to 4- mM solutions of the respective proteins in 85 mM phosphate buffer of pH 7.0 and 21 °C, shifts are reported with respect to DSS as an internal standard. For accuracy in control experiments, the labeled protein, S_A, was spiked with the native protein.

^bDefined as $\delta_{\text{labeled}} - \delta_{\text{native}}$.

Table III-6 (Continued)

<u>chemical shift,^a ppm</u>		assignment	<u>perturbn,^b</u>	
native	labeled		ppm	references
-2.53	-2.53	S-CH-CH ₃ in II	0	134-137
-2.82	-2.82	S-CH-CH ₃ in I	0	134-137
-4.48	-4.48	meso CH of heme	0	137
-6.39	-6.39	meso CH of heme	0	137
-24.70	-24.70	CH ₃ of Met 80	0	131,136
-28.1	-28.1	γCH ₂ of Met 80	0	137

which is transmitted to the heme and perhaps causes a slight tilt in the pyrrole ring II. This hypothesis of the correlated motions of heme and the backbone finds support in the previous crystallographic comparisons between the ferro- and ferricytochrome c.^{138,139} These studies revealed that the change in the oxidation state is accompanied by the movement of the heme and also of the polypeptide chain between residues 17 (the Cys link) and 33 (the labeled His in the horse protein), exactly the segment implicated in our hypothesis.¹³⁸

The slight perturbation of the β -CH₂ group might be attributed to the direct electrostatic attraction between the propionate anion and the Pt(trpy)²⁺ label. An indirect interaction, too, is conceivable: labeling of His 33 perhaps causes a slight movement of the proximate Tyr 48, which is hydrogen-bonded to the propionate chain of the ring IV.

CONCLUSIONS AND PROSPECTS

The complex $\text{Pt}(\text{trpy})\text{Cl}^+$ is well-suited for tagging biological macromolecules on account of its reactivity, selectivity, stability, and spectroscopic properties. Owing to an interplay between the steric and electronic effects of the ancillary trpy ligand, the selectivity of $\text{Pt}(\text{trpy})\text{Cl}^+$ is entirely opposite from that of PtCl_4^{2-} . This example shows that unusual selectivity of transition-metal complexes toward biological ligands can be achieved by a judicious choice of ancillary ligands.

Stability of the $\text{Pt}(\text{trpy})^{2+}$ tags permits storage, dialysis, cation-exchange chromatography of the modified proteins. The tags can be removed, however, and the native protein restored easily by treatment with highly nucleophilic ligands such as CN^- , SCN^- , and I^- . This combination of stability under ordinary conditions and easy removability under conditions harmless to the protein renders the Pt reagent particularly useful.

Perhaps the greatest advantage of the new reagent lies in the strong absorption bands of the $\text{Pt}(\text{trpy})\text{L}^{n+}$ chromophore, characterized by the extinction coefficients of $13,000\text{-}30,000 \text{ M}^{-1}\text{cm}^{-1}$, which permit easy detection and quantitation. The charge-transfer bands in the region of 320-350 nm, unobscured by protein absorption, are sensitive not only to the nature of the binding site (i.e., the identity of ligand L), but also to the environment in which the site is found.

This reagent can also serve to probe the accessibility of histidine on the surface of a protein. The yields of the separable modified proteins are easy to quantitate and these agree with the accessibility of the histidines, as was shown in this work with cytochrome c. Lastly, the labels are noninvasive, they do not perturb the conformation and redox ability of cytochrome c.

SECTION IV.

**GUANIDYL GROUPS: NEW METAL-BINDING LIGANDS IN BIOMOLECULES.
REACTIONS OF $PT(TRPY)CL^+$ WITH ARGININE IN CYTOCHROMES AND
WITH OTHER GUANIDYL LIGANDS**

INTRODUCTION

The recognized functions of arginine (Arg) residues in proteins – binding of cofactors and anions – involve electrostatic attraction to the guanidinium cation.^{140,141} Although transition metals are common in metalloproteins and in metal-activated enzymes, their covalent binding to Arg side chain has not been proposed. Indeed, metal-guanidyl complexes are barely known.¹⁴²

The precedent reported here shows that Arg can bind metals, and that inorganic complexes hold promise as heavy-atom and spectroscopic tags for Arg.^{143,144}

This work resulted from the attempts to study the effect of increasing pH on the yields of histidine-modified cytochromes on incubation with $\text{Pt}(\text{trpy})\text{Cl}^+$. As discussed in Section III, $\text{Pt}(\text{trpy})\text{Cl}^+$ reacts readily and noninvasively with His residues at pH 5.0. The yield of $\text{Pt}(\text{trpy})\text{His}^{2+}$ depends on the accessibility and the pK value of the imidazole. The tag is stable, and its strong UV-vis bands are characteristic of His and its environment.

EXPERIMENTAL SECTION

Chemicals

The proteins were obtained from Sigma Chemical Co. Tuna-heart cytochrome c of type XI was used as received. Horse-heart cytochrome c (of types VI and III) was oxidized with $K_3Fe(CN)_6$ and then purified by cation-exchange chromatography on CM 52 cellulose. Chloro(2,2':6',2'-terpyridine)platinum (II) dihydrate, $[Pt(trpy)Cl]Cl \cdot 2H_2O$, was purchased from Strem Chemicals. Compound $[Co(phen)_3](ClO_4)_3$ was prepared according to the published procedure. The CM 52 resin was obtained from Whatman or Sigma. Other chemicals were used as received from Aldrich Chemical Co.

Methods

UV-visible spectra were obtained using an IBM 9430 spectrophotometer with a double-grating. 1H NMR spectra were obtained with a Bruker WM 300 or a Nicolet NT 300 instrument using deuteriated solutions and residual water, or acetone as internal standards. A Fisher Accumet pH meter was used for pH measurements.

Protein Modification

Ferricytochrome c was incubated with an equimolar amount of $[Pt(trpy)Cl]Cl$ at room temperature in 85 mM potassium phosphate buffer at pH 7.0 for 24 hours. The concentration of each was 2 mM. Procedures involving 5.0 or 25 mg of the protein and

0.20 or 1.0 mg of the platinum complex, were normally used. The incubation was terminated by ultrafiltration of the reaction mixture in the same buffer. The components of the reaction mixture were separated on a CM 52 column, previously equilibrated with the same phosphate buffer. About 1 mg of cytochrome was applied per 1 mL of resin. The modification of the horse cytochrome yielded the following in their elution order: native (N), minor singly-labeled (S_C), major singly-labeled (S_A), minor singly-labeled (S_B), doubly-labeled (D_1), doubly-labeled (D_2), and triply-labeled (T). The first four fractions were eluted with 85 mM phosphate buffer, fractions designated D_1 and D_2 required gradients to 125 mM buffer, but the last fraction required a gradient with excess salt. Incubation with tuna protein gave the following derivatives in their elution order: native (N), very minor singly-tagged (S_C), minor singly-tagged (S_B), and doubly-tagged (D).

Reactions with Potential Ligands

Amino acids Arg, Gly, Lys, Trp, Asp, Asn, Glu, Gln, Pro, Thr, Ser, Tyr, and Met were incubated with $[Pt(trpy)Cl]Cl$ under the general conditions of protein modification for a long time (ca. 2 months), only the solution with Arg gave a distinct color change, from yellow to red. With heating the solutions containing Arg gave the same color change in which standing for a long period of time did. Heating of the solutions containing Gly, Lys, and Tyr did not effect any change in their color as well as in their UV-visible spectra.

Reactions with Guanidyl-Containing Ligands

Guanidine (Gua), methylguanidine (MeGua), canavanine (Can), arginine (Arg), and N-acetyl arginine (AceArg) when incubated with an equivalent amount of $[\text{Pt}(\text{trpy})\text{Cl}]\text{Cl}$ in 85 mM phosphate buffer of pH 7.0 produced new complexes after heating at 80° C. Ion exchange chromatography of the heated solutions gave a red band and a yellow band having distinct UV-visible spectra unlike that of unreacted $\text{Pt}(\text{trpy})\text{Cl}^+$. Only solutions with canavanine did not require any heating for any new complex formation in 5 d. Heating at 80° C for 4 d surprisingly gave 30 % red complex formation for a 2 $\text{Pt}(\text{trpy})\text{Cl}^+$:1 MeGua mixture in 100 mM acetate buffer of pH 5.0.

Mixtures containing different mole fractions of canavanine and of $[\text{Pt}(\text{trpy})\text{Cl}]\text{Cl}$ in 100 mM potassium phosphate buffer of pH 8.0 were prepared. After 30 min, solutions of N_{can} in the range 0.5 to 0.9 became lighter. After 41 hours, superimposition of the UV-visible spectra of 15 μM solutions of N_{can} in the range 0.5 to 0.9 was evident. This spectrophotometric titration thus shows the formation of the 1 $\text{Pt}(\text{trpy})^{2+}$: 1 Can complex or $\text{Pt}(\text{trpy})\text{CanH}^{2+}$.

RESULTS AND DISCUSSION

The Binding Site

The increase in incubation from pH 5.0 to 7.0 evidently yielded a new binding site. Figure IV-1 shows the spectrum of the new derivative, triply-tagged horse cytochrome (T) obtained. The difference UV-visible spectra of 10 μ M solutions of singly-tagged (S_C) - native horse protein and triply tagged (T) - doubly-tagged (D) horse proteins show similar spectra. However, these spectra clearly differ from that of imidazole complexes of $Pt(trpy)^{2+}$. Table IV-1 shows typical extinction coefficients of the new derivatized proteins.

The binding site was identified indirectly, but conclusively, by control experiments and structural considerations. Since both horse and tuna consistently produced new derivatives on changing the pH of incubation, the new binding site must be accessible in both horse and tuna cytochromes c, and there must be few such ligands (because only one reacts).

Table IV-2 shows the list of amino acid residues that are found on the surface of both horse and tuna proteins.^{112,113} From this list, only three residues – Tyr 74, Tyr 97, and Arg 91 – satisfy both requirements. Further tests, with heating, confirming the unreactivity of Tyr (as well as of Gly and Lys) and the reactivity of Arg suggest that Arg must be the new binding site.

Reactions of the guanidyl-containing ligands with heating and upon separation on a cation-exchange column yielded homologous complexes (shown in Figure IV-2). The yellow complex obtained has UV-visible properties (see Table IV-1 and Figure IV-3 and the previous section's Figure III-2) unlike those of unreacted $Pt(trpy)Cl^+$ and those of its

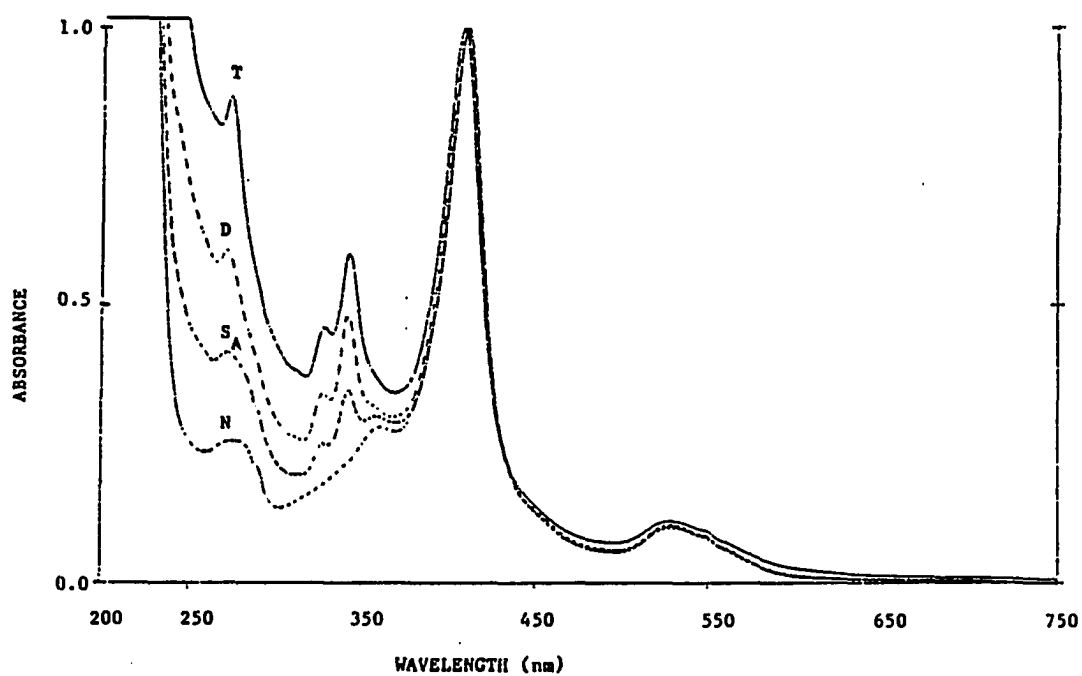


Figure IV-1. Absorption Spectra of Cytochrome c and of its $\text{Pt}(\text{trpy})^{2+}$ Derivatives. The derivatives designated S_A , D, and T are tagged with $\text{Pt}(\text{trpy})^{2+}$ chromophore: singly at His 33, doubly at His 33 and His 26, and triply at Arg 91, His 33, and His 26, respectively

Table IV-1. Extinction Coefficients of the New Pt(trpy)²⁺ Derivatives of Horse-heart Cytochrome c

Protein ^a	λ_{max} , nm	ϵ , M ⁻¹ cm ⁻¹
Singly-tagged-Native	345	10 000
(S _C -N)	327	11 000
	277	25 000
	249	30 000
Tripoly-tagged-Doubly tagged	346	12 000
(T-D)	330	12 000
	275	29 000
	244	29 000

^aIn 85 mM phosphate buffer of pH 7.0.

Table IV-2. Potential Ligands of Transition Metals that are Exposed on the Surface of Both Horse and Tuna Cytochromes

amino acid	number of residues
Glu ^a	> 3
Asp ^a	3
Gln ^b	2
Asn ^b	2
Tyr ^c	2
Met ^d	1
Lys ^a	> 3
His ^e	1
Arg ^f	1

^aNumber of residues preclude selective binding at only one site.

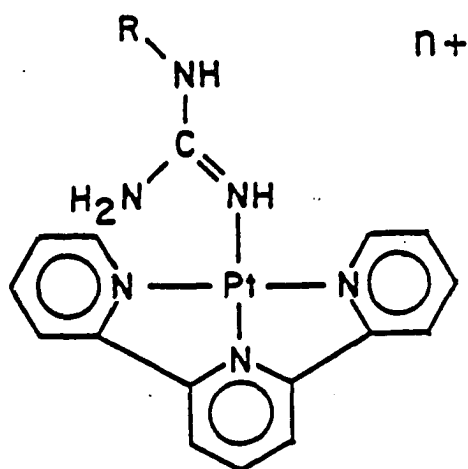
^bTreated as one common group, the total number precludes selective binding at only one site.

^cTyr 74 and Tyr 97 are potential ligands.

^dMet 65 has been precluded for Pt(trpy)Cl⁺, see Section III.

^eHis 26 is a minor binding site, see Section III.

^fArg 91 is a potential ligand.



Gua	R	Gua pK _a	Reactivity toward Pt(trpy)Cl ⁺
MeGua	CH ₃	13.5	pH 8, 80° or pH 10, R.T.
Arg	(CH ₂) ₃ CH(NH ₂)COO ⁻	12.5	pH 8, 80° or pH 10, R.T.
Can	O(CH ₂) ₂ CH(NH ₂)COO ⁻	7.0	pH 7, R.T.
Arg 91	cyt c	<12.5	pH 7, 5°

Figure IV-2. Reactivity of Guanidine Compounds with Pt(trpy)Cl⁺

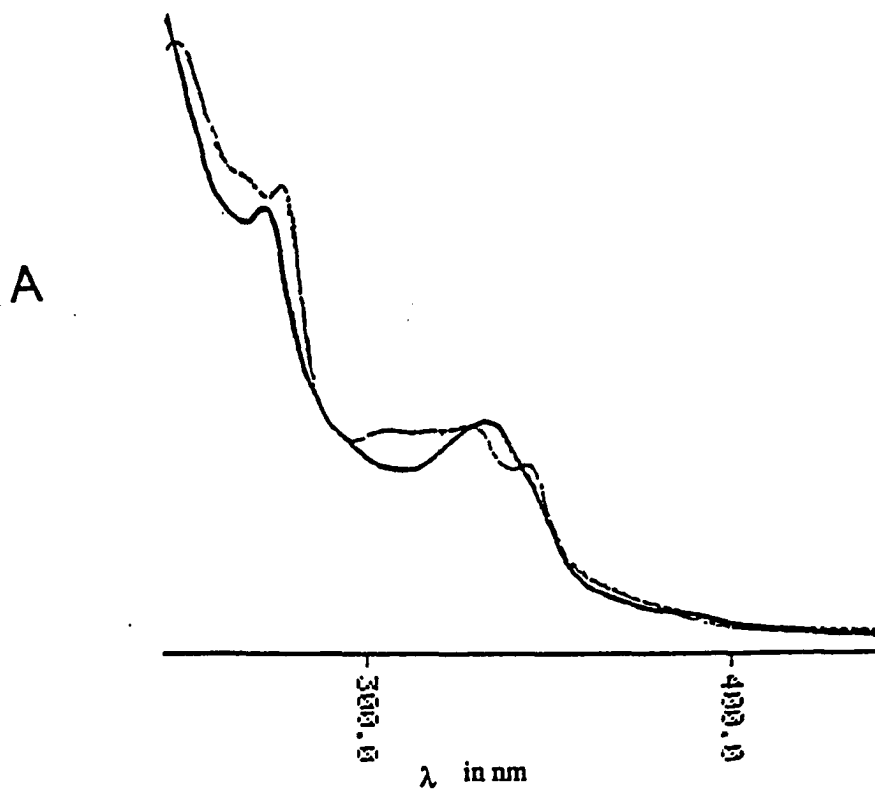


Figure IV-3. Absorption Spectra of $\text{Pt}(\text{trpy})\text{CanH}^{2+}$ (—) and $\text{Pt}(\text{trpy})\text{Cl}^+$ (---) in 100 mM Phosphate Buffer of pH 8.0

imidazole complexes.¹⁷ The similarity in the UV-vis properties of the yellow complexes (see Figure IV-3) obtained from the various guanidyl-containing ligands confirm their coordination to the same site, the guanidyl group. The presence of the guanidyl ligands was also proven by the thin-layer chromatography of the acid-cleaved complexes, for these gave identical ninhydrin reactions and R_f values with the corresponding free compounds.

The yellow complex could not be obtained by itself, its formation was always accompanied by the red complex formation. This new and interesting coordination chemistry of the guanidine compounds are thus further studied in the next Section.

Thus, the aforementioned new derivatives contain Pt(trpy)²⁺ tags at the following residues: at 91, at 33 and 91, and at 26, 33, and 91 in the horse protein; at 91, at 26 and 91 in the tuna protein.

Rationale for Arg 91 Reactivity

Why Arg 91 reacts at pH 7.0 despite the guanidine basicity becomes evident from the crystal structure.^{112,113} Barely exposed on the surface (hence its low labeling yield of 10 %), Arg 91 abuts the N-terminus of the α -helical segment 92-102 (see Figure IV-4). Both the helical macrodipole and the hydrophobic environment lower its pK_a value.¹⁴⁵⁻¹⁴⁹ Indeed, canavanine (Can) whose pK_a is 7.0¹⁵⁰ forms Pt(trpy)CanH²⁺ readily under the conditions of protein labeling.

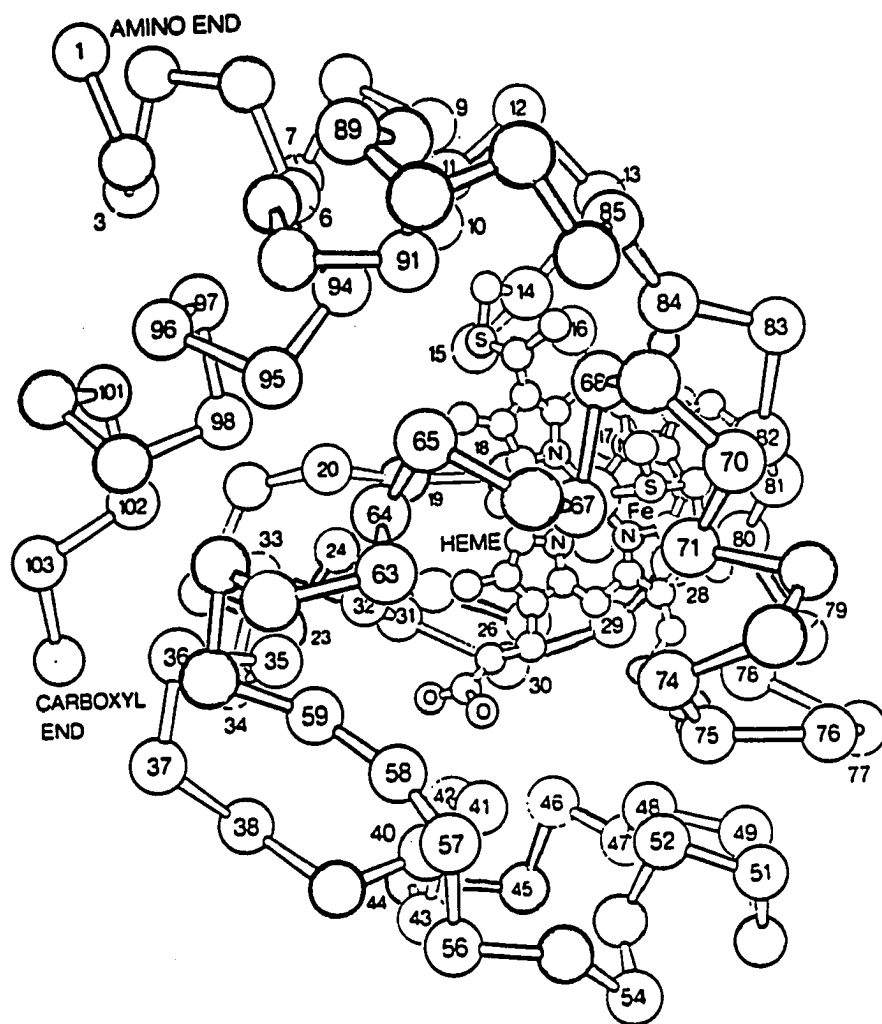


Figure IV-4. Alpha-helical Structure of Cytochrome c

Attempts at Direct Identification of Arg Binding Site in Cytochrome c

The standard procedures for peptide mapping of cytochrome c require handling and chromatography of the peptide mixture at pH < 3.0.^{87,88} Under these conditions, the Pt(trpy)²⁺ tag is displaced from the basic guanidine group by a proton. Such a displacement was observed with the horse cytochrome c derivatives that contain a Pt(trpy)²⁺ tag at Arg 91 and also with model guanidine complexes. This instability, which ruled out the use of peptide mapping in the identification of the labeled site, is discussed below.

If a selective, irreversible modification of Arg 91 in the protein precluded the subsequent formation of those Pt(trpy)²⁺ derivatives that form at pH 7.0 (but not at pH 5.0) when the native protein is treated with Pt(trpy)Cl⁺, a direct proof of Arg 91 as a binding site would be at hand. Unfortunately, the modification of Arg 91 with 2,3-butanedione according to the published procedure¹⁵¹ is incomplete and reversible regardless of the reaction time and of the protein:2,3-butanedione ratio. The borate buffer, which is required for the stabilization of the modified guanidine group,¹⁵¹ proved unsuitable for the subsequent incubation of the (partially) modified cytochrome c with Pt(trpy)Cl⁺; much of the protein became denatured. The denatured matter was removed by centrifugation and the remaining solution of the protein was dialyzed, by ultrafiltration, in the 85 mM phosphate buffer at pH 7.0. Chromatography with CM 52,

which otherwise yields good separation of the tagged derivatives, produced an unusual fast-moving band and a red-brownish smear on the column.

The $\text{Pt}(\text{trpy})\text{ArgH}^{2+}$ complex in the triply-tagged horse protein is unstable already at pH 5.0. Incubation of the triply-tagged protein in 0.10 M acetate buffer of pH 5.0 for two hours at 4 °C and subsequent ultrafiltration into the same buffer or into the phosphate buffer of pH 7.0 yielded in either case, a filtrate containing $\text{Pt}(\text{trpy})\text{L}^{2+}$ complex. This finding is consistent with the absence of labeling arginine when cytochrome c is incubated with $\text{Pt}(\text{trpy})\text{Cl}^+$ at pH 5.0, as discussed in Section III.

Since the guanidine group in free arginine is more basic ($\text{pK}_a = 12.5$) than this group in Arg 91 of cytochrome c, the model complex $\text{Pt}(\text{trpy})\text{ArgH}^{2+}$ is even more labile than the tag on the protein. A 1.0 mM solution of the yellow model complex was prepared by mixing equimolar amounts of $[\text{Pt}(\text{trpy})\text{Cl}]\text{Cl}$ and arginine in 0.10 M phosphate buffer at pH 9.6. When 75 μL of this solution was added to 5.0 mL of phosphate buffer of pH 8.0, the pH of the resulting mixture was ca. 8.1. Its UV-visible spectrum showed that the main complex present was $\text{Pt}(\text{trpy})\text{Cl}^+$. Similarly, incubation of $[\text{Pt}(\text{trpy})\text{Cl}]\text{Cl}$ with arginine and N-acetylarginine in various mole ratios at $\text{pH} \leq 8.2$ did not cause a reaction even after 3 weeks at room temperature. At $\text{pH} > 8.5$ the reactions proceeded.

Since the guanidine group in canavanine is less basic ($\text{pK}_a = 7.0$)¹⁵⁰ than that in arginine, the $\text{Pt}(\text{trpy})\text{CanH}^{2+}$ complex is more resistant than the $\text{Pt}(\text{trpy})\text{ArgH}^{2+}$ complex to mild acids. This complex is fairly stable in the 0.10 M phosphate buffer at

pH 7.0, although the formation of the red complex, as will be discussed in the subsequent section occurs with time. The complex decomposes slowly (over several hours) when the pH of the buffered solution is lowered by careful addition of HCl, to ca. 5.0. The UV-vis spectrum of the acidified solution showed the presence of the $\text{Pt}(\text{trpy})\text{Cl}^+$ complex.

CONCLUSIONS AND PROSPECTS

This report of platinum(II) binding to Arg in proteins and a previous report of the bioactive metals Cu(II), Co(II), Zn(II), and Cr(III) binding to tetramethylguanidine¹⁵² together demonstrate that Arg side chain is a potential ligand. Most likely to bind metals is a guanidyl group whose basicity is diminished owing to its environment; for the binding to occur on the protein surface, this group should also be accessible. Since guanidine probably is a π acceptor, its coordination may be facilitated if other ligands bonded to the same metal are π donors. Therefore Arg is particularly likely to bind metals in conjunction with Cys or Tyr.

The coordination of Arg in site-directed mutagenesis experiments of metalloproteins and metal-activated proteins will be of growing interest. This report demonstrating Arg as a potential ligand may perhaps shed light into why some mutated metalloproteins or metal-activated proteins whose side chains have been replaced by Arg remain functional despite presumable loss of metal coordination.

SECTION V.
TERMINAL AND BRIDGING COORDINATION OF
GUANIDINE LIGANDS TO PLATINUM(II)

INTRODUCTION

The known functions of arginyl residues in enzymes and in other proteins depend on the positive charge of its side chain. The guanidinium cation, whose normal pKa value is ca. 12.5, exists throughout the usual pH range of protein stability. It participates in recognition of anionic substrates, binds cofactors, forms internal hydrogen bonds and salt bridges, and enhances protein hydrophilicity.^{140,141,153} Although transition metals are common in metalloproteins and in metal-activated enzymes, coordination of such a metal to arginyl side chain in a protein has only been recently observed, as discussed in Section IV.

This unexpected and unprecedented binding of Arg 91 in cytochrome c necessitated the syntheses of model complexes of $\text{Pt}(\text{trpy})\text{Cl}^+$ with free arginine and with its analogs. Few conclusive studies of transition-metal complexes with guanidine ligands have been made.^{142,154,155} This work begins a detailed study of the interesting coordination chemistry of guanidines (see Table V-1) as revealed in the preliminary studies in Section IV.

Table V-1. The Guanidine Ligands^a

Symbol	Formula ^b	pK _a of Gua	Charge
ArgH	$\text{H}_2\text{NC}(=\text{NH})\text{NH}(\text{CH}_2)_3\text{CH}(\text{NH}_3^+)\text{COO}^-$	12.5	0
Arg	$\text{H}_2\text{NC}(=\text{NH})\text{NH}(\text{CH}_2)_3\text{CH}(\text{NH}_2)\text{COO}^-$	12.5	-1
AcArg	$\text{H}_2\text{NC}(=\text{NH})\text{NH}(\text{CH}_2)_3\text{CH}(\text{NHCOCH}_3)\text{COO}^-$	12.5	-1
CanH	$\text{H}_2\text{NC}(=\text{NH})\text{NH}(\text{O})(\text{CH}_2)_2\text{CH}(\text{NH}_3^+)\text{COO}^-$	7.0	0
Can	$\text{H}_2\text{NC}(=\text{NH})\text{NH}(\text{O})(\text{CH}_2)_2\text{CH}(\text{NH}_2)\text{COO}^-$	7.0	-1
Gua	$\text{H}_2\text{NC}(=\text{NH})\text{NH}_2$	13.5	0
MeGua	$\text{H}_2\text{NC}(=\text{NH})\text{NHCH}_3$	13.5	0

^aWith neutral guanidine group, as in the platinum(II) complexes.

^bThe part set in boldface corresponds to group R in the structural formulas in the text.

EXPERIMENTAL SECTION

Chemicals

The guanidine compounds (L-enantiomers of the amino acids) and the chromatographic materials were obtained from Sigma Chemical Co.; the deuteriated solvents and KPF_6 , from Aldrich Chemical Co.; NaBPh_4 , from J.T. Baker Chemical Co.; and $[\text{Pt}(\text{trpy})\text{Cl}]\text{Cl}_2 \cdot 2\text{H}_2\text{O}$, from Strem Chemicals and from Aldrich Chemical Co. Distilled water was demineralized to the resistance greater than $16 \text{ M}\Omega \text{ cm}$. The common solvents and other chemicals were of the reagent grade.

Methods

Absorption Spectroscopy The UV-visible spectra were recorded with an IBM 9430 spectrophotometer equipped with a double grating. The IR spectra between 4000 and 200 cm^{-1} were recorded with an IBM IR98 Fourier-transform instrument, whose sample chamber was flushed with dry air. The mulls of the dried samples in Nujol were smeared on CsI plates; the pellets of the dried samples in KBr (for the middle IR region) were prepared by grinding ca. 1 mg of solid sample with 100 mg KBr.

NMR Spectroscopy The ^1H spectra of solutions in D_2O , $(\text{CD}_3)_2\text{CO}$, and $(\text{CD}_3)_2\text{SO}$ were recorded at 300 MHz with Nicolet NT 300 and Bruker WM 300 spectrometers, using residual protons or dioxane as internal references. Complexes prepared in H_2O were dissolved in D_2O by successive cycles of lyophilization and dissolution in D_2O . The ^{13}C spectra of solutions in $\text{D}_2\text{O} - \text{H}_2\text{O}$, if present, did not need to be removed completely – were recorded with the same spectrometers, using acetone or

dioxane as internal standards. The ^{195}Pt spectra of solutions were recorded at 64.4 and 42.9 MHz with the Bruker WM 300 and WM 200 spectrometers, respectively. A deuteriated solution 0.20 M both in K_2PtCl_4 and in NaCl was an external reference (0 ppm). The resonances were sought between +1450 and -2000 ppm. Two-dimensional NOESY spectra of a degassed 10 mM solution of $[\{\text{Pt}(\text{trpy})\}_2\text{Can}]\text{Cl}_3$ in D_2O were recorded with the Nicolet NT 300 spectrometer; the mixing time was 300 ms.

Mass Spectrometry The FAB spectra were obtained with a Kratos MS 50 spectrometer. The samples were dissolved as follows: $[\{\text{Pt}(\text{trpy})\}_2\text{Arg}](\text{BPh}_4)_3$ in CH_3CN , $[\{\text{Pt}(\text{trpy})\}_2\text{McGua}](\text{BPh}_4)_4$ in CH_2Cl_2 , and $[\{\text{Pt}(\text{trpy})\}_2\text{Can}](\text{ClO}_4)_3$ in 3-nitrobenzyl alcohol. In the first two cases 3-nitrobenzyl alcohol was added as a liquid matrix.

Other Procedures The pH values were measured with a Fisher Accumet 805 MP instrument; the results were not corrected when D_2O was the solvent. Elemental analyses were performed by Galbraith Laboratories, Inc.

Synthesis and Reactions

Stability of $[\text{Pt}(\text{trpy})\text{Cl}]\text{Cl}$ in Basic Solution Aqueous solutions that were 50 mM in $[\text{Pt}(\text{trpy})\text{Cl}]\text{Cl}$ and 25, 50, or 100 mM in NaOH showed no irreversible change in their UV-vis spectra over 10 d at room temperature. A 10-mM solution of this complex, kept at 70°C for 16 d with occasional adjustment of pH to ca. 9.0, also did not show any significant spectral changes. A 15-mM solution of the complex in 30 mM phosphate buffer of pH 8.0, kept at 80° for 5 d, yielded a single band of $\text{Pt}(\text{trpy})\text{Cl}^+$ upon chromatography on CM 52, with 85-mM phosphate buffer of pH 7.0 as eluent.

Synthesis of [Pt(trpy)ArgH]Cl₂, [(Pt(trpy))₂Arg]Cl₃, [(Pt(trpy))₂Arg](PF₆)₃, and [(Pt(trpy))₂Arg](BPh₄)₃ A solution containing 96.4 mg (0.18 mmol) of [Pt(trpy)Cl]Cl·2H₂O and 31.4 mg (0.18 mmol) of L-arginine in 4 mL of water was kept at 70 °C for 7 d. At the beginning, and occasionally during the reaction, the pH was adjusted to ca. 9.0 by addition of 1.0 M NaOH solution. The color turned from orange to dark red. The reaction mixture was filtered, evaporated to the minimum volume, and chromatographed on a column of CM 52 cation exchanger; both the equilibration and elution were done with 85-mM potassium phosphate buffer of pH 7.0. A minor yellow band (ca. 10 %) and a major red band (ca. 90 %) were eluted in this order. Since the yellow fraction gradually converts into the red one at room temperature, the chromatographic separation is best carried out at 4 °C at least until the first band is eluted off the column. Since the red fraction is stable upon heating, the rest of the separation can be done either at 4 °C or at room temperature. Addition of a concentrated solution of KPF₆, followed by standing or evaporation, caused copious precipitation of the red compound. The precipitates were filtered off by centrifugation, washed with cold water and cold methanol, and dried in vacuo. Recrystallization of the red solid from a mixture of acetone and water (1:1) yielded tiny needles that were dried in vacuo. Percentages, calculated for C₃₆H₃₅N₁₀O₂F₁₈P₃Pt₂ and found: C, 29.52 (28.47); H, 2.41 (3.01); N 9.56 (9.11); and F, 23.34 (20.75). The red fraction from another similar synthesis was evaporated to ca. 10 mL, and a saturated solution of NaBPh₄ was added dropwise to it. The brownish-red precipitate was filtered off by centrifugation, washed with cold water in the same way, and dried in vacuo. The yield, 34 mg or 34 % with respect to [Pt(trpy)Cl]Cl. Percentages, calculated for C₁₀₈H₉₅N₁₀O₂B₃Pt₂ and found: C, 65.24 (60.91); H, 4.83 (4.67); N, 7.05 (6.80); B, 1.61 (1.66); and Pt, 19.64 (19.62). Principal fragments, m/z values, and relative abundancies: [(Pt(trpy))₂Arg]BPh₄⁺,

1348, 1.2; $[\{\text{Pt}(\text{trpy})\}_2\text{Arg}]\text{BPh}_3^+$, 1270, 1.7; $[\{\text{Pt}(\text{trpy})\}_2\text{Arg}]\text{BPh}_2^+$, 1192, 1.8; $[\text{Pt}(\text{trpy})\}_2\text{Arg}^+$, 1029, 6.0; $[\text{Pt}(\text{trpy})\}_2(\text{ArgH-CO}_2)^+$, 984, 1.4; and $\text{Pt}(\text{trpy})^+$, 428, 100.

Synthesis of $[\{\text{Pt}(\text{trpy})\}_2\text{Arg}](\text{PF}_6)_3$ A solution containing 67.5 mg (0.50 mmol) of $[\text{Pt}(\text{trpy})\text{Cl}]\text{Cl}\cdot 2\text{H}_2\text{O}$ and 43.6 mg (0.25 mmol) of arginine in 10 mL of water was kept at 70 ° for 7 d, and the pH was adjusted to ca. 9.0 as before. Because the chromatography yielded only the red product, this step can be omitted from the procedure. The PF_6^- salt was prepared as before.

Reaction of $[\text{Pt}(\text{trpy})\text{Cl}]\text{Cl}$ with N α -Acetyl-L-Arginine A solution containing 60.0 mg (0.030 mmol) of $[\text{Pt}(\text{trpy})\text{Cl}]\text{Cl}\cdot 2\text{H}_2\text{O}$ and 6.5 mg (0.030 mmol) of the arginine derivative in 1 mL of water was treated like the corresponding mixture containing arginine; see above. The color changed, and the pH decreased, as in the other reaction.

Synthesis of $[\text{Pt}(\text{trpy})\text{CanH}]\text{Cl}_2$, $[\{\text{Pt}(\text{trpy})\}_2\text{Can}]\text{Cl}_3$, and $[\{\text{Pt}(\text{trpy})\}_2\text{Can}](\text{PF}_6)_3$ A solution containing 100.0 mg (0.187 mmol) of $[\text{Pt}(\text{trpy})\text{Cl}]\text{Cl}\cdot 2\text{H}_2\text{O}$ and 32.9 mg (0.187 mmol) of canavanine in 7 mL of 85-mM potassium phosphate buffer of pH 8.5 was kept at 40 °C for 9 h. The color turned from orange to deep red. The reaction mixture was filtered and evaporated to the minimum volume. Cation-exchange chromatography on CM 52 with the same buffer as an eluent, yielded two bands. The yellow fraction, whose yield with respect to $[\text{Pt}(\text{trpy})\text{Cl}]\text{Cl}$ was 65 %, was eluted at 4 °C with the 85-mM buffer flowing at a rate of ca. 15 mL h⁻¹. The red fraction, whose yield was 35 % was eluted at room temperature with the 125-mM buffer flowing at a rate of ca. 30 ml h⁻¹. Both buffers were of pH 8.5. The same products were obtained when 51.2 mg (0.187 mmol) of canavanine sulfate were used instead of the equimolar amount of the free base. The treatment with KPF_6 , as in the case of arginine complexes, yielded very little yellow precipitate and much red precipitate.

Synthesis of $[\{\text{Pt}(\text{trpy})\}_2\text{Can}](\text{PF}_6)_3$ A mixture containing 225 mg (0.42 mmol) of $[\text{Pt}(\text{trpy})\text{Cl}]\text{Cl}\cdot 2\text{H}_2\text{O}$ and 57.5 mg (0.21 mmol) of canavanine sulfate in 10 mL of water was kept at 40 °C for 4 d, and the pH was occasionally adjusted to ca. 9.0 with 1.0 M NaOH solution. The reaction mixture yielded a single red band on the CM 52 column; this band was eluted as before. The red solution was evaporated in vacuo to a concentration of ca. 120 mM. To 0.20 mL of this solution was added 0.60 mL of a saturated aqueous solution of KPF_6 , and the mixture was left at 4 °C. The red precipitate was filtered and washed with cold methanol and cold diethyl ether. Yield, 34 mg or 92 %; decomposes at 187 °C. Percentages, calculated for $\text{C}_{35}\text{H}_{33}\text{N}_{10}\text{O}_3\text{F}_{18}\text{P}_3\text{Pt}_2$ and found: C, 28.66 (27.99); H, 2.27 (2.67); N, 9.55 (8.83); and Pt, 26.60 (24.80).

Synthesis of $[\{\text{Pt}(\text{trpy})\}_2\text{Can}](\text{ClO}_4)_3\cdot 5.5\text{H}_2\text{O}$ A mixture containing 112.5 mg (0.210 mmol) of $[\text{Pt}(\text{trpy})\text{Cl}]\text{Cl}\cdot 2\text{H}_2\text{O}$ and 18.5 mg (0.105 mmol) of free-base canavanine in 5.0 mL of water was heated and adjusted with NaOH as in the previous procedure, but not rechromatographed. To this solution was added a saturated solution of 551 mg (4.5 mmol) of NaClO_4 in water. The first precipitate was filtered, washed with water, and dried in vacuo. The filtrate was concentrated to ca. 1.0 mL, and the second precipitate was similarly obtained. Total yield, 90 mg or 66 %. Percentages calculated for $\text{C}_{35}\text{H}_{44}\text{N}_{10}\text{O}_{20.5}\text{Cl}_3\text{Pt}_2$ and found: C, 29.40 (29.82); H, 3.08 (3.39); N, 9.80 (9.77); Cl, 7.46 (6.95); and Pt, 27.30 (26.22). Principal fragments, m/z values, and relative abundancies: $[\{\text{Pt}(\text{trpy})\}_2\text{CanH}](\text{ClO}_4)_2^+$, 1231, 22.5; $[\{\text{Pt}(\text{trpy})\}_2\text{Can}]\text{ClO}_4^+$, 1130, 28.2; $\{\text{Pt}(\text{trpy})\}_2\text{Can}^+$, 1031, 8.4; and $\text{Pt}(\text{trpy-H})^+$, 427, 100.

X-ray Crystallographic Analysis of $[\{\text{Pt}(\text{trpy})\}_2\text{Can}](\text{ClO}_4)_3\cdot 5.5\text{H}_2\text{O}$ A solution of 60 mg of this compound in ca. 1.0 mL of hot water was left to cool to room temperature and to evaporate slowly through pinholes for 1 week.

Table V-2. Crystallographic Data for $[\{\text{Pt}(\text{trpy})\}_2\text{Can}](\text{ClO}_4)_3 \cdot 5.5 \text{H}_2\text{O}$

formula: $\text{C}_{35}\text{H}_{44}\text{N}_{10}\text{O}_{20.5}\text{Cl}_3\text{Pt}_2$	space group: $\text{P}2_1$ (No. 4)
$a = 12.733$ (3) Å	$T = -50 \pm 1$ $^\circ\text{C}$
$b = 27.039$ (4) Å	$\lambda = 0.71073$ Å
$c = 14.813$ (3) Å	$\rho_{\text{calcd}} = 2.058$ g cm^{-3}
$\beta = 115.219$ (8) $^\circ$	$\mu = 63.83$ cm^{-1}
$V = 4614$ Å^3	transmission coeff: 0.9954-0.7086
$Z = 4$	$R(F_0 \text{ or } F_0^2) = 0.0418$
$\text{FW} = 1429.3$	$R_w(F_0 \text{ or } F_0^2) = 0.0572.$

pinacoidal crystals grew. One of them was cleaved to the approximate dimensions: $0.51 \times 0.52 \times 0.54$ mm. Although a C-centered orthorhombic cell with all angles of $90.00 \pm 0.05^\circ$ was a possibility, axial photographs ruled out mmm symmetry. The technical details are summarized in Table V-2. The structure was solved by direct methods, with an Enraf-Nonius CAD4 diffractometer and the standard programs. Only the four independent platinum atoms were located from the E-map; the other nonhydrogen atoms were found by repeated least-squares refinements and difference-Fourier syntheses. Hydrogen atoms bonded to carbon atoms were placed in calculated positions and used only for the calculation of structure factors. Only the platinum and oxygen atoms in the cations and the chlorine atoms in the anions were refined with anisotropic thermal parameters.

Analysis of $[(Pt(trpy))_2Can]Cl_3$ by Job's Method Solutions containing various mole fractions of $[Pt(trpy)Cl]Cl$ and of canavanine sulfate were prepared in 85-mM phosphate buffer of pH 8.5-8.9 and were kept in sealed tubes, at 40° , for up to 22 d. The total concentration of the reactants was 1.00 mM. In the preliminary experiments, aliquots were examined spectrophotometrically throughout the reaction. In definitive experiments, the absorbances were measured only at the end in order to avoid evaporation. Formation of the complex was accompanied by the growth of a new band at 480 nm. For mole fractions of $[Pt(trpy)Cl]Cl$ above 0.67, the absorbance at 480 nm was corrected by subtracting the small contribution of this compound. In order to minimize deviations from the Beer law, the solutions were diluted to 100 μ M and their spectra recorded in a 10-cm cell.

Synthesis of $[(Pt(trpy))_2MeGua](BPh_4)_4$ A mixture containing 128.6 mg (0.24 mmol) of $[Pt(trpy)Cl]Cl \cdot 2H_2O$ and 13.3 mg (0.12 mmol) of methylguanidine hydrochloride in 5 mL of water was kept at $70^\circ C$ for 10 d, and the pH was occasionally

adjusted to ca. 9.0 with NaOH. Since an aliquot of the reaction mixture gave a single band on a CM 52 column, the bulk of it was not chromatographed. The precipitate, obtained by adding to the reaction mixture an excess of saturated solution of NaBPh₄ in water, was filtered, washed with water, and dried. Yield, 140 mg or 53 %. Principal fragments, m/z values, and relative abundancies: $[(\text{Pt}(\text{trpy}))_2(\text{MeGua-H})](\text{BPh}_4)_2^+$, 1566, 1.4; $[(\text{Pt}(\text{trpy}))_2(\text{MeGua-H})]\text{BPh}_4^+$, 1247, 10.4; $\{\text{Pt}(\text{trpy})\}_2(\text{MeGua-H})^+$, 928, 100; and $\text{Pt}(\text{trpy})^+$, 428, 33.3.

Reactions of $[\text{Pt}(\text{trpy})\text{Cl}]\text{Cl}$ with Guanidine A solution containing 16.0 mg (0.030 mmol) of $[\text{Pt}(\text{trpy})\text{Cl}]\text{Cl}\cdot 2\text{H}_2\text{O}$ and 5.8 mg (0.060 mmol) of guanidine hydrochloride in 1 mL of water was treated like the corresponding mixture containing methylguanidine hydrochloride. The color changed, and the pH decreased, as in this other reaction. The minor yellow (ca. 10 %) and the major red (ca. 90 %) products were separated on the CM 52 column, as before.

Stability of the Complexes Effects of acids and of added nucleophiles on the complexes in aqueous solutions were examined by UV-vis spectrophotometry. All the red complexes proved stable indefinitely at $7 < \text{pH} < 9$ and upon heating. The yellow complexes, however, converted into their red counterparts upon concentration and heating, and therefore had to be cooled. The reverse conversion occurred, albeit slowly, upon addition of an excess of the guanidine ligands to the mildly acidic solutions of the corresponding red complexes. The following experiments were done at room temperature. At $\text{pH} < 5$, the red complex $\{\text{Pt}(\text{trpy})\}_2\text{Arg}^{3+}$ decomposed slowly in the presence of an excess of Cl^- anions; at $\text{pH} < 2$, it decomposed immediately even when the noncoordinating H_3PO_4 and H_2SO_4 were used for acidification. The yellow complex $\text{Pt}(\text{trpy})\text{CanH}^{2+}$ remained stable as the pH was lowered to 2 with H_2SO_4 . Separate additions of the 100-fold, 10,000-fold, and 20,000-fold excesses, respectively,

of the KI, KBr, and KCl caused no apparent decomposition of $\text{Pt}(\text{trpy})\text{CanH}^{2+}$ after 2 h; decomposition became evident after 1 d, and pronounced after 2 d. The red complex $\{\text{Pt}(\text{trpy})\}_2\text{Can}^{3+}$ proved stable at pH 8.5 even in the presence of a 70,000-fold excess of KBr. The complex decomposed, however, as the pH was lowered to 4.5 with H_2SO_4 .

Conversion of the yellow $\text{Pt}(\text{trpy})\text{CanH}^{2+}$ into the red $\{\text{Pt}(\text{trpy})\}_2\text{Can}^{3+}$ in aqueous solution was followed by the growth of absorption at 480 nm. The solutions of the yellow complex were thermostated in closed containers, and aliquots were examined spectrophotometrically. The reaction was considered complete when the absorbance quotient A_{480}/A_{244} ceased increasing. At 40 °C for 48 h, a 77 μM solution remained stable; a 0.31 mM solution reacted slightly; and a 1.5 mM solution reacted noticeably. At 80 °C, the full conversion of the yellow complex into the red complex took the following times: 40, 18, and 6 h for the 77 μM , 0.31 mM, and 1.5 mM solutions, respectively. A solution that was 50 μM in the yellow $\text{Pt}(\text{trpy})\text{CanH}^{2+}$ and a solution that was 50 μM both in this complex and in $\text{Pt}(\text{trpy})\text{Cl}^+$ underwent the conversion into the red $\{\text{Pt}(\text{trpy})\}_2\text{Can}^{3+}$ at approximately the same rate.

RESULTS AND DISCUSSION

Reactivity of $\text{Pt}(\text{trpy})\text{Cl}^+$ toward Guanidine Ligands

The complex $\text{Pt}(\text{trpy})\text{Cl}^+$ is stable under the reaction conditions, and it is unreactive toward amino and carboxylate groups of amino acids.¹⁷ As the ligands in Table V-1 react with this complex, all of them release protons; when the pH becomes constant, the substitution is completed. The ligands whose reactions were studied in more detail all yield similar products. Evidently, it is the guanidine group that displaces the Cl^- ligand and coordinates to the $\text{Pt}(\text{trpy})^{2+}$ fragment.

Basicity of Guanidine Ligand The reactivity of $\text{Pt}(\text{trpy})\text{Cl}^+$ toward guanidine ligands depends on their intrinsic basicity and on the reaction conditions, as established in systematic examination (by cation-exchange chromatography and UV-vis spectrophotometry) of the reaction mixtures held for various times, at different temperatures, and in solutions of different basicity. Other conditions being equal, canvanine ($\text{pK}_a = 7.0$)¹⁵⁰ is more reactive than other ligands (pK_a ca. 13); it reacts already at room temperature and in neutral solutions, whereas the other ligands require heating, mild basicity, or both. The substitution reaction is accelerated, and the preponderance of the red product over the yellow product is enhanced, at higher pH values. The pH of the reaction mixture was kept below ca. 9.5 lest the hydroxide ions attack the complexes irreversibly.

Lability of Chloride Ligand Since $\text{Pt}(\text{trpy})\text{Cl}^+$ reacts with the very basic ligands in mildly basic solution, where only a miniscule fraction of the guanidine group (pK_a ca. 13) is deprotonated, the chloride ligand must be labile. This lability probably is caused by the aromatic terpyridine ligand. Indeed, the chloride ion is displaced from

$\text{Pt}(\text{trpy})\text{Cl}^+$ approximately 10^3 - 10^4 times faster than from the analogous aliphatic complex, $\text{Pt}(\text{dien})\text{Cl}^+$.¹⁰⁶ This facile reactivity, together with its other advantages, makes $[\text{Pt}(\text{trpy})\text{Cl}]\text{Cl}$ useful as a selective and noninvasive reagent for labeling of proteins.^{6,17,18,156}

The ^{195}Pt NMR spectra recorded during the reaction between $\text{Pt}(\text{trpy})\text{Cl}^+$ and canavanine show the decline of the signal at -1206 ppm and the growth of the pair of signals at -959 and -974 ppm. The corresponding conversion of the yellow $\text{Pt}(\text{trpy})\text{CanH}^{2+}$ to the red $[\text{Pt}(\text{trpy})]_2\text{Can}^{3+}$ may amount simply to addition of the second $\text{Pt}(\text{trpy})^{2+}$ group to the yellow complex.

Characterization of the Guanidine Complexes

In approximately neutral aqueous solutions the yellow complexes have the net charge +2 because arginine and canavanine ligands exist as the zwitterions. The red complexes of these ligands have the net charge +3 because two $\text{Pt}(\text{trpy})^+$ groups diminish the basicity of the α -amino group, and the amino acids exist as carboxylate anions. The red complex of methylguanidine, which cannot be deprotonated in this way, has a charge of +4. The relative mobilities on the CM 52 cation exchanger are consistent with these charges. The yellow products are eluted faster than the red complex of arginine under identical chromatographic conditions. The various spectroscopic methods of characterization yield consistent descriptions of the new compounds in solution.

Mass Spectra The FAB mass spectra show that the red complexes each contain two $\text{Pt}(\text{trpy})^{2+}$ groups per guanidine-containing ligand. Only the singly-charged fragments occurred in significant amounts; multiply-charged ones were evident only in

the first few scans. The same phenomenon was observed in similar studies of other transition-metal complexes with polypyridyl ligands.¹⁵⁷⁻¹⁶⁰

Absorption Spectra The electronic spectra (shown in Table V-3 and in the previous Section's Figure IV-3) permit both qualitative comparisons among the complexes and their quantitative determination in solution. The charge-transfer bands in the region 300-350 nm depend on the identity of the ligand L in $\text{Pt}(\text{trpy})\text{L}^{\text{n}+}$, whereas the aromatic bands in the region 200-300 nm are characteristic of the $\text{Pt}(\text{trpy})^{2+}$ fragment itself. Displacement of the chloride ligand from $\text{Pt}(\text{trpy})\text{Cl}^+$ by the guanidine ligands causes changes in the former region, but does not affect the latter one markedly. The spectra of all the yellow complexes containing guanidine, arginine, canavanine, and methylguanidine are similar to one another. So are the spectra of the red complexes; evident in all of them is an additional band at ca. 480 nm. Because all of the guanidine-containing compounds react similarly with $\text{Pt}(\text{trpy})\text{Cl}^+$, all of them probably coordinate to platinum(II) in the same way - through the guanidine group.

The yellow and the red products always occur together. The former cannot be obtained by itself, since it converts into the latter, the latter can be obtained alone if the mixture of $[\text{Pt}(\text{trpy})\text{Cl}]\text{Cl}$ and the guanidine ligand in the correct ratio is heated for several days. Therefore, the composition of the yellow complex could not, but that of the red complex of canavanine, which is representative of the red complexes with the other ligands as well. As Figure V-1 shows, the complex contains exactly two $\text{Pt}(\text{trpy})^{2+}$ groups per canavanine ligand.

IR Spectra The strong band at 344 cm^{-1} (see Table V-4) in the far IR spectrum of $[\text{Pt}(\text{trpy})\text{Cl}]\text{Cl}$, corresponding to the Pt-Cl stretch, disappears upon formation of the complexes. The bands at 1663 and 1684 cm^{-1} in the middle IR spectra (see Table V-4)

Table V-3. Extinction Coefficients of the Pt(trpy)Lⁿ⁺ and {Pt(trpy)}₂Lⁿ⁺ Complexes

Complex	λ_{\max} in nm (ϵ in M ⁻¹ cm ⁻¹) ^a		
Pt(trpy)Cl ⁺	342	270	242
	(13 300)	(24 300)	(27 800)
Pt(trpy)ArgH ²⁺	332	273	244
	(10 600)	(22 900)	(29 100)
{Pt(trpy)} ₂ Arg ³⁺	480	309	270
	(3 700)	(24 000)	(54 800)
			(66 000)
Pt(trpy)CanH ²⁺	336	274	244
	(10 400)	(19 300)	(27 500)
{Pt(trpy)} ₂ Can ³⁺	480	310	270
	(4 000)	(23 000)	(48 000)
			(60 000)
Pt(trpy)MeGua ²⁺	332	273	244
	(9 800)	(21 700)	(27 900)
{Pt(trpy)} ₂ MeGua ⁴⁺	490	309	270
	(3 600)	(26 100)	(59 700)
			(73 000)

^aFor 8- to 15- μ M solutions in 85-mM potassium phosphate buffer of pH 7.0.

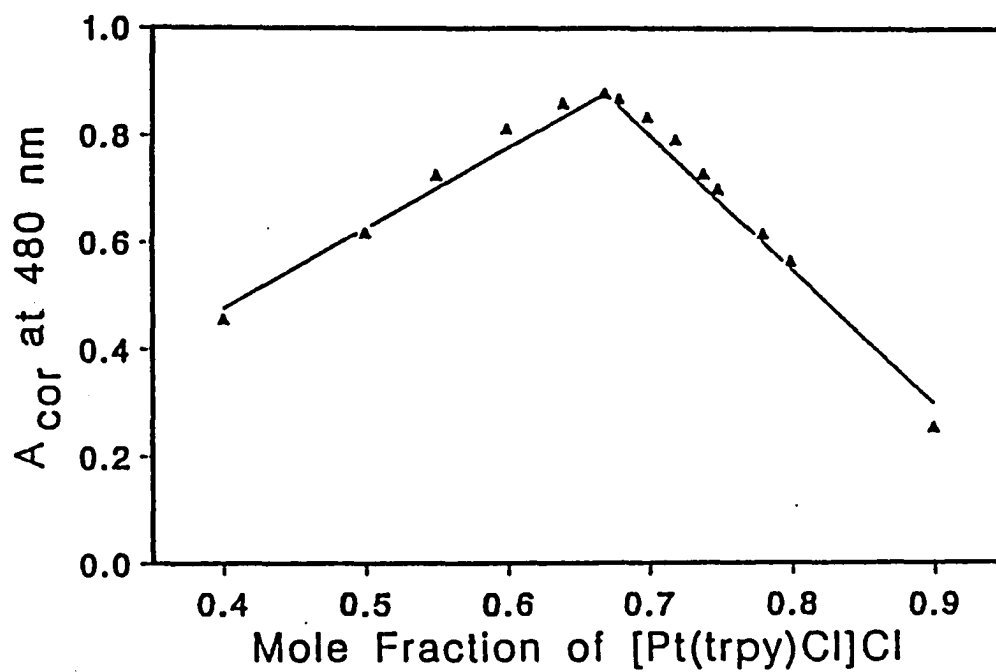


Figure V-1. Job's Plot of $\{Pt(trpy)\}_2Can^{3+}$

Table V-4. Infrared Bands (cm⁻¹)^a

compound	middle IR bands ^b				far IR bands ^c	
[Pt(trpy)Cl]Cl	3425	br,m	3117	sh,m	585	br,m
	2896	sh,s	2934	s	517	m
	1736	vs	1605	sh,s	476	w
	1468	s	1447	s	457	s
	1447	s	1383	sh,s	394	br,m
	1259	br,s	1173	sh,m	368	m
	1101	sh,vs	1022	s	344	s
	937	s	795	sh,s	294	br,s
	717	m	702	sh,m		
	Arginine	3489	vs	3346	sp,vs	662
3346		sp,vs	3288	br,vs	631	vs
3105		br,vs	2953	sp,vs	607	sp,m
2981		vs	2937	vs	552	sp,m
2868		vs	2351	m	495	w
2324		m	1705	vs	303	w
1684		vs	1645	vs		
1607		vs	1564	vs		
	1474	sp,s	1452	s		

^aAbbreviations: vs, very strong; s, strong; m, medium; w, weak; vw, very weak; sp, sharp; br, broad; and sh, shoulder.

^bKBr pellets, unless otherwise stated.

^cNujol mull on CsI, nujol absorptions are not reported.

Table V-4 (Continued)

compound	middle IR bands ^b				far IR bands ^c	
	1441	s	1423	sp,vs		
	1379	sp,s	1362	s		
	1331	sp,vs	1302	s		
	1188	s	1136	sp,vs		
	1121	s	1080	sp,s		
	1011	vs	928	m		
	854	s	811	s		
	797	vs	752	vs		
[[Pt(trpy)] ₂ Arg](PF ₆) ₃	3744	m	3406	br,vs	660	m
	3302	br,s	3096	br,s	648	m
	3028	br,m	2930	m	559	sp,vs
	2860	m	2361	m	517	m
	2336	m	1628	vs	461	m
	1603	sp,vs	1558	sp,vs	434	br,w
	1502	m	1477	sp,s		
	1452	sp,s	1446	s		
	1400	sp,s	1346	m		
	1315	sp,s	1292	m		
	1252	br,s	1188	m		
	1171	m	1140	m		
	1109	m	1094	m		
	1075	m	1032	sp,s		
	839	vs	773	sp,s		

Table V-4 (Continued)

compound	middle IR bands ^b		far IR bands ^c		
	741	m	723	m	
Canavanine	3489	vs	3346	sp,vs	696 br,s
	3288	br,vs	3105	br,vs	536 s
	2953	sp,vs	2937	vs	503 s
	2881	vs	2868	vs	455 s
	2361	m	2324	m	411 sp,m
	1705	vs	1684	vs	354 sp,m
	1645	vs	1607	vs	
	1564	vs	1474	sp,s	
	1452	s	1441	s	
	1423	sp,vs	1379	sp,s	
	1362	s	1331	sp,vs	
	1302	s	1236	sp,s	
	1188	s	1178	sp,s	
	1157	m	1144	m	
	1136	sp,vs	1096	sp,s	
	1068	sp,s	1026	sp,vs	
	941	sp,s	918	sp,s	
	878	sp,s	789	sp,s	
	766	sp,m	708	sp,s	
[Pt(trpy)CanH](PF ₆) ₂ ^d	3246	br,m	1730	sp,s	558 s
	1640	sh,s	1607	sp,s	519 m

^dNujol mull on CsI plates.

Table V-4 (Continued)

compound	middle IR bands ^b			far IR bands ^c		
[[Pt(trpy)] ₂ Can](PF ₆) ₃	1290	m	1169	w	447	br,m
	1074	w	841	s	394	m
	771	sp,s			308	m
	3662	br,m	3391	br,s	656	m
	2975	m	2926	sp,s	644	sp,m
	2875	m	2375	w	557	sp,s
	2362	w	1625	sh,s	518	m
	1607	s	1562	m	459	m
	1516	m	1479	sp,s	436	w
	1402	sp,s	1317	sp,s	352	w
	1288	m	1250	s		
	1188	w	1169	s		
	1144	m	1112	m		
	1094	sp,m	1034	sp,s		
Methylguanidine·HCl	843	vs	775	sp,s		
	750	sp,s	731	sp,s		
	3354	br,vs	3180	vs	563	br,s
	2926	sp,s	2854	sp,m		
	2349	sp,w	1663	vs		
	1460	sp,s	1427	sp,s		
	1377	sp,m	1173	s		
1067	br,m	912	sp,m			

Table V-4 (Continued)

compound	middle IR bands ^b				far IR bands ^c	
[Pt(trpy)MeGua](PF ₆) ₂	3447	vs	3000	m	662	w
	2975	s	2925	s	602	sp,m
	2363	sp,s	2338	s	559	sp,s
	2338	s	1641	s	518	w
	1609	sp,s	1479	sp,s	460	w
	1456	sp,s	1400	sp,s		
	1317	sp,m	1261	m		
	1034	m	843	vs		
	768	sp,s	744	sp,s		
	714	sp,s				
[Pt(trpy) ₂ MeGua](PF ₆) ₄	3433	br,s	2955	sp,vs	557	s
	2926	sp,vs	2850	sp,s	516	sp,m
	2361	sp,m	2325	m	458	m
	1645	br,s	1612	s	434	m
	1572	s	1538	w		
	1456	sp,s	1400	sp,s		
	1377	sp,s	1261	sp,s		
	1096	br,s	1032	s		
	845	s	804	sp,s		
	775	sp,m				

of the guanidine-containing compounds, corresponding to the C=N stretch, shift upon complexation by 18 to 59 cm^{-1} to lower frequencies.

^1H NMR Spectra ^1H NMR spectroscopy (see Table V-5) was useful because the resonances of the aromatic $\text{Pt}(\text{trpy})^{2+}$ group and of the aliphatic guanidine-containing ligands occur in separate regions of the spectra. The guanidine protons are undetectable in D_2O solutions because of exchange, but are evident when the spectra are recorded in $(\text{CD}_3)_2\text{SO}$ and $(\text{CD}_3)_2\text{CO}$ solutions. The relative intensities of the signals confirmed that the ratio of $\text{Pt}(\text{trpy})^{2+}$ to the ligand is 1:1 in the yellow complexes and 2:1 in the red complexes. As expected, the protons whose chemical shifts are most affected by coordination are those in the guanidine group and those that sit nearest to the guanidine group in the organic ligand (namely, H^δ in arginine and CH_3 in methylguanidine) and to the platinum atom in the $\text{Pt}(\text{trpy})^{2+}$ fragment (namely, H6 and H5).

^{13}C NMR Spectra The ^{13}C resonances in the guanidine-containing ligands shift downfield as they form the respective red complexes as shown in Table V-6. The great perturbations of the C^δ atoms confirm that all three ligands coordinate through the guanidine group. In the arginine complex, the perturbation increases monotonically along the amino acid chain toward the guanidine group. In the canavanine complex, however, even the carboxylate carbon atom is significantly affected by coordination. Perhaps the arginine chain in solution extends away from the $\text{Pt}(\text{trpy})^{2+}$ groups, whereas the canavanine chain in solution adopts a conformation in which the carboxylate anion is attracted to these positively-charged groups. On the one hand, noncovalent interactions

Table V-5. Proton NMR Chemical Shifts

compound	$\delta,^a$ ppm				
	Pt(trpy)		H	ligand	H
[Pt(trpy)Cl]Cl ^b	8.08	m	4,4'		
	7.88	d	3,3'		
	7.82	m	6		
	7.37	m	5		
Arginine				3.73	t α
				3.22	t δ
				1.87	m β
				1.67	m γ
[(Pt(trpy))Arg]Cl ₃	8.33	m	6,4'	3.75	t α
	8.19	t	4	3.51	t δ
	7.96	m	3,3'	2.09	m β
	7.58	t	5	1.85	m γ
Canavanine				3.93	m γ
				3.82	m α
				2.20	m β

^aFor 2- to 5- mM solutions in D₂O at pH* 9.0, δ vs. DSS with residual water as an internal reference; for solutions in (CD₃)₂CO or DMSO-d₆, δ vs. TMS with residual solvent or TMS as internal reference.

^bFor solution in D₂O at pH* 7.0.

Table V-5 (Continued)

compound	$\delta,^a$ ppm					
	Pt(trpy) H		ligand		H	
[Pt(trpy)CanH]Cl ₂ ^c	8.40	t	6	4.19	t	γ
	8.20	m	4,4'	3.63	t	α
	8.12	t	3,3'	2.10	m	β
	7.64	m	5			
[Pt(trpy)] ₂ Can]Cl ₃	8.25	m	6	4.27	t	γ
	8.12	m	4,4'	3.63	t	α
	7.86	m	3,3'	2.11	m	β
	7.49	m	5			
Methylguanidine				in D ₂ O:		
				2.81	s	CH ₃
				in DMSO:		
				7.79	s	NHCH ₃
				7.32	s	gua
				2.70	d	CH ₃
[Pt(trpy)] ₂ MeGua](PF ₆) ₄				in (CD ₃) ₂ CO:		
	8.72	d	6	6.53	br,s	NH ₂
	8.53	t	4'	5.12	s	NH
	8.40	t	4	3.31	d	CH ₃
	8.30	m	3,3'			
	7.80	t	5			

^cChloride is presumed to be the counterion even in the presence of sulfate ions; measured at pH* 7.0 in 3.0 M Na₂SO₄.

Table V-5 (Continued)

compound	$\delta,^a$ ppm					
	Pt(trpy)		H	ligand	H	
[[Pt(trpy)] ₂ MeGua]Cl ₄ ^d	8.29	m	6,4'	3.08	s	CH ₃
	8.17	t	4			
	7.92	m	3,3'			
	7.53	t	5			

^dFrom a reaction between equimolar amounts of [Pt(trpy)Cl]Cl and MeGua·HCl in D₂O at pH* 9.0; additional signal at 2.81 ppm corresponds to free methylguanidine.

Table V-6. Carbon-13 NMR Chemical Shifts

compound	δ in ppm ^a			
	Pt(trpy)	C	ligand	C
[Pt(trpy)Cl]Cl	157.0	3		
	153.5	3'		
	150.4	6		
	142.7	4		
	142.4	4'		
	129.1	5		
	125.4	2		
	124.1	2'		
Arginine			177.7	COO ⁻
			155.9	ζ
			54.9	α
			40.8	δ
			29.5	β
		24.3	γ	

^aFor 100-mM solutions in D₂O at pH 9.0, unless otherwise stated; the chemical shifts with respect to TMS using acetone or dioxane as internal reference.

Table V-6 (Continued)

compound	$\delta,^a$ ppm			
	Pt(trpy)	C	ligand	C
[[Pt(trpy)] ₂ Arg]Cl ₃	156.8	3	177.9	COO ⁻
	153.4	3'	165.2	ζ
	151.2	6	55.2	α
	142.9	4'	42.3	δ
	142.8	4	30.0	β
	129.7	5	25.4	γ
	125.5	2		
	124.0	2'		
Canavanine			174.0	COO ⁻
			157.6	ζ
			68.7	γ
			52.2	α
			29.0	β
[Pt(trpy)CanH]Cl ₂ ^b	156.7	3	173.3	COO ⁻
	153.9	3'	158.7	ζ
	151.1	6	70.5	γ
	142.5	4	51.3	α
	142.0	4'	28.2	β
	128.3	5		
	124.5	2		
	122.8	2'		

^bChloride is presumed to be the counterion even in the presence of sulfate ions; measured at pH 7.0 in 3 M Na₂SO₄.

Table V-6 (Continued)

compound	$\delta,^a$ ppm			
	Pt(trpy)	C	ligand	C
[[Pt(trpy)] ₂ Can]Cl ₃	154.3,155.1	3	176.2	COO ⁻
	152.0,152.6	3'	164.4	ζ
	150.5,150.7	6	71.1	γ
	142.1,142.4	4	52.0	α
	141.8	4'	29.8	β
	128.7,129.1	5		
	124.6,124.8	2		
	122.9,123.2	2'		
Methylguanidine			157.5	gua
			27.3	CH ₃
[[Pt(trpy)] ₂ MeGua]Cl ₄ ^c	155.3	3	166.0	gua
	152.8	3'	29.0	CH ₃
	151.1	6		
	143.0	4'		
	142.8	4		
	129.8	5		
	125.5	2		
	123.9	2'		

^cFrom a reaction between equimolar amounts of [Pt(trpy)Cl]Cl and MeGua·HCl in D₂O at pH 9.0; additional signals at 27.3 and 157.5 ppm correspond to free methylguanidine.

among ligands commonly manifest themselves in the perturbed chemical shifts.^{161,162} On the other hand, the two-dimensional ^1H NMR (NOESY) of $\{\text{Pt}(\text{trpy})\}_2\text{Can}^{3+}$ do not contain off-diagonal peaks attributable to an interaction between the terpyridine and α -CH protons. because, in molecules of this size, NOE effects may be absent for other reasons,¹⁶³ these ^1H NMR spectra do not rule out noncovalent interactions as the cause of the unusual ^{13}C chemical shifts.

The arginine and methylguanidine complexes each show a single set of ^{13}C terpyridine resonances, thus, indicating that the two $\text{Pt}(\text{trpy})^{2+}$ groups in each complex are equivalent. The canavanine complex, however, shows doubling of the terpyridine resonances. This indicates that the two $\text{Pt}(\text{trpy})^{2+}$ groups in it are inequivalent. It is uncertain whether this inequivalence stems from the putative noncovalent interactions as discussed above.

^{195}Pt NMR Spectra Since the ^{195}Pt chemical shift depends greatly on the ligands,^{12,13} ^{195}Pt NMR spectroscopy is well-suited to the study of the new guanidine complexes. The chemical shifts (see Table V-7), versus PtCl_4^{2-} , of the yellow complexes $\text{Pt}(\text{trpy})\text{L}^{2+}$ fall in the narrow range from -1166 to -1177 ppm (when L is MeGua or ArgH) and at -1206 ppm (when L is CanH), near the chemical shifts of $\text{Pt}(\text{trpy})\text{Im}^{2+}$ (-1150 ppm)¹⁷ and of $\text{Pt}(\text{trpy})\text{HisH}^{2+}$ (-1146 ppm).¹⁷ Since in the last two complexes imidazole and histidine are coordinated through the trigonal nitrogen atom,¹⁷ the guanidine ligands probably are also coordinated through such an atom. The canavanine complex differs from the methylguanidine and arginine complexes because it

Table V-7. Platinum-195 Chemical Shifts of Pt(trpy)Lⁿ⁺ and {Pt(trpy)}₂Lⁿ⁺ Complexes

Complex ^a	δ , ^b ppm	Conditions
Pt(trpy)Cl ⁺	-1080	pH 7.0, in H ₂ O
Pt(trpy)Im ²⁺	-1150	pH 7.0, in H ₂ O
Pt(trpy)ArgH ²⁺	-1168, -1177 (1.0 : 1.4)	pH 7.0, in 3 M potassium phosphate buffer
{Pt(trpy)} ₂ Arg ³⁺	-982	pH 9.0, in H ₂ O
	-957	pH 7.0, in 3 M potassium phosphate buffer
Pt(trpy)CanH ²⁺	-1206	pH 7.0, in 3 M Na ₂ SO ₄

^aIn aqueous solutions of the complexes, Cl⁻ is presumed to be the counterion even in the presence of sulfate or phosphate ions.

^bFor 5- to 30- mM solutions containing at least 30 % D₂O, unless other deuteriated solvent is used; the chemical shift with respect to PtCl₄²⁻ at 22 °C.

Table V-7 (Continued)

Complex ^a	$\delta,^b$ ppm	Conditions
$\{\text{Pt}(\text{trpy})\}_2\text{Can}^{3+}$	-959, -974	pH 9.0, in H ₂ O
	(1.0 : 1.0)	
	-970	saturated solution of the PF ₆ ⁻ salt in (CD ₃) ₂ CO
Pt(trpy)MeGua ²⁺	-1166	pH 7.0, in H ₂ O ^c
$\{\text{Pt}(\text{trpy})\}_2\text{MeGua}^{4+}$	-994	saturated solution of the PF ₆ ⁻ salt in (CD ₃) ₂ CO
	-960	pH 7.0, in H ₂ O ^c
	-969	pH 7.0, in 3 M potassium phosphate buffer

^cFrom a reaction mixture containing equimolar amounts of [Pt(trpy)Cl]Cl and MeGua·HCl in water, which was kept at 50^o C and pH 9.5 for 18 h and brought to pH 7.0; additional signals at -1073 and -957 ppm correspond respectively to [Pt(trpy)Cl]Cl and to $[\{\text{Pt}(\text{trpy})\}_2\text{MeGua}]\text{Cl}_4$.

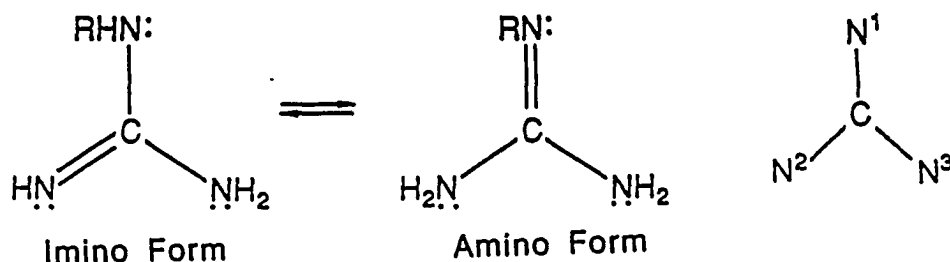
has an oxygen atom, whereas the other two have an organic substituent, attached to the guanidine group; see Table V-1. The methylguanidine and canavanine complexes show one signal each, whereas the arginine complex shows a major and a minor signal close to each other. These properties are related to the structures of the complexes as will be discussed in the succeeding discussion.

The ^{195}Pt NMR spectra of the red complexes $\{\text{Pt}(\text{trpy})\}_2\text{L}^{n+}$ containing three guanidine ligands L differ from those of the yellow complexes and among themselves. Their chemical shifts, in the narrow range from -957 to -994 ppm, are by more than 200 ppm lower than the shifts of the yellow complexes, presumably because guanidine coordinates weaker as a bridging than as a terminal ligand. The spectra of the methylguanidine and arginine complexes at ambient temperature, in aqueous solution, contain one signal each, whereas the spectrum of the canavanine complex contains two equal signals 15 ppm apart. This doubling probably is caused by the slightly different environments of two $\text{Pt}(\text{trpy})^{2+}$ groups in the same complex or by the coexistence of slightly different complexes. Since the difference is small, the two platinum atoms must have similar or identical ligands in the fourth coordination place. In aqueous solution at 325 K and in acetone solution the two signals coalesce into one. Evidently the two platinum atoms in the complex are easily converted into each other. The doubling of signals in the ^{13}C and ^{195}Pt NMR spectra of $\{\text{Pt}(\text{trpy})\}_2\text{Can}^{3+}$ probably has structural causes, which will be discussed later. The ^{195}Pt chemical shifts of the cationic complexes depend slightly on the anions in solution and somewhat more on the solvent,

as Table V-7 shows. The shift of the methylguanidine complex is independent of pH, whereas that of the arginine complex, which contain ionizable groups, changes in the pH range 7.0-9.0.

Structures of the Complexes

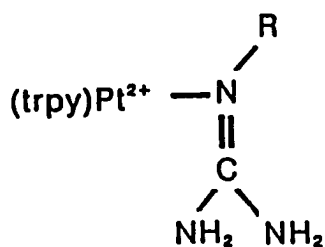
A neutral monosubstituted guanidine group can exist as two tautomers; with reference to the character of an unsubstituted nitrogen atom (designated N2), they are termed imino and amino forms.¹⁵⁰ (With reference to the substituted nitrogen atom, N1, these designations of the tautomers would be reversed. This revised nomenclature may be more logical because of the uniqueness of the atom N1, but we will adhere to the existing convention.) Little is known about this tautomerism, and the neutral monosubstituted guanidine group is generally assumed to exist in the imino form. Both



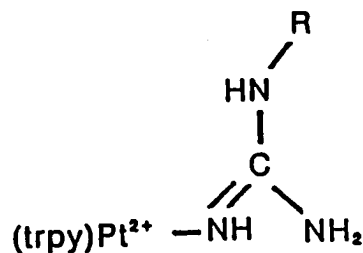
forms, however, seem to exist in the aqueous solution of arginine; the imino form is slightly favored.¹⁶⁴ Guanidine complexes containing aromatic¹⁶⁵ and electron-withdrawing¹⁵⁰ substituents seem to greatly favor the amino form. Indeed, the neutral guanidine group of canavanine exists exclusively as the amino tautomer in the solid

state.¹⁵⁰ To our knowledge, tautomerism of canavanine in solution and of methylguanidine in either solid or solution has not been studied. In the absence of such knowledge, the structures of the new complexes will be discussed tentatively.

Yellow Complexes, $Pt(trpy)L^{2+}$ The ^{195}Pt chemical shifts indicate that the guanidine group is coordinated through a trigonal nitrogen atom. It could be either N2 (in the imino tautomer) or N1 (in the amino tautomer). Therefore both of the structures shown below are possible. The methylguanidine and canavanine



Type A



Type B

complexes show one ^{195}Pt signal each, whereas the arginine complex shows two unequal signals only 9 ppm apart. If the ^{195}Pt chemical shift is sensitive to the slight difference between N1 and N2 atoms as donors, the first two complexes perhaps exist in solution as a single tautomer each, whereas the third complex in solution may be a mixture of two tautomers. Alternatively, the two signals in the last case may be due to noncovalent interactions between the flexible arginine chain and the $Pt(trpy)^{2+}$ group.^{161,162}

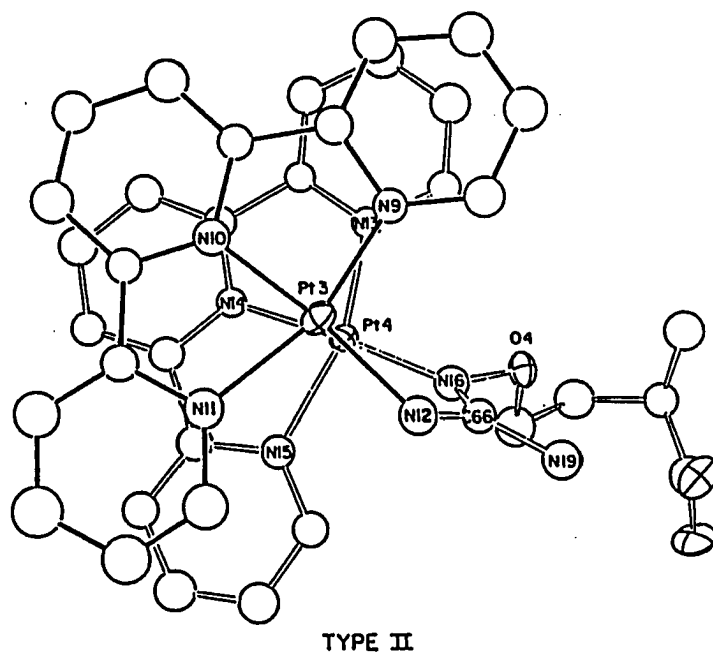
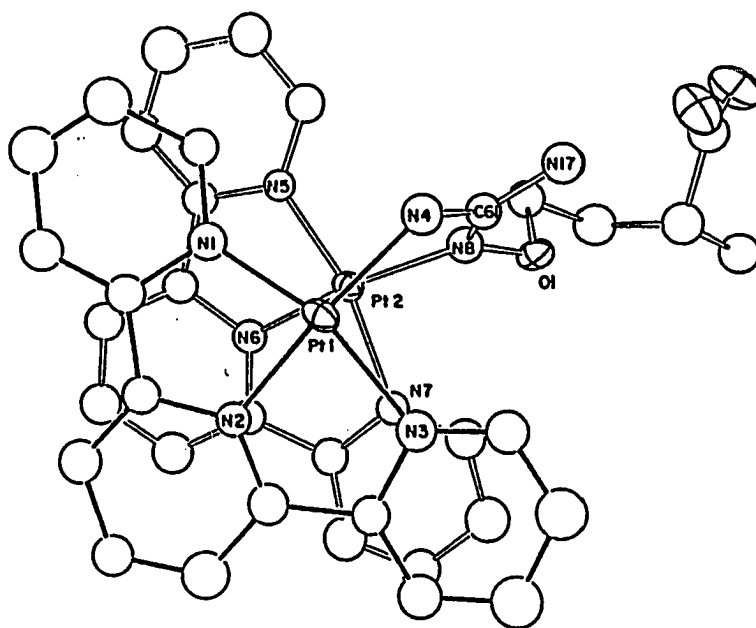
Red Complex, $\{\text{Pt}(\text{trpy})\}_2\text{Canr}^{3+}$ To our knowledge, this is the first transition-metal complex containing a coordinated guanidine to be analyzed crystallographically. The two independent complex cations, designated types I and II, are shown in Figures V-2 through V-4. The numerical findings are listed in Tables V-8 through V-10.

In both types the two $\text{Pt}(\text{trpy})^{2+}$ groups are attached to the unique nitrogen atom (N1) and to one of the other two nitrogen atoms (N2 or N3) in the canavanine side chain. (This local numbering within the guanidine group should not be confused with the numbering in the whole complexes; the latter system is used in Figures V-2 and V-3 and in Tables V-8 through V-10.) The two types differ from each other noticeably in the torsion angle about the $\text{C}^\alpha\text{-C}^\beta$ (C(63)-C(64) in type I and C(68)-C(69) in Type II) bond in the canavanine ligand, but this difference is insignificant. The canavanine COO^- group does not approach the $\text{Pt}(\text{trpy})^{2+}$ groups in the crystalline state. Although this finding militates against the possibility of noncovalent interactions in solutions, they cannot be ruled out (see above).

The four $\text{Pt}(\text{trpy})^{2+}$ groups have very similar dimensions – they are somewhat puckered, the bond angles involving the platinum atoms deviate from the ideal values of 90° , and the Pt-N distances within each group vary. These distortion, evident also in terpyridyl complexes of platinum(II)^{91,166,167} and palladium(II),^{168,169} show the strain in this tridentate ligand.

In complexes of both types the guanidine group is planar, and its bond angles are close to 120° . The two differ from each other in the bond distances involving the

Figure V-2. Molecular Structures (ORTEP Drawings with 50 % Ellipsoids) of the Two Types of Complex Cation that Coexist in the Crystal of $[\{\text{Pt}(\text{trpy})\}_2\text{Ca}]\text{(ClO}_4)_3 \cdot 5.5 \text{H}_2\text{O}$. The skeleton of the upper $\text{Pt}(\text{trpy})^{2+}$ group is darkened for clarity



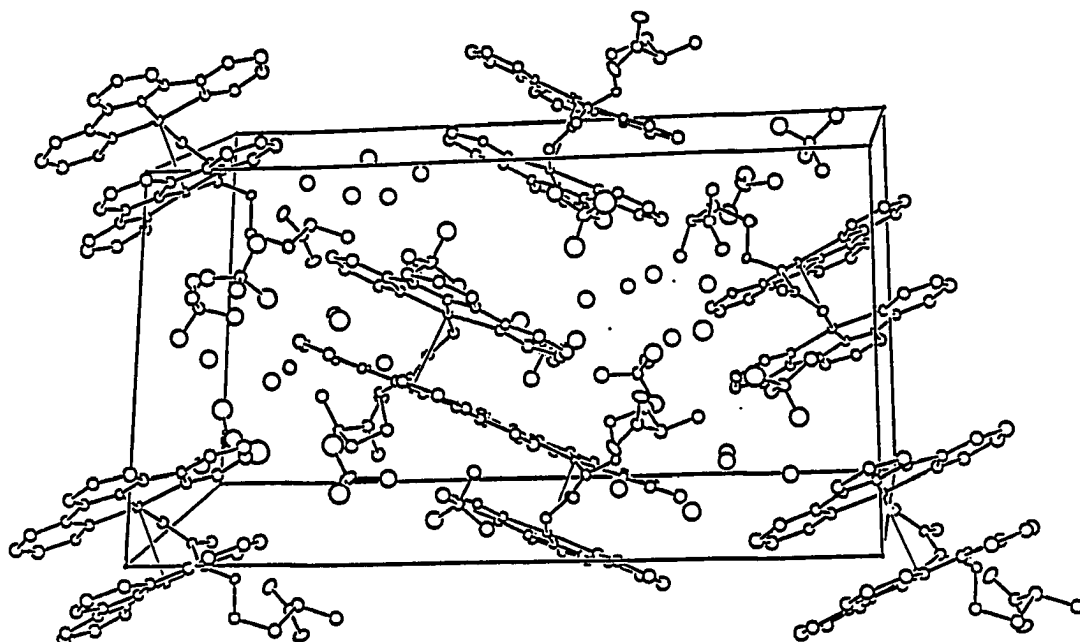


Figure V-3. An ORTEP Diagram of the Unit Cell of
 $[(\text{Pt}(\text{trpy}))_2\text{Can}](\text{ClO}_4)_3 \cdot 5.5\text{H}_2\text{O}$

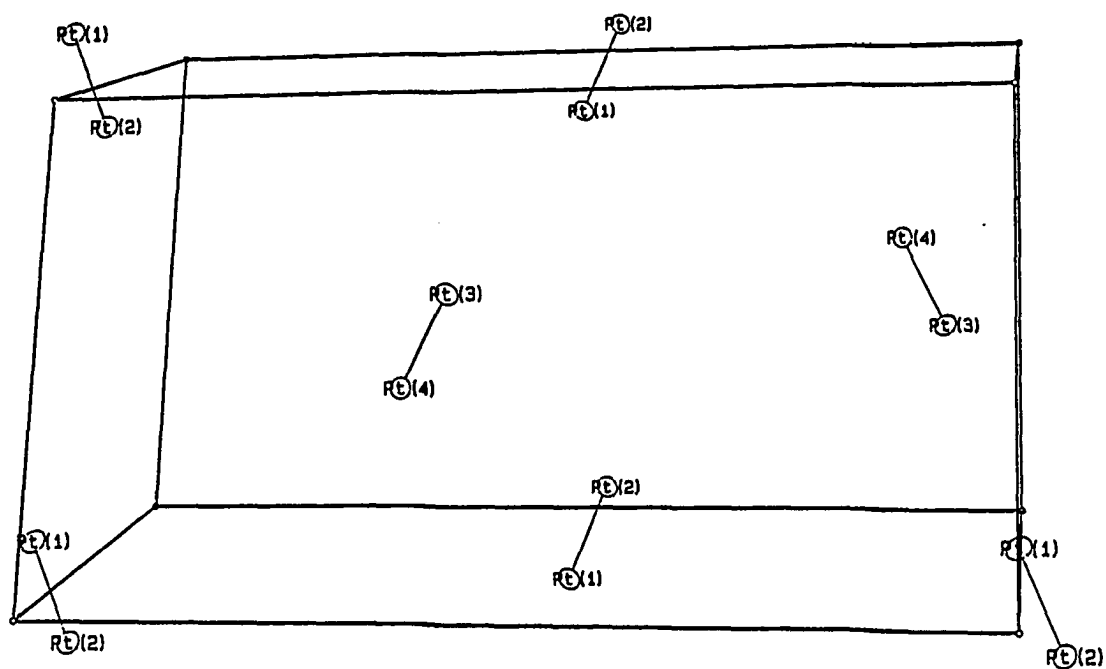
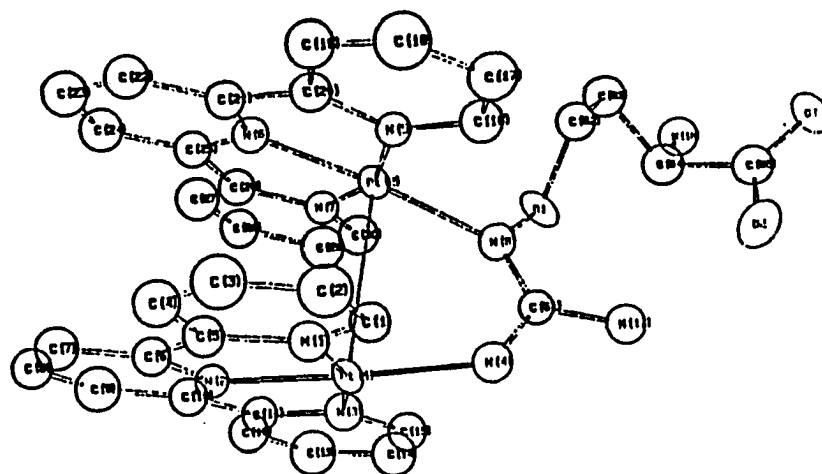
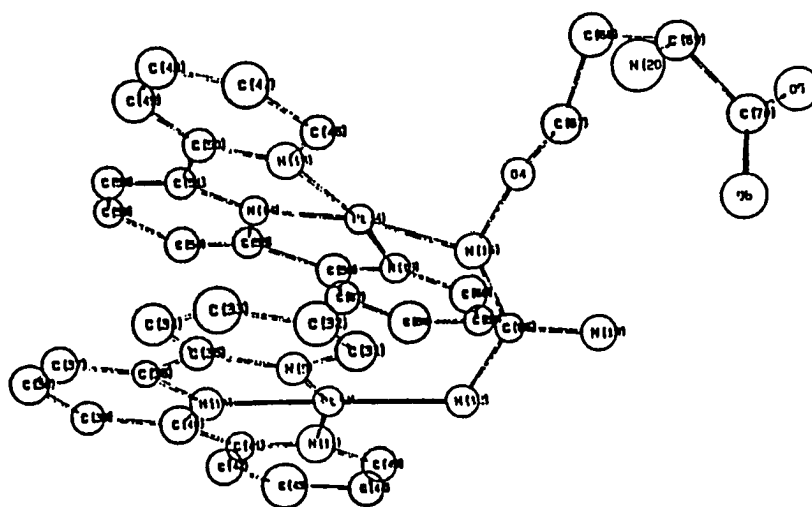


Figure V-4. A Diagram of the Unit Cell of $[\{\text{Pt}(\text{trpy})\}_2\text{Can}](\text{ClO}_4)_3$ Showing Only the Platinum Atoms

**Table V-8. Coordinates of the Nonhydrogen Atoms in the Complex Cation
Salt of $[(Pt(trpy))_2Can](ClO_4)_3 \cdot 5.5 H_2O$**



type I



type II

Table V-8 (Continued)

atom	x	y	z	B_{eq}^a, A^{O2}
		type I ^b		
Pt(1)	0.09206(4)	0.000	-0.12651	1.86(1)
Pt(2)	0.11250(4)	0.04220(2)	0.06676(3)	1.75(1)
O(1)	0.3061(8)	0.1139(4)	0.1039(6)	2.3(2)
O(2)	0.5921(8)	0.1294(5)	0.1896(8)	3.9(3)
O(3)	0.6607(9)	0.1711(5)	0.3314(8)	4.0(3)
N(1)	0.0779(9)	-0.0660(4)	-0.0857(8)	2.2(2) ^c
N(2)	-0.0783(8)	-0.0025(4)	-0.1934(7)	1.8(2) ^c
N(3)	0.0532(9)	0.0714(5)	-0.1933(8)	2.5(2) ^c
N(4)	0.2679(9)	0.0117(5)	-0.0505(8)	2.5(2) ^c
N(5)	0.1624(8)	-0.0197(4)	0.1364(7)	1.8(2) ^c
N(6)	-0.0354(9)	0.0242(4)	0.0620(8)	2.1(2) ^c
N(7)	0.0142(9)	0.1064(4)	0.0022(8)	2.0(2) ^c
N(8)	0.2610(9)	0.0685(5)	0.0585(8)	2.3(2) ^c
N(17)	0.4252(9)	0.0627(5)	0.0346(8)	2.7(2) ^c
N(18)	0.482(1)	0.2399(5)	0.2437(9)	3.3(3) ^c

^aAnisotropically refined atoms are given in the form of the isotropic equivalent displacement parameter defined as: $(4/3) * [a^2 * B(1,1) + b^2 * B(2,2) + c^2 * B(3,3) + ab(\cos \gamma) * B(1,2) + ac(\cos \beta) * B(1,3) + bc(\cos \alpha) * B(2,3)]$.

^bTwo independent molecules (types I and II) coexist in the unit cell, numbering scheme is shown.

^cAtoms refined isotropically.

Table V-8 (Continued)

atom	x	y	z	$B_{eq}^a A^{o2}$
C(1)	0.163(1)	-0.0970(5)	-0.0317(9)	2.1(2) ^c
C(2)	0.138(1)	-0.1457(7)	-0.007(1)	3.4(3) ^c
C(3)	0.031(1)	-0.1600(7)	-0.036(1)	3.5(3) ^c
C(4)	-0.060(1)	-0.1270(6)	-0.092(1)	2.9(3) ^c
C(5)	-0.037(1)	-0.0814(6)	-0.1199(9)	2.4(2) ^c
C(6)	-0.126(1)	-0.0445(5)	-0.1784(9)	2.2(2) ^c
C(7)	-0.244(1)	-0.0470(6)	-0.214(1)	2.8(3) ^c
C(8)	-0.311(1)	-0.0059(6)	-0.266(1)	2.6(3) ^c
C(9)	-0.258(1)	0.0355(7)	-0.276(1)	3.6(3) ^c
C(10)	-0.135(1)	0.0365(6)	-0.239(1)	2.5(3) ^c
C(11)	-0.065(1)	0.0797(5)	-0.2418(9)	2.2(2) ^c
C(12)	-0.106(1)	0.1237(6)	-0.288(1)	3.1(3) ^c
C(13)	-0.034(1)	0.1606(7)	-0.294(1)	4.2(4) ^c
C(14)	0.088(1)	0.1483(7)	-0.256(1)	3.9(3) ^c
C(15)	0.124(1)	0.1052(6)	-0.196(1)	2.8(3) ^c
C(16)	0.273(1)	-0.0368(6)	0.183(1)	2.7(3) ^c
C(17)	0.298(1)	-0.0820(6)	0.230(1)	3.2(3) ^c
C(18)	0.209(1)	-0.1119(7)	0.228(1)	3.9(4) ^c
C(19)	0.100(1)	-0.0934(6)	0.188(1)	3.0(3) ^c
C(20)	0.077(1)	-0.0465(5)	0.141(1)	2.3(2) ^c
C(21)	-0.039(1)	-0.0232(5)	0.0940(9)	2.2(2) ^c
C(22)	-0.148(1)	-0.0425(6)	0.076(1)	2.9(3) ^c
C(23)	-0.248(1)	-0.0146(6)	0.026(1)	3.3(3) ^c
C(24)	-0.239(1)	0.0333(6)	-0.005(1)	3.1(3) ^c
C(25)	-0.129(1)	0.0528(5)	0.0145(9)	2.3(2) ^c

Table V-8 (Continued)

atom	x	y	z	$B_{eq}^a A^{02}$
C(26)	-0.099(1)	0.1000(5)	-0.015(1)	2.4(3) ^c
C(27)	-0.179(1)	0.1373(7)	-0.059(1)	3.8(3) ^c
C(28)	-0.144(1)	0.1798(6)	-0.082(1)	3.1(3) ^c
C(29)	-0.025(1)	0.1866(7)	-0.062(1)	3.8(3) ^c
C(30)	0.045(1)	0.1472(6)	-0.019(1)	3.0(3) ^c
C(61)	0.315(1)	0.0489(5)	0.0135(9)	2.0(2) ^c
C(62)	0.356(1)	0.1097(6)	0.214(1)	2.7(3) ^c
C(63)	0.386(1)	0.1632(7)	0.253(1)	3.5(3) ^c
C(64)	0.464(1)	0.1872(7)	0.206(1)	3.5(3) ^c
C(65)	0.584(1)	0.1611(6)	0.248(1)	3.1(3) ^c
Cl(1)	0.4932(3)	-0.0952(1)	0.0361(3)	2.77(8)
Cl(2)	0.0785(3)	0.1320(2)	0.2917(3)	3.64(9)
Cl(3)	-0.5320(3)	0.0236(2)	-0.5735(3)	3.16(8)
O(7)	0.4547(9)	-0.0771(5)	0.1083(8)	3.9(2) ^c
O(8)	0.616(1)	-0.1057(5)	0.0848(9)	4.3(3) ^c
O(9)	0.472(1)	-0.0562(5)	-0.0334(9)	4.6(3) ^c
O(10)	0.424(1)	-0.1350(6)	-0.018(1)	6.3(4) ^c
O(11)	0.109(1)	0.0809(6)	0.295(1)	5.4(3) ^c
O(12)	-0.019(1)	0.1404(6)	0.310(1)	5.8(3) ^c
O(13)	0.059(1)	0.1559(7)	0.204(1)	7.3(4) ^c
O(14)	0.174(1)	0.1604(8)	0.363(1)	8.1(5) ^c
O(15)	-0.494(1)	-0.0097(7)	-0.488(1)	7.0(4) ^c
O(16)	-0.6499(9)	0.0280(5)	-0.6188(8)	4.1(2) ^c
O(17)	-0.492(1)	0.0073(6)	-0.6414(9)	5.1(3) ^c
O(18)	-0.485(1)	0.0713(7)	-0.541(1)	6.8(4) ^c

Table V-8 (Continued)

atom	x	y	z	$B_{eq}^a A^{o2}$
		type II ^b		
Pt(3)	0.87029(4)	-0.08060(2)	0.59128(3)	1.83(1)
Pt(4)	0.85714(4)	-0.12790(2)	0.40451(3)	1.629(9)
O(4)	0.6601(7)	-0.1923(3)	0.3595(6)	2.0(2)
O(5)	0.3220(9)	-0.2270(4)	0.1355(8)	3.6(3)
O(6)	0.3946(8)	-0.2168(4)	0.3008(7)	3.2(2)
N(9)	0.9133(8)	-0.1428(4)	0.6616(7)	1.8(2) ^c
N(10)	1.0331(9)	-0.0664(4)	0.6526(8)	2.1(2) ^c
N(11)	0.8795(9)	-0.0070(5)	0.5487(8)	2.4(2) ^c
N(12)	0.6971(9)	-0.0880(4)	0.5159(8)	2.3(2) ^c
N(13)	0.9572(8)	-0.1827(4)	0.4727(7)	1.8(2) ^c
N(14)	1.0026(8)	-0.1000(4)	0.4145(7)	1.7(2) ^c
N(15)	0.8015(9)	-0.0598(4)	0.3317(8)	2.1(2) ^c
N(16)	0.7079(9)	-0.1458(4)	0.4033(8)	2.2(2) ^c
N(19)	0.5376(9)	-0.1392(5)	0.4314(8)	2.5(2) ^c
N(20)	0.552(1)	-0.2857(5)	0.3358(9)	3.2(3) ^c
C(31)	0.842(1)	-0.1788(6)	0.667(1)	2.6(3) ^c
C(32)	0.889(1)	-0.2222(6)	0.720(1)	3.0(3) ^c
C(33)	1.003(1)	-0.2279(6)	0.767(1)	2.9(3) ^c
C(34)	1.079(1)	-0.1918(6)	0.766(1)	3.0(3) ^c
C(35)	1.036(1)	-0.1485(5)	0.715(1)	2.3(2) ^c
C(36)	1.103(1)	-0.1069(5)	0.7080(9)	2.0(2) ^c
C(37)	1.220(1)	-0.1031(6)	0.747(1)	2.8(3) ^c
C(38)	1.269(1)	-0.0576(6)	0.732(1)	2.8(3) ^c
C(39)	1.200(1)	-0.0194(6)	0.681(1)	2.8(3) ^c

Table V-8 (Continued)

atom	x	y	z	$B_{eq}^a A^{O2}$
C(40)	1.079(1)	-0.0251(5)	0.6386(9)	1.9(2) ^c
C(41)	0.991(1)	0.0086(5)	0.5796(9)	2.1(2) ^c
C(42)	1.012(1)	0.0556(6)	0.550(1)	3.2(3) ^c
C(43)	0.922(1)	0.0865(7)	0.495(1)	4.0(3) ^c
C(44)	0.805(1)	0.0697(7)	0.466(1)	3.6(3) ^c
C(45)	0.789(1)	0.0238(6)	0.492(1)	3.1(3) ^c
C(46)	0.921(1)	-0.2272(5)	0.4934(9)	2.1(2) ^c
C(47)	1.005(1)	-0.2629(6)	0.545(1)	3.1(3) ^c
C(48)	1.120(1)	-0.2561(7)	0.572(1)	3.5(3) ^c
C(49)	1.154(1)	-0.2114(6)	0.544(1)	2.8(3) ^c
C(50)	1.072(1)	-0.1760(5)	0.4936(9)	1.7(2) ^c
C(51)	1.100(1)	-0.1267(5)	0.4632(9)	2.1(2) ^c
C(52)	1.205(1)	-0.1083(6)	0.480(1)	2.7(3) ^c
C(53)	1.212(1)	-0.0608(6)	0.446(1)	3.0(3) ^c
C(54)	1.112(1)	-0.0331(6)	0.3940(9)	2.3(2) ^c
C(55)	1.009(1)	-0.0544(5)	0.381(1)	2.3(2) ^c
C(56)	0.889(1)	-0.0318(5)	0.327(1)	2.4(2) ^c
C(57)	0.870(1)	0.0139(6)	0.285(1)	2.5(3) ^c
C(58)	0.755(1)	0.0297(6)	0.236(1)	3.2(3) ^c
C(59)	0.666(1)	0.0029(6)	0.239(1)	3.1(3) ^c
C(60)	0.693(1)	-0.0441(5)	0.286(1)	2.4(2) ^c
C(66)	0.648(1)	-0.1256(5)	0.4537(9)	1.8(2) ^c
C(67)	0.610(1)	-0.1867(6)	0.254(1)	3.2(3) ^c
C(68)	0.583(1)	-0.2389(6)	0.209(1)	3.2(3) ^c
C(69)	0.499(1)	-0.2659(6)	0.236(1)	2.4(3) ^c

Table V-8 Continued

atom	x	y	z	$B_{eq}^a A^{o2}$
C(70)	0.397(1)	-0.2359(6)	0.226(1)	3.2(3) ^c
Cl(4)	0.5116(3)	-0.1393(2)	-0.3224(3)	3.17(8)
Cl(5)	0.4551(3)	0.0783(2)	-0.2141(3)	4.3(1)
Cl(6)	0.0930(4)	0.2926(2)	-0.1901(3)	4.4(1)
O(19)	0.625(1)	-0.1601(5)	-0.2891(9)	4.4(3) ^c
O(20)	0.496(1)	-0.1000(5)	-0.3895(8)	4.3(3) ^c
O(21)	0.497(1)	-0.1185(7)	-0.241(1)	7.7(5) ^c
O(22)	0.423(2)	-0.1749(8)	-0.363(1)	8.8(5) ^c
O(23)	0.477(1)	0.0364(6)	-0.152(1)	6.0(3) ^c
O(24)	0.348(1)	0.0982(7)	-0.243(1)	7.4(4) ^c
O(25)	0.526(2)	0.112(1)	-0.174(2)	12.7(8) ^c
O(26)	0.470(2)	0.0648(9)	-0.299(1)	9.7(6) ^c
O(27)	0.146(1)	0.3415(6)	-0.177(1)	5.6(3) ^c
O(28)	0.173(1)	0.2541(8)	-0.105(1)	8.4(5) ^c
O(29)	0.100(2)	0.2702(8)	-0.272(1)	9.3(5) ^c
O(30)	-0.006(1)	0.2923(8)	-0.174(1)	8.3(5) ^c

**Table V-9. Important Bond Distances (Å^o) in the Complex Cation of
 [(Pt(trpy))₂Can](ClO₄)₃ · 5.5 H₂O^a**

type I		type II	
Pt(1) – Pt(2)	2.9884(7)	Pt(3) – Pt(4)	2.9872(8)
Pt(1) – N(4)	2.06(1)	Pt(3) – N(12)	2.01(1)
Pt(2) – N(8)	2.07(1)	Pt(4) – N(16)	1.95(1)
Pt(1) – N(1)	1.92(1)	Pt(3) – N(9)	1.93(1)
Pt(1) – N(2)	1.965(9)	Pt(3) – N(10)	1.91(1)
Pt(1) – N(3)	2.13(1)	Pt(3) – N(11)	2.11(1)
Pt(2) – N(5)	1.93(1)	Pt(4) – N(13)	1.93(1)
Pt(2) – N(6)	1.92(1)	Pt(4) – N(14)	1.95(1)
Pt(2) – N(7)	2.12(1)	Pt(4) – N(15)	2.10(1)
C(61) – N(4)	1.34(2)	C(66) – N(12)	1.33(2)
C(61) – N(8)	1.26(2)	C(66) – N(16)	1.38(2)
C(61) – N(17)	1.36(2)	C(66) – N(19)	1.35(2)
N(8) – O(1)	1.40(1)	N(16) – O(4)	1.43(1)

^aTwo independent molecules (types I and II) coexist in the unit cell.

Table V-10. Important Bond Angles (deg) in the Complex Cation of
 $[\{\text{Pt}(\text{trpy})\}_2\text{Ca}]\text{ClO}_4)_3 \cdot 5.5 \text{H}_2\text{O}^{\text{a}}$

type I		type II	
N(1)–Pt(1)–N(4)	101.3(4)	N(9)–Pt(3)–N(12)	101.8(4)
N(1)–Pt(1)–N(2)	84.0(4)	N(9)–Pt(3)–N(10)	85.3(5)
N(2)–Pt(1)–N(3)	79.0(4)	N(10)–Pt(3)–N(11)	76.4(4)
N(3)–Pt(1)–N(4)	95.7(4)	N(11)–Pt(3)–N(12)	96.6(5)
Pt(1)–N(4)–C(61)	124(1)	Pt(3)–N(12)–C(66)	122(1)
N(5)–Pt(2)–N(8)	103.1(5)	N(13)–Pt(4)–N(14)	103.7(5)
N(6)–Pt(2)–N(6)	83.9(5)	N(13)–Pt(4)–N(15)	82.2(4)
N(7)–Pt(2)–N(8)	79.0(5)	N(14)–Pt(4)–N(16)	78.5(4)
Pt(2)–N(8)–C(61)	127.3(9)	Pt(4)–N(16)–C(66)	130.7(8)
N(4)–C(61)–N(8)	121(1)	N(12)–C(66)–N(16)	118(1)
N(8)–C(61)–N(17)	121(1)	N(16)–C(66)–N(19)	121(1)
N(4)–C(61)–N(17)	118(1)	N(12)–C(66)–N(19)	120(1)

^aTwo independent molecules (types I and II) coexist in the unit cell.

guanidine group and the platinum atoms. In type I, the C-N1 [C(61)-N(8)] distance is shorter than the other two C-N distances, as in canavanine itself,¹⁵⁰ and the two Pt-N distances are equal and relatively long. In type II, the three C-N distances are approximately equal, as in most crystals containing arginine,^{145,170,171} but the two Pt-N distances are unequal and relatively short. The complexes of types I and II may perhaps be considered derivatives, respectively, of the amino and imino tautomers of the guanidine group. Although canavanine itself in the crystalline state exists as the amino tautomer, the tautomeric equilibrium perhaps is affected by coordination to the platinum atoms.

The two Pt(trpy)²⁺ groups are nearly parallel with each other – the dihedral angle between the average planes is ca. 9° in type I and ca. 7° in type II. Although the Pt(trpy)²⁺ groups are oblique with respect to the guanidine plane – the corresponding dihedral angles in both types fall in the range 68-71° – this deviation from orthogonality probably is insufficient to allow significant overlap between the π orbitals of the Pt(trpy)²⁺ and guanidine groups.

The Pt(trpy)²⁺ groups in the crystal are nearly eclipsed with each other; they probably remain inequivalent in solution and give rise to two sets of ¹³C NMR resonances. It is difficult to determine whether the two ¹⁹⁵Pt NMR signals, which are only 15 ppm apart, arise from the difference between the complexes of types I and II or from the inequivalence of the platinum atoms within these complexes. The average torsion angle about the Pt-Pt axis – because of the non-90° bond angles it depends

somewhat on the choice of the other two defining atoms – in the complexes of both types I and II is ca. 21°. The distance between the average $\text{Pt}(\text{trpy})^{2+}$ planes (ca. 2.8 Å in both types I and II) is shorter than the typical interlayer distances in columnar platinum(II) complexes (3.1-4.2 Å)¹⁷²⁻¹⁷⁵ and shorter than these distances in analogous complexes $\text{Pt}(\text{trpy})(\text{SCH}_2\text{CH}_2\text{OH})^+$ ⁹¹ and $\text{Pd}(\text{trpy})\text{Cl}^+$ (3.40-3.50 Å).^{168,169} The last two complexes associate by noncovalent forces in the head-to-tail arrangement, and the $\text{M}(\text{trpy})^{2+}$ groups overlap only partially. The sole complex of the $\{\text{M}(\text{trpy})\}_2\text{L}^{n+}$ type known before this report is $\{\text{Pt}(\text{trpy})\}_2\text{Pt}(\text{SCH}_2\text{CH}_2\text{NH}_2)_2^{4+}$,¹⁶⁷ in which the torsion angle between the two $\text{Pt}(\text{trpy})^{2+}$ units appears to be ca. 90°.

The Pt-Pt distance in $\{\text{Pt}(\text{trpy})\}_2\text{Can}^{3+}$ (ca. 2.99 Å in both types I and II) is much shorter than the distances between nonbonded platinum atoms in $\{\text{Pt}(\text{trpy})\}_2\text{Pt}(\text{SCH}_2\text{CH}_2\text{NH}_2)_2^{4+}$ (ca. 4.42 Å)¹⁶⁷ and in stacked $\text{Pt}(\text{trpy})(\text{SCH}_2\text{CH}_2\text{OH})^+$ (ca. 3.57 Å),⁹¹ comparable to the distances between the weakly-bonded platinum atoms in the partially oxidized $\text{Pt}(\text{CN})_4^{(2-\delta)-}$ anions (2.8-3.0 Å);¹⁷⁵⁻¹⁷⁹ but longer than the distances between the singly-bonded platinum atoms in the binuclear Pt(III)-Pt(III) and Pt(I)-Pt(I) compounds (2.5-2.8 Å). The band at ca. 480 nm in the absorption spectra of the $\{\text{Pt}(\text{trpy})\}_2\text{L}^{3+}$ complexes with MeGua, Arg, and Can as bridging ligands L probably is due to electronic interactions between the π systems and between the metal orbitals of the two proximate $\text{Pt}(\text{trpy})^{2+}$ groups.

Red Complexes $\{\text{Pt}(\text{trpy})\}_2\text{MeGua}^{4+}$ and $\{\text{Pt}(\text{trpy})\}_2\text{Arg}^{3+}$ The structures of these complexes, in the main, probably are similar to the structure of their canavanine

homolog. Since they show one ^{195}Pt signal each, the two platinum atoms in each complex are equivalent or nearly so, at least in solution. Attempts so far to obtain a suitable crystal of either of these complexes have failed.

CONCLUSIONS AND PROSPECTS

This study shows, for the first time, that guanidine group can act as a bridging ligand in bimetallic complexes. The N-N distance of ca. 2.3 Å is compatible with single bonds involving first-row and second-row transition metals. In proteins, however, guanidine groups with low pKa may serve as terminal ligands to Pt(trpy)Cl⁺ complex, as in Arg 91 in cytochromes. These findings may point the way toward a heavy-atom tag for arginine residues in proteins, a tool needed by protein crystallographers. These findings also show that arginine side chain is a potential ligand in metalloproteins and in metal-dependent enzymes. Arginine coordination should be facilitated by environmental effects, such as hydrophobicity and proximity to α-helical polypeptide segments, that diminish the basicity of the guanidine group. Although arginine certainly is not as common a biological ligand as histidine, the similarity between the nitrogen atoms in the guanidine group and in the imidazole ring is worth noting.

SECTION VI.

INTERACTIONS OF $(PT(TRPY))_2CAN^{3+}$ WITH NUCLEIC ACIDS

INTRODUCTION

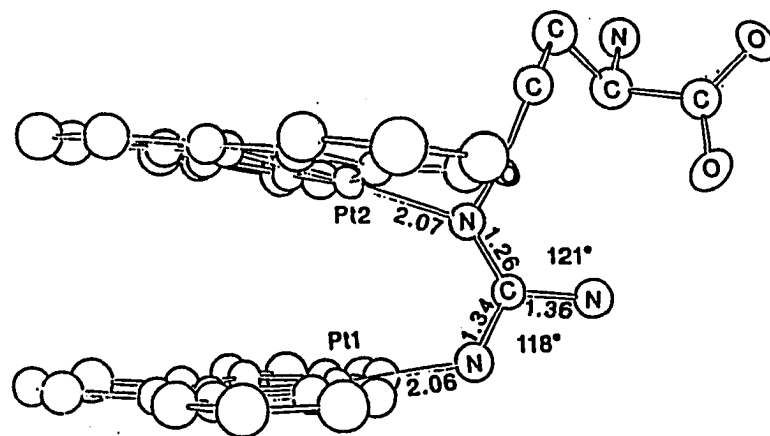
DNA is now increasingly recognized to have a heterogeneous structure¹⁸⁰⁻¹⁸³ and that DNA contributes to specificity of protein interaction by its ability to exist in alternate conformations or to deform its structure as it accommodates the protein.^{182,183} A wide range of unusual structural variations¹⁸⁰⁻¹⁸³ – bends, kinks, loops, single-stranded loops, left-handed sites, supercoils, cruciforms, and more recently, G-quartets¹⁸⁴ – may exist within a DNA.

Studies directed toward the design of site- and conformation- specific reagents are useful for rational drug design and as a means to develop chemical probes of polynucleotide structure, especially since standard structural methods are often difficult.^{7,34,182,183,185} In this regard, metal complexes have proven useful as chemical probes of DNA structure,^{7,34,185-193} as mediators for cleavage of duplex DNA,¹⁹⁴⁻¹⁹⁹ and as chemotherapeutic agents.^{34,185} Iron(III) chelates tethered to an intercalating or groove-binding group as well as metallointercalators with redox active centers which cleave DNA upon photoactivation have been successfully employed.¹⁹⁴⁻¹⁹⁸

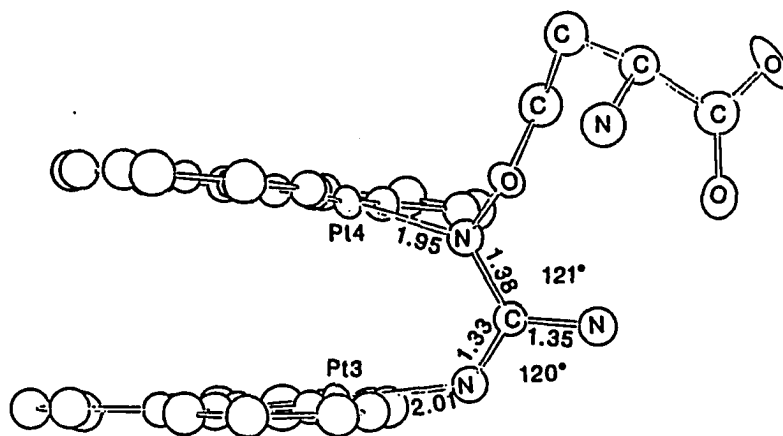
Platinum(II) complexes, in particular, are advantageous as biological probes for they are relatively kinetically inert, non-redox active, and are better behaved in the electron microscope than other heavy metals.^{34,185} Moreover, terpyridine platinum(II) complexes can bind by intercalation with nucleic acids leading to their utility as electron dense probes of intercalation and nucleic acid structure.^{30,34,37,91,185,200-203}

The complex $[(\text{Pt}(\text{trpy}))_2\text{Can}](\text{ClO}_4)_3$ in which the two $\text{Pt}(\text{trpy})^{2+}$ moieties are stacked and separated by ca. 3 Å⁰ (see Figure VI-1, from the crystallographic study in Section V) provides an interesting test case for double-decker type metallointercalation,

perhaps, with the unusual conformations within the DNA or for deformation of DNA structure to accommodate such an interaction.



Type I



Type II

Figure VI-1. ORTEP Drawing of $[(Pt(trpy))_2Can](ClO_4)_3 \cdot 5.5 H_2O$ Illustrating the π -Stacking Interactions

EXPERIMENTAL SECTION

Materials

Nucleic Acids Calf thymus DNA of Type XV [$\epsilon(P)_{260} = 6600 \text{ M(P)}^{-1} \text{ cm}^{-1}$] from Sigma Chemical Co., having an A_{260}/A_{280} greater than 1.8 which rules out protein contamination,^{204,205} was used as received. Closed circular superhelical PBR322 plasmid in the lyophilized form and Bacteriophage T4 DNA were used as received from Sigma. The synthetic polynucleotides poly(dA) [$\epsilon(P)_{257} = 8600 \text{ M(P)}^{-1} \text{ cm}^{-1}$],²⁰⁶ poly(dT) [$\epsilon(P)_{264} = 8520^{207}$ or $8400^{208} \text{ M(P)}^{-1} \text{ cm}^{-1}$], poly(dG) [$\epsilon(P)_{253} = 10100^{209}$ or $9700^{208} \text{ M(P)}^{-1} \text{ cm}^{-1}$], poly(dC) [$\epsilon(P)_{274} = 7400^{207}$ or $6800^{208} \text{ M(P)}^{-1} \text{ cm}^{-1}$], poly(dA)·poly(dT) [$\epsilon(P)_{260} = 6000 \text{ M(P)}^{-1} \text{ cm}^{-1}$],²¹⁰ poly(dG)·poly(dC) [$\epsilon(P)_{253} = 7400 \text{ M(P)}^{-1} \text{ cm}^{-1}$],²⁰⁸ poly(dA-dT)·poly(dA-dT) [$\epsilon(P)_{262} = 6600 \text{ M(P)}^{-1} \text{ cm}^{-1}$],²⁰⁸ and poly(dG-dC)·poly(dG-dC) [$\epsilon(P)_{254} = 8400 \text{ M(P)}^{-1} \text{ cm}^{-1}$],²¹⁰ were from Pharmacia-LKB Biotechnology. The ammonium salts of the oligonucleotides d(pA)₈, d(pC)₈, and d(pT)₈ were from Sigma Chemical Co.

Platinum Complexes The complex $[(\text{Pt}(\text{trpy}))_2\text{Can}](\text{ClO}_4)_3$ [$\epsilon_{480} = 4000 \text{ M}^{-1} \text{ cm}^{-1}$] was synthesized according to the previous Section. The complex $[\text{Pt}(\text{en})_3]\text{Cl}_4$ was prepared according to known procedures.^{211,212}

Buffers All experiments were carried out in the following buffers: (a) buffer 1 – 1 mM sodium phosphate, 3 mM NaCl, pH 6.8; (b) buffer 2 – 1 mM sodium phosphate, 3 mM NaCl, pH 7.5; (c) buffer 3 – 50 mM Tris·HCl, 100 mM NaCl, pH 7.5; (d) buffer 4 – 5 mM Tris·HCl, 10 mM NaCl, pH 7.5; (e) buffer 5 – 5 mM Tris·HCl, 50 mM NaCl, pH 7.5; (f) buffer 6 – 5 mM Tris·HCl, 100 mM NaCl, and (g) buffer 7 – 40 mM Tris, 20 mM Acetate, 1 mM EDTA, pH 8.0. All solutions were prepared using deionized water of resistivity $>16 \text{ M}\Omega \text{ cm}$.

Methods

Optical Spectroscopy UV-visible spectra of solutions in 1-cm pathlength cells were recorded using an IBM 9430 spectrophotometer with a double grating. The spectrum for the solid $[(\text{Pt}(\text{trpy}))_2\text{Can}](\text{ClO}_4)_3$ was obtained from a CsI pellet.

Thermal Denaturation Thermal denaturation curves were measured by monitoring at 260 nm the increase in absorbance for calf thymus DNA using the spectrophotometer and a thermostatted cell holder regulated by a Fisher isotemp circulator model 9500. Relative absorbancies from two to three trials were averaged. The melting temperature, T_m , corresponds to the temperature at half the change in maximum relative absorbance, according to the literature.²⁰²

Fluorescence Spectroscopy Fluorescence intensities of solutions in 1-cm quartz cells were measured with a SPEX FLUOROLOG 2 spectrofluorimeter at ambient temperature. For the ethidium bromide competitive inhibition studies, solutions were excited at 540 nm and emissions at 590 nm were observed.²¹³ The calf thymus DNA concentration was kept constant at 3.5 μM , while ethidium bromide concentrations were varied from 4.9 to 18 μM in the absence and in the presence of varying molar ratios of $[(\text{Pt}(\text{trpy}))_2\text{Can}](\text{ClO}_4)_3$ to DNA, M/D, in the range 0.22 to 2.2.

Viscosity Viscosity measurements were carried out in a Zimm-Crothers low shear viscometer^{214,215} at 25°C using a Forma Scientific 2067 Circulatory Bath for thermal regulation. Solutions in buffer 2 were filtered in a fine-fritted funnel prior to mixing. The concentration of DNA was kept constant at 99.7 μM while the amounts of $[(\text{Pt}(\text{trpy}))_2\text{Can}](\text{ClO}_4)_3$ were varied to give various r (ratio of bound complex to DNA) values, based on equilibrium binding analysis in buffer 2.

Equilibrium Dialysis Spectra-Por-3 dialysis tubing with cut-off MW of 3500 obtained from Fisher Scientific was prepared according to standard procedures.²¹⁶ One

ml of retentates (solutions within the dialysis bags) containing a 500 μM solution of calf-thymus DNA were dialyzed against 2.0 ml dialysates (solutions outside the bags) containing $[\{\text{Pt}(\text{trpy})\}_2\text{Can}](\text{ClO}_4)_3$ concentrations in the range 25 μM to 500 μM for 12 h at 22^o C, after which time equilibration was achieved. Upon equilibration, dialysates and retentates were separated and analyzed by UV-visible spectroscopy. Free concentrations of $\{\text{Pt}(\text{trpy})\}_2\text{Can}^{3+}$ were determined at 480 nm using $\epsilon=4000 \text{ M}^{-1} \text{ cm}^{-1}$ and at 370 nm using $\epsilon=7500 \text{ M}^{-1} \text{ cm}^{-1}$. To remove uncertainties for bound $\{\text{Pt}(\text{trpy})\}_2\text{Can}^{3+}$ concentrations, the retentates can be made 1.0 M NaCl to dissociate the platinum complex, and extinction coefficients for the free complex can be used.

Gel Electrophoresis The PBR322 plasmid was incubated in buffer 7 with varying amounts of metal complex in the range 5 μM to 120 μM for 2 h; usually, 0.3 μg of DNA per lane was used. After incubation, the solution was treated with ethanol, vortexed, centrifuged and decanted. The residue was then redissolved in buffer 7 and mixed with the 10x loading solution consisting of 30 % ficoll dye, 0.25% bromophenol blue and 0.2 M EDTA. The samples were then loaded onto a 20-well minigel made of 0.5 to 2.0 % agarose in buffer 7. The results from several trials using the same conditions can be averaged when the R_f values are based on the mobility of supercoiled circular plasmid. The 0.5% gels were formed by layering the 0.5 % agarose solution onto a previously molded 1 % agarose gel. This gel was kept at 4 ^oC and electrophoresis was carried out at 100 V for 3 h at 4^oC. The 1 and 2% gels were run at 50 V for 4 h at 22^oC.

The polynucleotides were incubated with equivalent amounts of $\{\text{Pt}(\text{trpy})\}_2\text{Can}^{3+}$ in buffer 7 for 10 minutes, mixed with the 10x loading solution of ficoll dye-bromophenol blue-EDTA and loaded onto 2 % agarose gels. Electrophoresis for 1.5 h at 50 V and 22 ^oC was usually employed.

The bands were visualized by staining with solutions in buffer 7 containing 0.5 $\mu\text{g}/\text{mL}$ ethidium bromide for 30 min (when necessary, the staining solution was also

made 100 mM NaCl to dissociate $\{\text{Pt}(\text{trpy})\}_2\text{Ca}^{3+}$ in highly loaded bands) and subsequent destaining in the same buffer solution for at least 2 hours was employed. Photographs using Polaroid 55 P/N film of the gel with UV light from below were taken for 30 s or 45 s exposure using the Fotodyne Camera Device.

RESULTS AND DISCUSSION

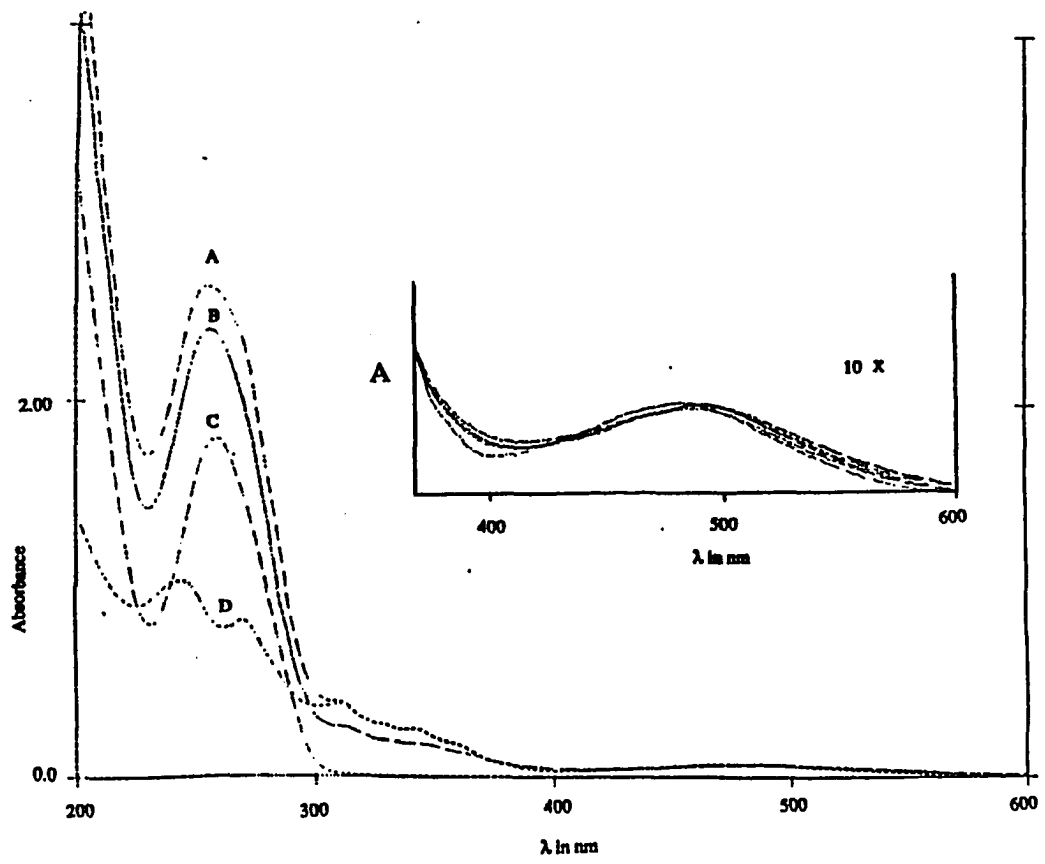
Spectroscopic Studies

Noncovalent and noncoulombic interactions,^{192,217,218} and electrostatic interactions¹⁹² can induce changes in the electronic spectra of molecules bound to DNA. However, intercalation, an example of the first type of interaction, has the greatest effect on the electronic properties.^{192,217}

Binding of $\{\text{Pt}(\text{trpy})\}_2\text{Ca}^{3+}$ with calf thymus DNA shows a decrease in absorption or hypochromicity and a corresponding increase in maximum wavelength or bathochromic shift. This hypochromic effect in the charge-transfer bands below 360 nm of $\{\text{Pt}(\text{trpy})\}_2\text{Ca}^{3+}$ as a result of binding to the polynucleotide is illustrated in Figure VI-2. The interaction is real as shown by the overlay of the hypothetical addition spectrum of the DNA and metal complex in which no physical interaction occurs and of the actual mixture of DNA and metal complex (see Figure VI-2). There appears to be an isosbestic point at 370 nm from this overlay of spectra.

The inset shows the large shift in the red band of $\{\text{Pt}(\text{trpy})\}_2\text{Ca}^{3+}$ from 480 nm to 490 nm. This red band is believed to arise from metal to ligand charge transfer, in which the interaction between the two platinum atoms which exist in the solid state structure contributes to this band in solution as it does in the solid state spectrum (see Figure VI-3). The solid state spectrum below 260 nm has strong contributions from the CsI matrix, hence, this range is not shown. The near-UV range bands become broader and less distinct, perhaps, due to the sensitivity of these bands to the environment. The ratios of the extinction coefficients in these range of λ to that of the 480 nm band are at best close to the ratios for the solution spectrum. Perhaps the strong contribution of the platinum

Figure VI-2. Absorption Spectra of $\{Pt(trpy)\}_2Can^{3+}$ in the Absence and in the Presence of Calf Thymus DNA in Buffer 1. Curve A is the hypothetical addition spectrum of 270 μM DNA and 12.5 μM $\{Pt(trpy)\}_2Can^{3+}$, B is the actual spectrum of a solution containing 270 μM DNA and 12.5 μM complex, C is the spectrum of 270 μM native DNA and D is the spectrum of 12.5 μM free complex. In the inset, the red band at 480 nm upon interaction with DNA is shown to shift to the red with increasing DNA to $\{Pt(trpy)\}_2Can^{3+}$ molar ratio



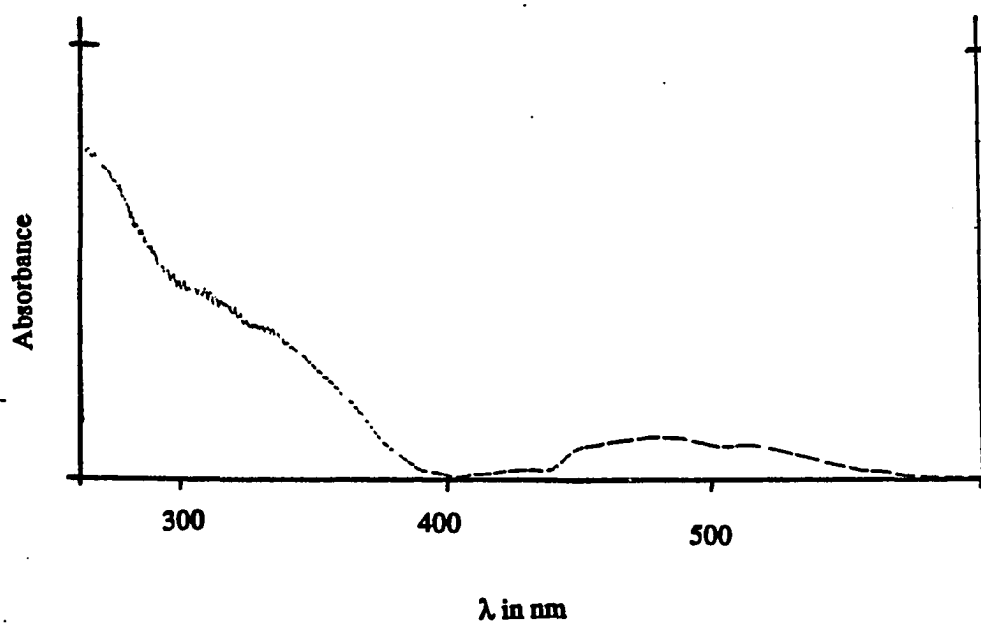


Figure VI-3. Absorption Spectrum of Solid $[\text{Pt}(\text{trpy})_2]_2\text{Can}(\text{ClO}_4)_3 \cdot 5.5 \text{H}_2\text{O}$ as a CsI Pellet

interactions accounts for the retention of the 480 nm band feature in the solid state spectrum in contrast to the almost featureless charge transfer bands in the near-UV range.

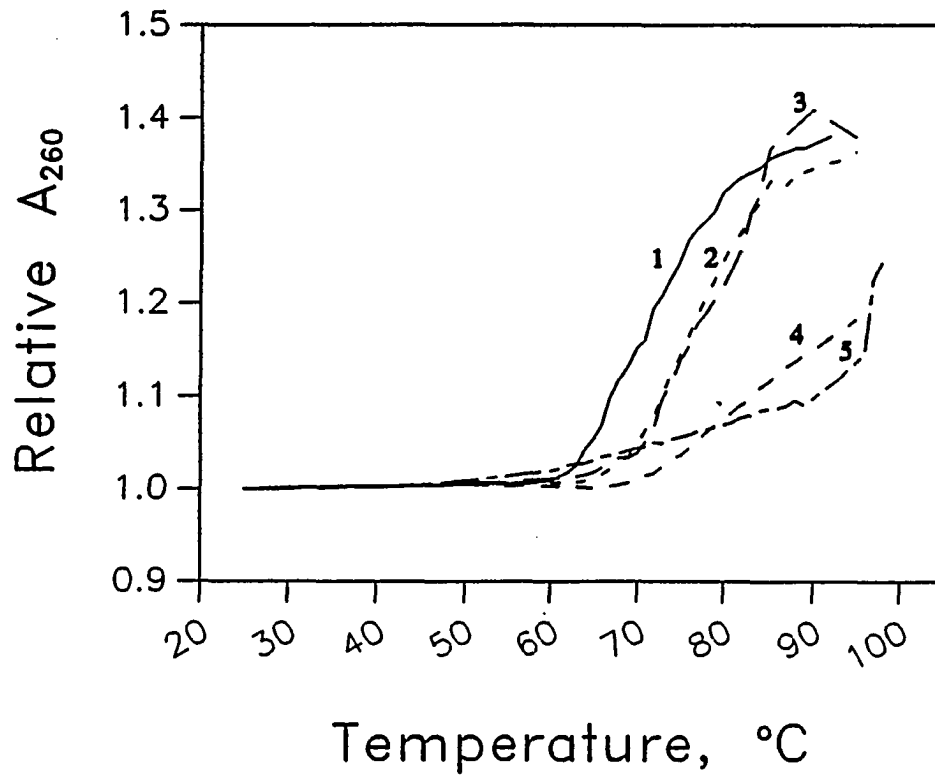
The hypochromic effect below 360 nm as shown in Figure VI-2 is comparable to the $M(\text{phen})_3^{n+}$ complexes⁷ and is lower than its related metallointercalator, $\text{Pt}(\text{trpy})\text{HET}^+$.²⁰⁰ Use of tandem cells for mixing DNA and $\{\text{Pt}(\text{trpy})\}_2\text{Can}^{3+}$ solutions, however, showed a decreased hypochromic effect below 360 nm, and an apparent isosbestic point at 362 nm. These apparent differences with respect to Figure VI-2 may be related to slight increases in absorbance due to slight sample turbidity resulting from the quick mixing of concentrated DNA and $\{\text{Pt}(\text{trpy})\}_2\text{Can}^{3+}$ solutions. In either procedures the large shift to 490 nm is evident and unquestionable. Small shifts in wavelengths at higher energy is found – about 1 to 2 nm only for bands between 300 to 350 nm.

Thermal Denaturation of DNA

The melting behavior of DNA can be affected by molecules bound to DNA that stabilize its duplex nature.^{192,204,218} Electrostatic interaction on the one hand can be differentiated from intercalation or noncovalent and noncoulombic interactions on the other on the basis of T_m curves.¹⁹²

To compare the effect of a highly charged platinum complex on the melting temperature profile, the complex $\text{Pt}(\text{en})_3^{4+}$ was used. At a low molar ratio of metal complex to DNA, M/D of 1/22, (see Figure VI-4) the T_m profile shows similarity in the curve width with native calf thymus DNA, although, the electrostatic interactions have caused a slight increase in T_m – from 71.3 to 76.8 °C or ΔT_m of 5.5 °C. In contrast, the complex $\{\text{Pt}(\text{trpy})\}_2\text{Can}^{3+}$ at the same loading shows a marked difference in curve width and a T_m of 81.7 °C or ΔT_m of 10.4 °C. The different effects on the T_m profiles

Figure VI-4. T_m Curves for Calf Thymus DNA in the Absence (line 1, -) and in the Presence of Varying Metal Complex to DNA Molar Ratios in Buffer 1. The curves obtained in the presence of $\text{Pt}(\text{en})_3^{4+}$ are: line 2, - - -, at M/D of $1/22$ and line 3, — — — , at M/D of $1/5$. The curves obtained in the presence of $\{\text{Pt}(\text{trpy})\}_2\text{Ca}^{3+}$ are: line 4, - - -, at M/D of $1/22$ and line 5, - - -, at M/D of $1/5$



produced by the electrostatic binder, $\text{Pt}(\text{en})_3^{4+}$, and the noncovalently and nonelectrostatically bound complex, $\{\text{Pt}(\text{trpy})\}_2\text{Ca}^{3+}$ become more evident at a high load of metal complex to DNA (see Figure VI-4) than at a lower load – reminiscent of the different effects on the T_m profiles by the nonintercalating and by the intercalating ruthenium complexes.¹⁹² At an M/D of 1/5, the curve width in the case of $\text{Pt}(\text{en})_3^{4+}$ is basically similar and an additional slight increase in T_m or ΔT_m of 6.8 °C is observed. In the latter complex, the curve width is drastically altered and a great increase in T_m or ΔT_m of 22.5 °C is observed.

Binding of $\{\text{Pt}(\text{trpy})\}_2\text{Ca}^{3+}$

Equilibrium Dialysis The results of equilibrium dialysis of calf thymus DNA with $\{\text{Pt}(\text{trpy})\}_2\text{Ca}^{3+}$ at 22 °C in 5 mM Tris buffers of varying NaCl concentrations in the range 10 mM to 100 mM are in the form of Scatchard plots. Conventional Scatchard analysis²⁰¹ by linear regression fits to the Scatchard equation

$$r/C_f = (n-r) K_{\text{app}}$$

gave the apparent binding constants of $\{\text{Pt}(\text{trpy})\}_2\text{Ca}^{3+}$ to calf thymus DNA and n or maximum number of binding sites per nucleotide as listed in Table VI-1. Figure VI-5 shows the dependence of K_{app} on the total positive ion concentration, $[\text{M}^+]$, in solution. The binding affinity as expected from a highly charged species decreases appreciably with increasing ionic strength or increasing $[\text{M}^+]$. The linear plot of $\log K_{\text{app}}$ vs $\log [\text{M}^+]$ may be expressed^{201,219,220} as

$$\log K_{\text{app}} = -m'\psi \log [\text{M}^+] + \log K_0$$

in which K_0 is the value of K_{app} at 1 M Na^+ and is assumed to be free of electrostatic components. Extrapolation to 1 M Na^+ yields a K_0 of $2.9 \times 10^3 \text{ M}^{-1}$. This value which is intrinsic to the nature of the complex is most informative of the strength of binding to

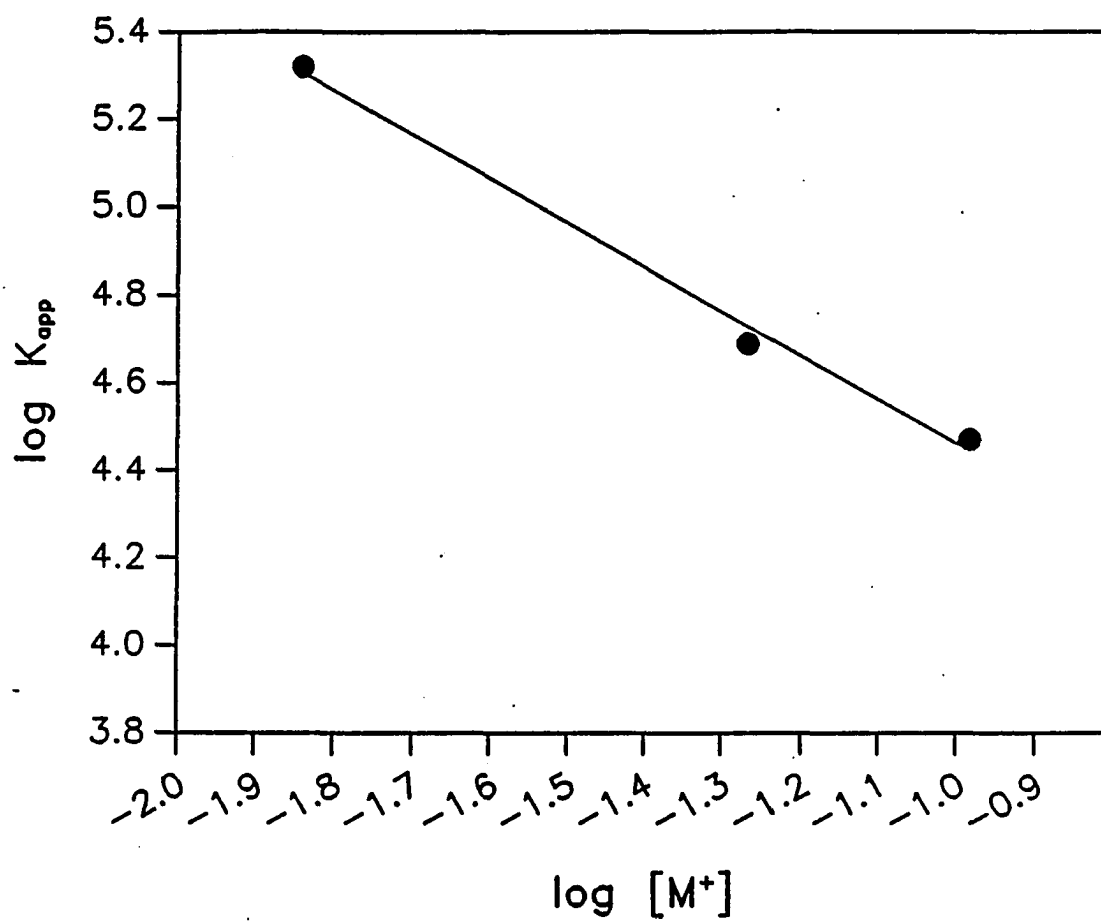


Figure VI-5. Apparent Binding Constant as a Function Total Positive Ion Concentration, M^+

the DNA in the absence of electrostatic contributions. Its K_0 is comparable to $3.5 \times 10^3 \text{ M}^{-1}$, the K_0 value for both the intercalators $\text{Pt}(\text{trpy})\text{HET}^+$ and $\text{Pt}(\text{o-phen})(\text{en})^{2+}$, and one order of magnitude less than the K_0 for ethidium, $7.4 \times 10^4 \text{ M}^{-1}$.²⁰¹ The electrostatic component, given by the slope of 1.0 and indicating the release of 1 monocation per 1.1 phosphate residues, is surprisingly lower than expected value of 3. This is indicative of drastic changes in the phosphate backbone on interaction with the platinum complex. The K_{app} for $\{\text{Pt}(\text{trpy})\}_2\text{Can}^{3+}$ is less than the K_{app} for $\text{Pt}(\text{trpy})\text{HET}^+$ and (see Table VI-1)²⁰¹ and is greater than for $\text{Ru}(\text{phen})^{2+}$ (*vide infra*).²²⁰

Competitive Inhibition by Fluorescence Analysis The fluorescence Scatchard plots for competitive inhibition of ethidium bromide by $\{\text{Pt}(\text{trpy})\}_2\text{Can}^{3+}$ in buffer 3 (see Figure VI-6) shows that at high ionic strength, the highly charged $\{\text{Pt}(\text{trpy})\}_2\text{Can}^{3+}$ cannot compete with the monocation, ethidium bromide. The luminescence of the ethidium bromide-DNA complex is not quenched by the $\{\text{Pt}(\text{trpy})\}_2\text{Can}^{3+}$ at low molar ratios of metal complex to DNA. At the higher limit (M/D of 2.2), slight quenching of luminescence is evident. The platinum complex at this higher loading is now able to compete through noncovalent interactions perhaps at the minor groove.

At low ionic strengths such as in buffer 2 wherein the DNA is easily saturated with binding ligands both by electrostatic and by noncoulombic modes, the presence of $\{\text{Pt}(\text{trpy})\}_2\text{Can}^{3+}$ affects drastically the luminescence of ethidium bromide bound to DNA. Even at low levels of metal complex to DNA (M/D of 0.22), the luminescence of solutions containing DNA and ethidium bromide approaches that of free ethidium bromide. This indicates that ethidium bromide is not intercalated into the DNA in this mixture containing $\{\text{Pt}(\text{trpy})\}_2\text{Can}^{3+}$. Hence, $\{\text{Pt}(\text{trpy})\}_2\text{Can}^{3+}$ has effectively blocked the intercalation sites of ethidium bromide in buffer 2, perhaps by its strong electrostatic interaction for the polyphosphate backbone as well as through its noncovalent and

Table VI-1. Binding Parameters of $\{\text{Pt}(\text{trpy})\}_2\text{Can}^{3+}$ and $\text{Pt}(\text{trpy})\text{HET}^+$ to Calf Thymus DNA at Various Concentrations of Sodium Chloride^a

[Na ⁺],M	$\{\text{Pt}(\text{trpy})\}_2\text{Can}^{3+}$		$\text{Pt}(\text{trpy})\text{HET}^+$	
	$K_{\text{app}} \times 10^{-4}, \text{M}^{-1}$	n	$K_{\text{app}} \times 10^{-4}, \text{M}^{-1}$	n
0.100	2.1	0.14	8.5	0.14
0.050	4.9	0.24	17	0.19
0.010	21	0.23		

^aThe values for $\text{Pt}(\text{trpy})\text{HET}^+$ using 50 mM Tris buffer of pH 7.5, were taken from Ref.

201. The results for $\{\text{Pt}(\text{trpy})\}_2\text{Can}^{3+}$ used 5 mM Tris buffer of pH 7.5.

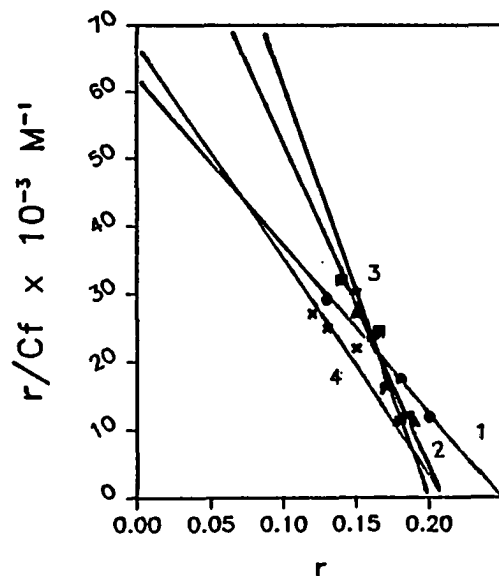


Figure VI-6. Fluorescence Scatchard Plots of Ethidium Bromide Bound to Calf Thymus DNA in Buffer 3 (•, line 1) and in the Presence of Increasing Concentrations of $\{\text{Pt}(\text{trpy})\}_2\text{Ca}^{3+}$ in Metal Complex to DNA Molar Ratios, M/D , of 0.22 (Δ , line 2), of 0.55 (\blacksquare , line 2), of 1.1 (\times , line 3), and of 2.2 (\times , line 4)

noncoulombic interactions with the bases. No Scatchard plots could be obtained in this buffer since essentially negligible binding of ethidium with DNA is observed. This quenching effect of $\{\text{Pt}(\text{trpy})\}_2\text{Can}^{3+}$ or its virtually complete inhibition of ethidium intercalation is illustrated by the plot of I/I_0 vs. increasing amounts of ethidium bromide in various ratios of metal complex to DNA (see Figure VI-7) wherein I_0 is the fluorescence intensity of the free ethidium bromide.

Hydrodynamic Properties

Viscosity Viscosity measurements show that $\{\text{Pt}(\text{trpy})\}_2\text{Can}^{3+}$ like most intercalators^{200,217} and groove binders²²¹ increases the viscosity of DNA. The specific viscosity, η_{sp} , of the DNA solution increases with increasing amounts of $\{\text{Pt}(\text{trpy})\}_2\text{Can}^{3+}$ -bound DNA reaching a saturation value at limiting r (see Figure VI-8). There is an increase in intrinsic viscosity $[\eta]$ by a factor of 1.7.

Electrophoretic Mobility Electrophoretic mobility of DNA may be affected by the presence of a bound ligand on DNA. There is usually a 15 % retardation in DNA mobility for gels containing ethidium bromide.²¹⁶ The effect is more pronounced in the case of supercoiled circular plasmid DNA. An intercalator can cause unwinding of supercoils (form I) to give a relaxed circular DNA (form I_0), and even nicking of DNA to give a retarded DNA band (form II).³⁴

Interestingly, the complex $\{\text{Pt}(\text{trpy})\}_2\text{Can}^{3+}$ induces formation of a highly retarded plasmid that is distinctively seen on the gel. Although at low loadings a less distinct and trailing band occurs with R_f values lower than supercoiled circular plasmid. For 0.3 μg pBR322 in the presence of varying concentrations of $\{\text{Pt}(\text{trpy})\}_2\text{Can}^{3+}$, the trailing has a maximum R_f of: 0.9, 0.8, 0.7, and 0.7 for 10-, 20-, 30-, and 40- μM $\{\text{Pt}(\text{trpy})\}_2\text{Can}^{3+}$, respectively. At higher concentrations of $\{\text{Pt}(\text{trpy})\}_2\text{Can}^{3+}$, the band smears down to a

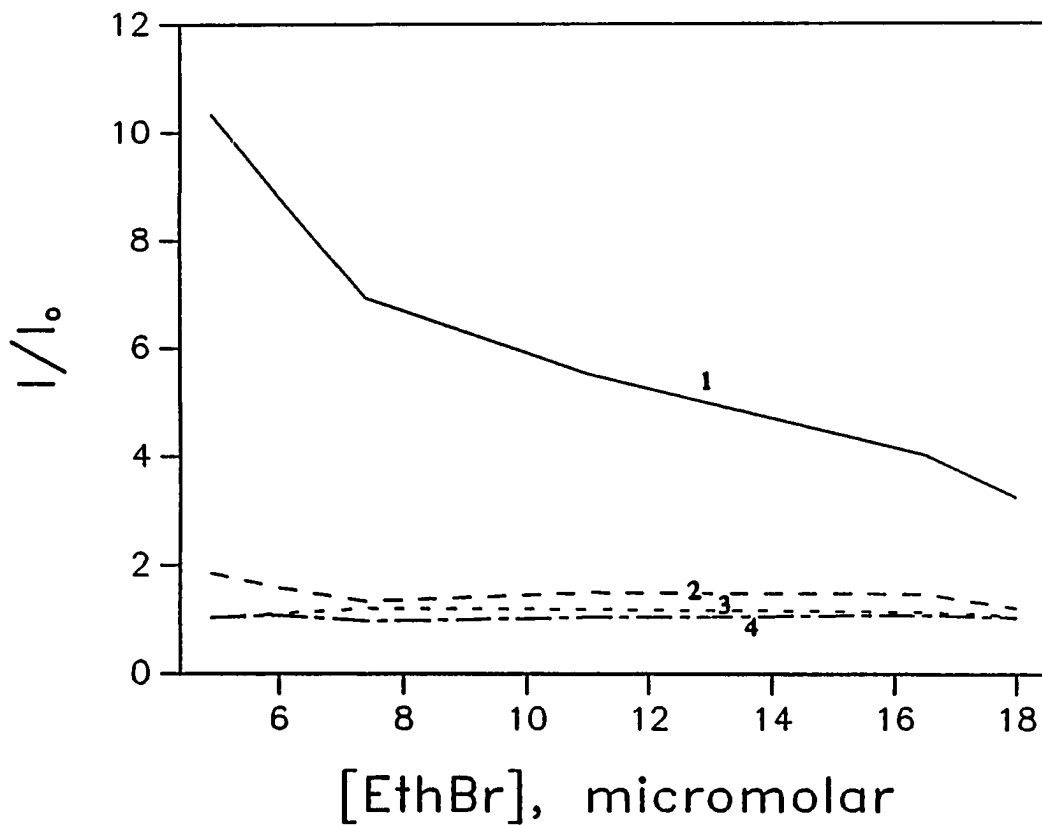


Figure VI-7. Luminescence Quenching of Ethidium Bromide Bound to Calf Thymus DNA in Buffer 2 in the Presence of Various $\{Pt(trpy)\}_2Can^{3+}$ to DNA Molar Ratios, M/D, of 6 (line 1, -), of 0.22 (line 2, ---), of 0.55 (line 3, -.-), and of 1.1 (line 4, ---) with Varying Amounts of Ethidium Bromide (4.9 μM to 18 μM)

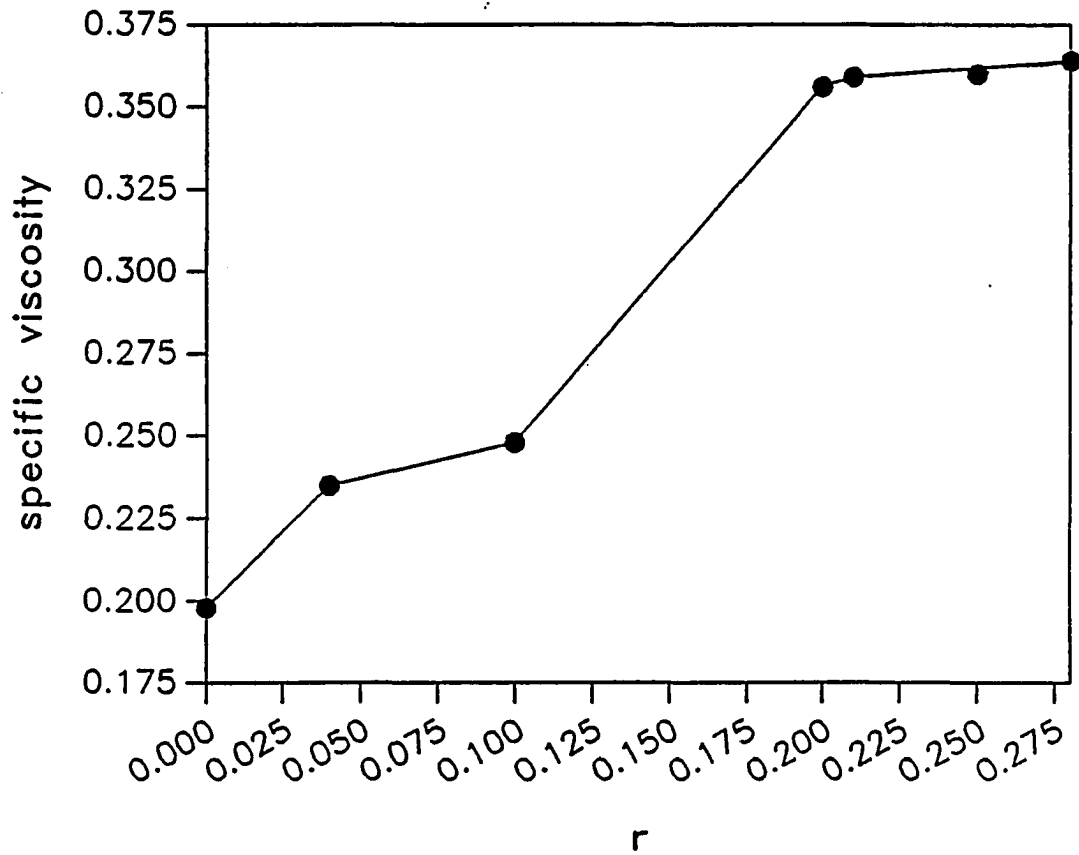


Figure VI-8. Specific Viscosity of Calf Thymus DNA at 25 °C as a Function of r in Buffer 2

maximum R_f of 0.4, which corresponds to form II or nicked DNA. Regardless of $\{\text{Pt}(\text{trpy})\}_2\text{Can}^{3+}$ concentration, the relatively immobile and very distinct band with R_f close to 0.02 is evident in the gel. The smearing or trailing of the band is perhaps indicative of shearing stress on the DNA.

In the case of poly (dG-dC)·poly (dG-dC) a more distinct band is observed with R_f of 0.87 in the presence of low molar ratios of $\{\text{Pt}(\text{trpy})\}_2\text{Can}^{3+}$ to duplex DNA. Increasing the molar ratio in the range 0.4 to 1.0 produces only the relatively immobile band with an R_f close to 0.03. Again, the mere presence of the $\{\text{Pt}(\text{trpy})\}_2\text{Can}^{3+}$ is enough to produce the relatively immobile band.

This relatively immobile band is not simply due to sticking on the agarose well, for it also moves, albeit, at a very slow rate. Compared to supercoiled circular plasmid pBR322, it has an R_f of 0.02. Attempts to move this band farther away from the loading site was successful when a low concentration (0.5 % agarose) gel using 100 V for 3 h at 4 °C was employed. Even so, the band only moved a few mm away from the well, no R_f value could be obtained for the standard supercoiled circular plasmid had gone past the gel's end. No precedents for such immobility in agarose is known.

The electrostatic binder, $\text{Pt}(\text{en})_3^{4+}$, does not affect the mobility of the plasmid regardless of loading ratios. The metallointercalator, $\text{Pt}(\text{trpy})\text{HET}^+$, produces unwinding of DNA causing slight retardation in DNA mobility.⁹¹ Covalent binding with $\text{Pt}(\text{trpy})\text{Cl}^+$ will produce a retarded but mobile band.⁹¹ The relatively immobile band is uniquely present only with the $\{\text{Pt}(\text{trpy})\}_2\text{Can}^{3+}$. The $\text{Zn}(\text{phen})\text{Cl}_2$ shows complete formation of nicked DNA at 40 μM having an R_f of 0.4.²²² At concentrations greater than 40 μM $\{\text{Pt}(\text{trpy})\}_2\text{Can}^{3+}$, complete conversion of the supercoiled form I, however, to both nicked DNA (form II) and immobile bands occurs.

It is possible that the immobile band may be due to polyhelical forms that may have aggregated through external intercalative displacement²²³ forming a G-quartet¹⁸⁴ type

of interaction with the two stacked $\text{Pt}(\text{trpy})^{2+}$ moieties serving as templates. The similarity in the mobility of the immobile band from poly d(G-C)·poly d(G-C) and from the pBR322 may imply similar conformations in both bands. Perhaps, in the case of the circular plasmid, linearization may have to occur initially as the strain of the bulky $\{\text{Pt}(\text{trpy})\}_2\text{Can}^{3+}$ causes not only nicking but breakage of the other phosphate backbone as well – unless the quartet type conformation is possible even with intact or nicked circular DNA.

Site-Specificity

The noncovalent interaction of $\{\text{Pt}(\text{trpy})\}_2\text{Can}^{3+}$ with DNA in low ionic strength buffer as evidenced by the increase in λ_{max} to 490 nm. The effects of various deoxynucleic acids, oligonucleotides, and polynucleotides on the 480 nm band of $\{\text{Pt}(\text{trpy})\}_2\text{Can}^{3+}$ are summarized in Table VI-2.

The 490 nm band in a solution containing both calf thymus DNA and $\{\text{Pt}(\text{trpy})\}_2\text{Can}^{3+}$ decreases back to 480 nm in the presence of formaldehyde. Formaldehyde reacts with purine bases and separates the duplex into single strands. This result initially indicated a requirement for a secondary structure in which the purine and pyrimidine bases are hydrogen-bonded for $\{\text{Pt}(\text{trpy})\}_2\text{Can}^{3+}$ interaction to occur.

Incubations with oligonucleotides, $\text{d}(\text{pA})_8$, $\text{d}(\text{pC})_8$, and $\text{d}(\text{pT})_8$ were consistent with this hypothesis for no bathochromic shifts in the 480 nm band were observed. The homopolymer, poly(dG) showed a bathochromic shift to 494 nm. This was not surprising since poly(dG),²²⁴⁻²²⁶ G-rich regions of immunoglobulin switch regions,²²⁷ and perhaps telomeric G-strings, are known or had been proposed to form four-stranded helices or tetrameric aggregates. Perhaps, $\{\text{Pt}(\text{trpy})\}_2\text{Can}^{3+}$ simply stacked with these

square planar array of guanosine residues. Furthermore, interactions with poly(dG) with intercalating agents had been reported.²²⁸

To verify whether the initial results with the oligonucleotides would be true for their corresponding homopolymers, incubations with poly(dA), poly(dC), and poly(dT) were carried out. Both homopolypyrimidines, poly(dC) and poly(dT), did not show any bathochromic shift in its 480 nm band, again indicating that the interaction with duplex DNA was not simply electrostatic. The result with poly(dA) was somewhat unexpected. Like poly(dG), the bathochromic shift observed was considerably high and its interactions with intercalating agents as had been previously cited²²⁸ may be similar. Alternatively, it is tempting to consider a square planar array of adenosine residues perhaps induced by the $\{\text{Pt}(\text{trpy})\}_2\text{Can}^{3+}$ as a template. Interestingly, this latter view is consistent with the previous discussion on the formation of the highly immobile bands.

Why the oligonucleotide d(pA)_g fails to give the same result is unknown. Perhaps, the $\{\text{Pt}(\text{trpy})\}_2\text{Can}^{3+}$ needs a highly charged polyphosphate backbone for the formation of a tightly bound adduct²²⁹ or that it needs a longer stretch of DNA which is able to form coils and a tertiary structure with a large hydrophobic pocket.

The duplexes of the homopolymers, poly(dG)·poly(dC) and poly(dA)·poly(dT) as well as the duplexes, poly(dG-dC)·poly(dG-dC) and poly(dA-dT)·poly(dA-dT) gave bathochromic shifts of the 480 nm band. It is difficult to assess any preference in binding of the $\{\text{Pt}(\text{trpy})\}_2\text{Can}^{3+}$ complex using the absorption spectra of the mixtures. Other techniques such as NMR, footprinting, and competitive binding analysis by electrophoresis and by circular dichroism will probably be more useful in studying the base or sequence specificity of the platinum complex.

The platinum complex was also incubated with a bacteriophage T4 DNA in which the major groove has already been blocked by the presence of sugar groups.²³⁰ Any interaction with the DNA is thought to arise from interactions with the minor groove.²²⁰

Initially, only a slight increase in λ_{max} was observed. After an hour, the λ_{max} gradually increased to 490 nm and stayed constant, in contrast to the practically instantaneous change to 490 nm with calf thymus DNA which is unglycosylated. Perhaps, $\{\text{Pt}(\text{trpy})\}_2\text{Ca}^{3+}$ interacts at the major groove in unglycosylated DNA and its interaction at the minor groove is kinetically slow compared to its interaction at the major groove.

Table VI-2. Effect of Various Nucleic Acids on the 480 nm Band of $\{Pt(trpy)\}_2Can^{3+}$ in Buffer 1 at a Molar Ratio M/D of 1/22

nucleic acid	effect on 480 nm band
calf thymus DNA	increased to 490 nm
calf thymus DNA + formaldehyde	490 nm band decreased back to 480 nm
d(pA) ₈	no effect
d(pC) ₈	no effect
d(pT) ₈	no effect
poly(dG)	increased to 494 nm
poly(dA)	increased to 495 nm
poly(dC)	no effect
poly(dT)	no effect
poly(dG)·poly(dC)	increased to 490 nm
poly(dG-dC)·poly(dG-dC)	increased to 490 nm
poly(dA)·poly(dT)	increased to 490 nm
poly(dA-dT)·poly(dA-dT)	increased to 490 nm
bacteriophage T4 DNA	gradually increased to 490 nm

CONCLUSIONS AND PROSPECTS

The complex $\{Pt(trpy)\}_2Ca^{3+}$ indeed interacts noncovalently and not solely electrostatically with nucleic acids. Its binding to DNA is sensitive to the ionic strength of the medium as befits a highly charged complex and yet its noncovalent and noncoulombic interactions are strong enough and comparable to its related platinum intercalators.

The formation of an immobile band on agarose gel electrophoresis regardless of the amount of complex incubated with DNA is unique to this complex. Further studies to unambiguously ascribe this phenomenon will be needed. It is interesting to note that the complex interacts with poly(dG) and poly(dA) to give large bathochromic shifts. Whether induction of a square planar array of adenosine residues by suitable templates – akin to the formation of G-quartets and inosine-quartets – occurs will have to be considered in the future.

It appears that the complex is able to interact with the minor groove of the DNA. Since interactions with the minor groove involve more specificity in binding by hydrogen bonding as well as stacking interactions, further studies in that direction might be of merit. There is also an increasing interest for molecules that bind by intercalative displacement,²²³ studies with this platinum complex might shed light in this area.

Once the binding modes of this platinum complex as well as its specificity is unambiguously determined, modifications in the ligand tail can be performed and a metal active site introduced for photoactivated strand scission of specific sites in the nucleic acid. With two heavy atoms in the platinum complex, electron microscopy of nucleic acids with this complex will be very promising.

GENERAL SUMMARY

The use of transition metal complexes as tags and probes for biomolecules is indeed advantageous. With platinum(II) complexes, the reactivity towards amino acid residues in proteins, such as cytochrome c, can be tailored through the choice of ancillary ligand. In the case of the common reagent, PtCl_4^{2-} , reactivity towards the thioethers or methionine is favored. In the case of the new reagent, $\text{Pt}(\text{trpy})\text{Cl}^+$, reactivity and selectivity towards cysteines, histidines, and arginines can be achieved by the proper choice of reaction conditions. Since cysteines are very reactive, selectivity towards cysteine may be achieved through short incubation times. In the case of cytochrome c, wherein the protein has no available cysteines, histidines are the only reactive residues at slightly acidic conditions. Increasing the pH, may effect modification of arginine residues whose pK_a of the guanidyl group have been lowered by its proximity to hydrophobic regions and α -helices, as was seen in the cytochrome c case.

The sensitivity of the $\text{Pt}(\text{trpy})$ chromophore to its environment makes this tag useful in probing the environment of histidine residues in proteins. The covalent modification procedures are mild and nondestructive to the protein. The yields obtained, as in the case of cytochrome c, reflect the accessibility of the binding sites or residues to the inorganic label, thus, making this tag potentially useful in mapping out exposures of residues in proteins especially those whose crystal structures are not yet available. Studies exploring the use of this tag as probes for histidines in active sites of enzymes have been addressed.²³¹

The unprecedented binding of guanidines as well as the arginine in protein to a transition metal complex, shows that arginine can be a potential ligand in metalloproteins and in metal-activated enzymes. Arginine can now no longer be disregarded as an innocuous species in metal-containing proteins. This study now opens up the unexplored

coordination chemistry of the guanidines - for guanidines can not only form terminally coordinated complexes, it can also bridge two metals.

The $\text{Pt}(\text{trpy})^{2+}$ -containing complexes are potentially useful probes for polynucleotide structure. The very electron dense complex, $\{\text{Pt}(\text{trpy})\}_2\text{Ca}^{3+}$, can indeed interact noncovalently with nucleic acids. The unusual phenomenon on gel electrophoresis of DNA incubated with this complex suggests formation of aggregates perhaps with the stacked trpy units serving as templates. Further studies on this unusual occurrence may lead to the area of intercalative displacement in DNA binding, a field that is yet in its infancy. Another generation of DNA-binding metal complexes is in store²³² for potential use as probes of nucleic acids.

BIBLIOGRAPHY

1. Lundblad, R. L.; Noyes, C. M. *Chemical Reagents for Protein Modification*; CRC Press: Columbus, OH, 1984; Vols. I and II.
2. Means, G. E.; Feeney, R. E. *Chemical Modification of Proteins*; Holden-Day: New York, 1971.
3. Sulkowski, E. *Trends Biotech.* 1985, 3, 1.
4. Meares, C. F.; Wensel, T. G. *Acc. Chem. Res.* 1984, 17, 202.
5. Blundell, T. L.; Johnson, L. N. *Protein Crystallography*; Academic Press: New York, 1976; Chapter 8.
6. Kostić, N. M. *Comments Inorg. Chem.* 1988, 8, 137.
7. Barton, J. K. *Comments Inorg. Chem.* 1985, 3, 321 and references cited therein.
8. *Metal-Ligand Interaction in Organic Chemistry and Biochemistry*; Pullman, B., Goldblum, N., Ed.; D. Reidel: Boston, 1977.
9. Hartley, F. R. *The Chemistry of Platinum and Palladium*; Wiley: New York, 1973.
10. Belluco, U. *Organometallic and Coordination Chemistry of Platinum*; Academic Press: New York, 1974.
11. Howe-Grant, M. E.; Lippard, S. J. *Metal Ions Biol. Syst.* 1980, 11, 63.
12. Pregosin, P. S. *Coord. Chem. Rev.* 1982, 44, 247.
13. Pregosin, P. S. *Annu. Rep. NMR Spectrosc.* 1986, 17, 285.
14. Dickerson, R. E.; Eisenberg, D.; Varnum, J.; Kopka, M. L. *J. Mol. Biol.* 1969, 45, 77.

15. Gummin, D. D.; Ratilla, E. M. A.; Kostić, N. M. *Inorg. Chem.* **1986**, *25*, 2429.
16. Galbraith, J. A.; Menzel, K. A.; Ratilla, E. M. A.; Kostić, N. M. *Inorg. Chem.* **1987**, *26*, 2073.
17. Ratilla, E. M. A.; Brothers, H. M., II; Kostić, N. M. *J. Am. Chem. Soc.* **1987**, *109*, 4592.
18. Ratilla, E. M. A.; Kostić, N. M. *J. Am. Chem. Soc.* **1988**, *110*, 4427.
19. Ratilla, E. M. A.; Scott, B. K.; Moxness, M. S.; Kostić, N. M. *Inorg. Chem.* **1990**, *29*, 918.
20. Albano, V. G.; Bellon, P. L.; Scatturin, V. *Chem. Commun.* **1966**, 507.
21. Thomas, T. W.; Underhill, A. E. *Chem. Soc. Rev.* **1972**, *1*, 99.
22. Stucky, G. D.; Schultz, A. J.; Williams, J. M. *Ann. Rev. Mater. Sci.* **1977**, *7*, 301.
23. Basolo, F.; Pearson, R. G. *Mechanisms of Inorganic Reactions*; John Wiley: New York, **1967**.
24. Mureinik, R. J. *Coord. Chem. Rev.* **1978**, *25*, 1.
25. Peloso, A. *Coord. Chem. Rev.* **1973**, *10*, 123.
26. Zhou, Xia-Ying, M.S. Thesis, Iowa State University, 1989.
27. Melius, P.; Friedman, M. E. *Inorg. Perspect. Biol. Med.* **1977**, *1*, 1.
28. Volshtein, L. M. *Sov. J. Coord. Chem.* **1975**, *1*, 483.
29. Thomson, A. J.; Williams, R. J. P.; Reslova, S. *Struct. Bonding (Berlin)*, **1972**, *11*, 1.
30. Howe-Grant, M.; Wu, K. C.; Bauer, W. R.; Lippard, S. J. *Biochemistry* **1976**, *15*, 4339.
31. Friedman, M. E.; Teggin, J. E. *Biochim. Biophys. Acta* **1974**, *341*, 277.

32. Sherman, S. E.; Gibson, D.; Wang, A. H. J.; Lippard, S. J. *J. Am. Chem. Soc.* **1988**, *110*, 7368.
33. Mansy, S.; Chu, Y.-H.; Duncan, R. E.; Tobias, R. S. *J. Am. Chem. Soc.* **1978**, *100*, 607.
34. Lippard, S. J. *Acc. Chem. Res.* **1978**, *11*, 211.
35. Miller, S. K.; Marzilli, L. G. *Inorg. Chem.* **1985**, *24*, 2421.
36. Sparks, S. W.; Ellis, P. D. *J. Am. Chem. Soc.* **1986**, *108*, 3215.
37. Strothkamp, K. G.; Lippard, S. J. *Proc. Natl. Acad. Sci. U.S.A.* **1976**, *73*, 2536.
38. Abel, E. W.; Bhargava, S. K.; Orrell, K. G. *Prog. Inorg. Chem.* **1984**, *32*, 1.
39. Kjaer, A.; Wagner, S. *Acta Chem. Scand.* **1955**, *9*, 721.
40. Wheeler, G. P.; Ingersoll, A. W. *J. Am. Chem. Soc.* **1951**, *73*, 4604.
41. Goggin, P. L.; Goodfellow, R. J.; Haddock, S. R.; Taylor, B. F.; Marshall, R. H. *J. Chem. Soc., Dalton Trans.* **1976**, 459.
42. Theodorou, V.; Hadjiliadis, N. *Polyhedron* **1985**, *4*, 1283.
43. Livingstone, S. E.; Nolan, J. D. *Inorg. Chem.* **1968**, *7*, 1447.
44. Roulet, R.; Barbey, C. *Helv. Chim. Acta* **1973**, *56*, 2179.
45. Goggin, P. L.; Goodfellow, R. J.; Haddock, S. R.; Reed, F. J. S.; Smith, J. G.; Thomas, K. *M. J. Chem. Soc., Dalton Trans.* **1972**, 1904.
46. Scott, J. D.; Puddephatt, R. J. *Organometallics* **1983**, *2*, 1643.
47. Sutherland, I. O. *Annu. Rep. NMR Spectrosc.* **1971**, *4*, 71.
48. Gunther, H. *NMR Spectroscopy*; John Wiley: New York, 1980; Chapter 8.
49. Binsch, G.; Kessler, H. *Angew. Chem., Int. Ed. Engl.* **1980**, *19*, 411.

50. Sandstrom, J. *Dynamic NMR Spectroscopy*; Academic Press: New York, 1982; Chapters 6 and 7.
51. Cross, R. J.; Green, T. H.; Keat, R. *J. Chem. Soc., Dalton Trans.* 1976, 1150.
52. Cross, R. J.; Green, T. H.; Keat, R.; Patterson, J. F. *J. Chem. Soc., Dalton Trans.* 1976, 1486.
53. McFarlane, W. *J. Chem. Soc., Dalton Trans.* 1974, 324.
54. Pregosin, P. S.; Sze, S. N.; Salvadori, P.; Lazzaroni, R. *Helv. Chim. Acta* 1977, 60, 2514.
55. Shinoda, S.; Yamaguchi, Y.; Saito, Y. *Inorg. Chem.* 1979, 18, 673.
56. Erickson, L. E.; McDonald, J. W.; Howie, J. K.; Clow, R. P. *J. Am. Chem. Soc.* 1968, 90, 6371.
57. Jezowska-Trzebiatowska, B.; Allain, A.; Kozlowski, H. *Inorg. Nucl. Chem. Lett.* 1979, 15, 279.
58. Theodorou, V.; Photaki, I.; Hadjiliadis, N.; Gellert, R. W.; Bau, R. *Inorg. Chim. Acta* 1982, 60, 1.
59. Kozlowski, H.; Siatecki, Z.; Jezowska-Trzebiatowska, B.; Allain, A. *Inorg. Chim. Acta* 1980, 46, L25.
60. Erickson, L. E.; Dappen, A. J.; Uhlenhopp, J. C. *J. Am. Chem. Soc.* 1969, 91, 2510.
61. Erickson, L. E.; Fritz, H. L.; May, R. J.; Wright, D. A. *J. Am. Chem. Soc.* 1969, 91, 2513.
62. Erickson, L. E.; Erickson, M. D.; Smith, B. L. *Inorg. Chem.* 1973, 12, 412.
63. Battaglia, L. P.; Bonamartini Corradi, A.; Grasselli Palmieri, C.; Nardelli, M.; Vidoni Tani, M. E. *Acta Crystallogr., Sect. B: Struct. Crystallogr. Cryst. Chem.* 1973, B29, 762.

64. **Burgeson, I. E.; Kostić, N. M., Dept. of Chemistry, Iowa State University, Research in Progress.**
65. **Pielak, G. J.; Urdea, M. S.; Legg, J. I. *Biochemistry* 1984, 23, 596.**
66. **Legg, J. I.; Igi, K.; Pielak, G. J.; Warner, B. D.; Urdea, M. S. *ACS Symp. Ser.* 1980, 119, 195.**
67. **Legg, J. I. *Coord. Chem. Rev.* 1978, 25, 103.**
68. **Johansen, J. T.; Livingston, D. M.; Vallee, B. L. *Biochemistry* 1972, 11, 2574.**
69. **Sokolovsky, M.; Riordan, J. F.; Vallee, B. L. *Biochem. Biophys. Res. Commun.* 1967, 27, 20.**
70. **Benisek, W. F.; Richards, F. M. *J. Biol. Chem.* 1968, 243, 4267.**
71. **Werber, W. M.; Lanir, A. *Isr. J. Chem.* 1981, 21, 34 and references cited therein.**
72. **Pecoraro, V. L.; Rawlings, J.; Cleland, W. W. *Biochemistry* 1984, 23, 153.**
73. **Werber, M. M.; Danchin, A. *Methods Enzymol.* 1977, 46, 312.**
74. **Recchia, J.; Matthews, C. R.; Rhee, M.-J.; Horrocks, W. DeW. *Biochim. Biophys. Acta* 1982, 702, 105.**
75. **Nocera, D. G.; Winkler, J. R.; Yocom, K. M.; Bordignon, E.; Gray, H. B. *J. Am. Chem. Soc.* 1984, 106, 5145.**
76. **Kostić, N. M.; Margalit, R.; Che, C.-M.; Gray, H. B. *J. Am. Chem. Soc.* 1983, 105, 7765.**
77. **Isied, S. S.; Kuehn, C.; Worosila, G. J. *J. Am. Chem. Soc.* 1984, 106, 1722.**
78. **Cruthcley, R. J.; Ellis, W. R.; Gray, H. B. *J. Am. Chem. Soc.* 1985, 107, 5002.**
79. **Brautigan, D. L.; Ferguson-Miller, S.; Margoliash, E. *Methods Enzymol.* 1978, 53, 129.**

80. Howe-Grant, M.; Lippard, S. J. *Inorg. Synth.* 1980, 20, 101.
81. Schilt, A. A.; Taylor, R. C.; *J. Inorg. Nucl. Chem.* 1959, 9, 211.
82. Markley, J. L. *Acc. Chem. Res.* 1975, 8, 70.
83. Botelho, L. H.; Gurd, F. R. N. *Biochemistry* 1978, 17, 5188.
84. Dobson, C. M.; Moore, G. R.; Williams, R. J. P. *FEBS Lett.* 1975, 51, 60.
85. Campbell, I. D.; Dobson, C. M.; Williams, R. J. P.; Xavier, A. V. *J. Magn. Reson.* 1973, 11, 172.
86. Brevard, C.; Granger, P. *Handbook of High Resolution Multinuclear NMR*; John Wiley: New York, 1981.
87. Yocom, K. M.; Shelton, J. B.; Shelton, J. R.; Schroeder, W. A.; Worosila, G.; Isied, S. S.; Bordignon, E.; Gray, H. B. *Proc. Natl. Acad. Sci. U.S.A.* 1982, 79, 7052.
88. Brautigam, D. L.; Ferguson-Miller, S.; Tarr, G. E.; Margoliash, E. *J. Biol. Chem.* 1978, 253, 140.
89. Eddowes, M. M.; Hill, H. A. O. *J. Am. Chem. Soc.* 1979, 101, 4461.
90. Hall, M. B.; Fenske, R. F. *Inorg. Chem.* 1972, 11, 768.
91. Jennette, K. W.; Gill, J. T.; Sadowick, J. A.; Lippard, S. J. *J. Am. Chem. Soc.* 1976, 98, 6159.
92. Spofford, W. A.; Amma, E. L.; Senoff, C. V. *Inorg. Chem.* 1971, 10, 2309.
93. Barnes, J. C.; Hunter, G.; Lown, M. W. *J. Chem. Soc., Dalton Trans.* 1977, 458.
94. Bales, J. R.; Mazid, M. A.; Sadler, P. J.; Aggarwal, A. A.; Kuroda, R.; Neidle, S.; Gilmour, D. W.; Peart, B. J.; Ramsden, C. A. *J. Chem. Soc., Dalton Trans.* 1985, 795.

95. Carmichael, J. W.; Chan, N.; Cordes, A. W.; Fair, C. K.; Johnson, D. A. *Inorg. Chem.* **1972**, *11*, 1117.
96. Perrin, D. D. *Dissociation Constants of Organic Bases in Aqueous Solution*; Butterworth and Co., Ltd.: London, England, 1965; p 1393.
97. Ismail, I. M.; Sadler, P. J. In *Platinum, Gold, and Other Metal Chemotherapeutic Agents*; Lippard, S. J., Ed.; ACS Symposium Series 209; American Chemical Society: Washington, DC, 1983; pp 171-190.
98. Tran, T.; Lintner, K.; Toma, F.; Femandjian, S. *Biochim. Biophys. Acta* **1977**, *492*, 245.
99. Nakamura, A.; Jardetzky, O. *Proc. Natl. Acad. Sci. U.S.A.* **1967**, *58*, 2212.
100. Kozlowski, H.; Matczak-Jon, E. *Inorg. Chim. Acta* **1979**, *32*, 143.
101. van Kralingen, C. G.; de Ridder, J. K.; Reedjik, J. *Inorg. Chim. Acta* **1979**, *36*, 69.
102. van Kralingen, C. G.; Reedjik, J. *Inorg. Chim. Acta* **1978**, *30*, 171.
103. Cattalini, L.; Martelli, M.; Kirschner, G. *Inorg. Chem.* **1968**, *7*, 1488.
104. Pearson, R. G.; Sobel, H.; Songstad, J. J. *Am. Chem. Soc.* **1968**, *90*, 319.
105. Murray, S. G.; Hartley, F. R. *Chem. Rev.* **1981**, *81*, 365.
106. Mureinik, R. J.; Bidani, M. *Inorg. Chim. Acta* **1978**, *29*, 37.
107. Mureinik, R. J.; Bidani, M. *Inorg. Nucl. Chem. Lett.* **1977**, *13*, 625.
108. Bonivento, M.; Canovese, L.; Cattalini, L.; Marangoni, G.; Michelson, G.; Tobe, M. L. *Inorg. Chem.* **1983**, *22*, 802.
109. Schejter, A.; George, P. *Biochemistry* **1964**, *3*, 1045.
110. Myer, Y. P.; MacDonald, L. H.; Verma, B. C.; Pande, A. *Biochemistry* **1980**, *19*, 199.

111. Makinen, M. W.; Chung, A. K. In *Iron Porphyrins, part I*; Lever, A. B. P.; Gray, H. B., Eds.; Addison-Wesley: Reading, Massachusetts, 1983; p 141.
112. Dickerson, R. E.; Takano, T.; Eisenberg, D.; Kallai, O. B.; Samson, L.; Cooper, A.; Margoliash, E. *J. Biol. Chem.* **1971**, *246*, 1511.
113. Takano, T.; Kallai, O. B.; Swanson, R.; Dickerson, R. E. *J. Biol. Chem.* **1973**, *248*, 5234.
114. Swanson, R.; Trus, B. L.; Mandel, N.; Mandel, G.; Kallai, O. B.; Dickerson, R. E. *J. Biol. Chem.* **1977**, *252*, 759.
115. Takano, T.; Trus, B. L.; Mandel, N.; Mandel, G.; Kallai, O. B.; Swanson, R.; Dickerson, R. E. *J. Biol. Chem.* **1977**, *252*, 776.
116. Cohen, J. S.; Hayes, M. B.; *J. Biol. Chem.* **1974**, *249*, 5472.
117. Horinishi, H.; Kurihara, K.; Shibata, K. *Arch. Biochim. Biophys.* **1965**, *111*, 520.
118. Stellwagen, E. *Biochem. Biophys. Res. Commun.* **1966**, *23*, 29.
119. Ando, K.; Matsubara, H.; Okunuki, K. *Biochim. Biophys. Acta* **1966**, *118*, 240.
120. Harbury, H. A. In *Hemes and Hemoproteins*; Chance, B., Estabrook, R.; Yonetani, Eds.; Academic Press: New York, 1966; p 391.
121. Ando, K.; Matsubara, H.; Okunuki, K. *Biochim. Biophys. Acta* **1966**, *118*, 256.
122. Brautigan, D. L.; Ferguson-Miller, S.; Margoliash, E. *J. Biol. Chem.* **1978**, *253*, 130.
123. Moore, G. R.; Eley, C. G. S.; Williams, G. *Adv. Inorg. Bioinorg. Mech.* **1984**, *3*, 1.
124. Petsko, G. A.; Phillips, D. C.; Williams, R. J. P.; Wilson, I. A. *J. Mol. Biol.* **1978**, *120*, 345.
125. Salmeen, I.; Palmer, G. *J. Chem. Phys.* **1968**, *48*, 2049.

126. Morton, R. A.; Bohan, T. L. *Can. J. Biochem.* 1971, 49, 328.
127. Brautigan, D. L.; Feinberg, B. A.; Hoffman, B. M.; Margoliash, E.; Peisach, J.; Blumberg, W. E. *J. Biol. Chem.* 1977, 252, 574.
128. Saterlee, J. D. *Annu. Rep. NMR Spectrosc.* 1986, 17, 79.
129. Toi, H.; La Mar, G. N.; Margalit, R.; Che, C.-M.; Gray, H. B. *J. Am. Chem. Soc.* 1984, 106, 6213.
130. La Mar, G. N. In *Biological Applications of Magnetic Resonance*; Shulman, R. G., Ed.; Academic Press: New York, 1979; p 305.
131. Wuthrich, K. *Struct. Bonding (Berlin)* 1970, 8, 53.
132. Williams, G.; Clayden, N. J.; Moore, G. R.; Williams, R. J. P. *J. Mol. Biol.* 1985, 183, 447.
133. Wuthrich, K. *NMR In Biological Research: Peptides and Proteins*; Elsevier North Holland: Netherlands, 1976.
134. McDonald, C. C.; Phillips, W. D. *Biochemistry* 1973, 12, 3170.
135. Moore, G. R.; Williams, G. *Biochim. Biophys. Acta* 1984, 788, 147.
136. Gupta, R. K.; Redfield, A. G. *Science (Washington, DC)* 1970, 169, 1204.
137. Redfield, A. G.; Gupta, R. K. *Cold Spring Harbor Symp. Quant. Biol.* 1971, 36, 405.
138. Takano, T.; Dickerson, R. E. *J. Mol. Biol.* 1981, 153, 95.
139. Takano, T.; Dickerson, R. E. *Proc. Natl. Acad. Sci. U.S.A.* 1980, 77, 6371.
140. Riordan, J. F.; McElvany, K. D.; Borders, C. L., Jr. *Science (Washington, D.C.)* 1977, 195, 884.

141. Schneider, F. *Z. Naturwissenschaften* 1978, 65, 376.
142. Mehrota, R. In *Comprehensive Coordination Chemistry*; Wilkinson, G., Gillard, R. D., McCleverty, J. A., Eds.; Pergamon Press: New York, 1987; p 269 and references cited therein.
143. Petsko, G. A. *Methods Enzymol.* 1985, 114, 147.
144. Wilson, I. A.; Skerál, J. J.; Wiley, D. C. *Nature (London)* 1981, 289, 366.
145. Ramachandran, G. N.; Mazumdar, S. K.; Venketasan, K.; Lakshminarayanan, A. V. J. *Mol. Biol.* 1966, 15, 232.
146. Hol, W. G. J.; van Duijnen, D. T.; Berendsen, H. J. C. *Nature (London)* 1978, 273, 443.
147. Ploegman, J. H.; Drent, G.; Kalk, K. H.; Hol, W. G. J. *Mol. Biol.* 1979, 127, 149.
148. Pathy, L.; Thesz, J. *Eur. J. Biochem.* 1980, 105, 387.
149. Soman, G.; Hurst, M. O.; Graves, D. J. *Int. J. Peptide Protein Res.* 1985, 25, 517.
150. Boyar, A.; Marsh, R. E. *J. Am. Chem. Soc.* 1982, 104, 1995.
151. Pande, J.; Myer, Y. P. *J. Biol. Chem.* 1980, 255, 11094.
152. Longhi, R.; Drago, R. S. *Inorg. Chem.* 1965, 4, 11.
153. Schulz, G. E.; Schirmer, R. H. *Principles of Protein Structure*; Springer-Verlag: New York, 1979; p 12.
154. Mitewa, M.; Gencheva, G.; Bontchev, P. R.; Angelova, O.; Macicek, J. *Polyhedron* 1988, 7, 1273.
155. Chevion, M.; Peisach, J.; Blumberg, W. E. *J. Biol. Chem.* 1977, 252, 3637.
156. Brothers, H. M., II; Kostić, N. M. *Inorg. Chem.* 1988, 27, 1761.

157. Cerny, R. L.; Sullivan, B. P.; Bursey, M. M.; Meyer, T. J. *Anal. Chem.* **1983**, *55*, 1954.
158. Cerny, R. L.; Sullivan, B. P.; Bursey, M. M.; Meyer, T. J. *Inorg. Chem.* **1985**, *24*, 397.
159. Balasanmugan, K.; Day, R. J.; Hercules, D. M. *Inorg. Chem.* **1985**, *24*, 397.
160. Dobson, J. C.; Taube, H. *Inorg. Chem.* **1989**, *24*, 4477.
161. Okawa, H. *Coord. Chem. Rev.* **1988**, *92*, 1.
162. Sigel, H. *Pure Appl. Chem.* **1989**, *61*, 923.
163. Derome, A. E. *Modern NMR Techniques for Chemistry Research*; Pergamon Press: Oxford, England, 1987; pp 97-127.
164. Kanamori, K.; Roberts, J. D. *J. Am. Chem. Soc.* **1983**, *105*, 4698 and references cited therein.
165. Botto, R. E.; Schwartz, J. H.; Roberts, J. D. *Proc. Natl. Acad. Sci. U.S.A.* **1980**, *77*, 23.
166. Wong, Y.-S.; Lippard, S. J. *J. Chem. Soc., Chem. Commun.* **1977**, 824.
167. Dewan, J. C.; Lippard, S. J.; Bauer, W. R. *J. Am. Chem. Soc.* **1980**, *102*, 858.
168. Intille, G. M.; Pflugger, C. E.; Baker, W. A., Jr. *Cryst. Struct. Commun.* **1973**, *2*, 217.
169. Intille, G. M.; Pflugger, C. E.; Baker, W. A., Jr. *J. Cryst. Mol. Struct.* **1973**, *3*, 47.
170. Watson, W. H.; Johnson, D. R.; Celap, M. B.; Kamberi, B. *Inorg. Chim. Acta* **1972**, *6*, 591.
171. Duarte, M. T. L. S.; Carrondo, M. A. A. F. de C. T.; Goncalves, M. L. S. S.; Hursthouse, M. B.; Walker, N. P. C.; Dawes, H. M. *Inorg. Chim. Acta* **1986**, *124*, 41.
172. Martin, D. S., Jr.; Hunter, L. D.; Kroening, R.; Coley, R. F. *J. Am. Chem. Soc.* **1971**, *93*, 5433.

173. Mais, R. H.; Owston, P. G.; Wood, A. M. *Acta Crystallogr., Sect. B: Struct. Crystallogr. Cryst. Chem.* **1972**, *B28*, 393.
174. Gliemann, G.; Yersin, H. *Struct. Bonding* **1985**, *62*, 87.
175. Williams, J. M. *Adv. Inorg. Chem. Radiochem.* **1983**, *26*, 235.
176. Balch, A. L. *Comments Inorg. Chem.* **1984**, *3*, 51.
177. O'Halloran, T. V.; Lippard, S. J. *Isr. J. Chem.* **1985**, *25*, 130.
178. Cotton, F. A.; Walton, R. A. *Struct. Bonding (Berlin)* **1985**, *62*, 1.
179. Roundhill, D. M.; Gray, H. B.; Che, C.-M. *Acc. Chem. Res.* **1989**, *22*, 55.
180. Wells, R. D. *J. Biol. Chem.* **1988**, *263*, 1095.
181. Wells, R. D.; Harvey, S. C., Eds. *Unusual DNA Structures*; Springer-Verlag: New York, 1988.
182. Barton, J. K. *Chem. Eng. News* **1988**, *66*, 30.
183. Tullius, T. D. In *Metal-DNA Chemistry*; Tullius, T. D., Ed.; ACS Symposium Series 402; American Chemical Society: Washington, DC, 1989; Chapter 1.
184. Williamson, J. R.; Raghurama, M. K.; Cech, T. R. *Cell*, **1989**, *59*, 871.
185. Barton, J. K.; Lippard, S. J. In *Nucleic Acid-Metal Ion Interactions with Nucleic Acids*; Spiro, T. G., Ed.; John-Wiley: New York, 1980; Volume I, Chapter 2.
186. Barton, J. K. *Science (Washington, DC)* **1986**, *233*, 727.
187. Fleisher, M. B.; Mei, H. Y.; Barton, J. K. *Nucleic Acids Mol. Biol.* **1988**, *2*, 65.
188. Barton, J. K. *J. Biomol. Struct. Dyn.* **1983**, *1*, 621.
189. Neidles, S.; Abraham, Z. *CRC Crit. Rev. Biochem.* **1984**, *17*, 73.

190. Dougherty, G.; Pilbrow, J. R. *Int. J. Biochem.* 1984, 16, 1179.
191. Hard, T.; Norden, B. *Biopolymers* 1986, 25, 7827.
192. Kelley, J. M.; Tossi, A. B.; McConnell, D. J.; OhUigin, C. *Nucleic Acids Res.* 1985, 13, 6017.
193. Kelley, J. M.; Murphy, M. J. *Nucleic Acids Res.* 1985, 13, 167.
194. Dervan, P. B. *Science (Washington, DC)* 1986, 232, 464.
195. Sigman, D. S.; Chen, C. B. In *Metal-DNA Chemistry*; Tullius, T. D., Ed., ACS Symposium Series 402; American Chemical Society: Washington, DC, 1989; Chapter 2.
196. Subramanian, R.; Meares, C. F. *J. Am. Chem. Soc.* 1986, 108, 6427.
197. McGall, G. H.; Rabow, L. E.; Stubbe, J.; Kozarich, J. W. *J. Am. Chem. Soc.* 1987, 109, 2936.
198. Basile, L. A.; Raphael, A. L.; Barton, J. K. *J. Am. Chem. Soc.* 1987, 109, 7550.
199. Barton, J. K.; Raphael, A. L. *Proc. Natl. Acad. Sci. USA* 1985, 82, 6460.
200. Jennette, K. W.; Lippard, S. J.; Vassiliades, G. A.; Bauer, W. R. *Proc. Natl. Acad. Sci. USA* 1974, 71, 3839.
201. Howe-Grant, M.; Lippard, S. J. *Biochemistry* 1979, 18, 5762.
202. Bond, R. J.; Langridge, R.; Jennette, K. W.; Lippard, S. J. *Proc. Natl. Acad. Sci. USA* 1975, 72, 4825.
203. Barton, J. K.; Lippard, S. J. *Biochemistry* 1979, 18, 2661.
204. Marmur, J.; Doty, P. *J. Mol. Biol.* 1962, 5, 109.
205. Carter, M. T.; Rodriguez, M.; Bard, A. J. *J. Am. Chem. Soc.* 1989, 111, 8901.

206. Chamberlin, M. J. *Federation Proc.* 1965, 24, 144.
207. Ts'o, P. O. P.; Rapaport, S. A.; Bollum, F. J. *Biochemistry* 1966, 5, 4153.
208. Pharmacia LKB Biotechnology, Inc., Piscataway, New Jersey, Unpublished Results.
209. Lefler, C. F.; Bollum, F. J. *J. Biol. Chem.* 1969, 244, 594.
210. Wells, R. D.; Larson, J. E.; Grant, R. C.; Shortle, B. E.; Cantor, C. E. *J. Mol. Biol.* 1970, 54, 465.
211. Basolo, F.; Bailar, J. C.; Tarr, B. R. *J. Am. Chem. Soc.* 1950, 72, 2433.
212. Gagarin, R. *Gmelins Handbuch der Anorganischen Chemie* 1957, 68D, 470.
213. LePecq, J.-B.; Paoletti, C. *J. Mol. Biol.* 1967, 27, 87.
214. Zimm, B. H.; Crothers, D. M. *Proc. natl. Acad. Sci. USA* 1962, 48, 905.
215. Drummond, D. S.; Pritchard, N. J.; Simpson-Gildemeister, V. F. W.; Peacocke, A. R. *Biopolymers* 1965, 4, 971.
216. Maniatis, T.; Fritsch, E. F.; Sambrook, J. *Molecular Cloning*; Cold Spring Harbor Laboratory: Cold Spring Harbor, NY, 1982.
217. Hahn, F. E., Ed. *Progress in Molecular and Subcellular Biology*; Springer-Verlag: Berlin, 1971; Volume 2.
218. Burckhardt, G.; Zimmer, Ch.; Baguley, B. *J. Biomol. Struct. Dynamics* 1987, 4, 813.
219. Record, M. T., Jr.; Lohman, T. M.; DeHaseth, P. *J. Mol. Biol.* 1976, 107, 145.
220. Barton, J. K.; Goldberg, J. M.; Kumar, C. V.; Turro, N. J. *J. Am. Chem. Soc.* 1986, 108, 2081.

221. Luck, G.; Reinart, K. E.; Baguley, B.; Zimmer, Ch. *J. Biomol. Struct. Dynamics* **1987**, *4*, 1079.
222. Barton, J. K.; Dannenberg, J. J.; Raphael, A. L. *J. Am. Chem. Soc.* **1982**, *104*, 4967.
223. Shea, R. G.; Hopkins, P. B.; Olson, A. J. *J. Biomol. Struct. Dynamics* **1987**, *5*, 313.
224. Zimmerman, S. B.; Cohen, G. H.; Davies, D. R. *J. Mol. Biol.* **1975**, *92*, 181.
225. Gellert, M.; Lipsett, M. N.; Davies, D. R. *Proc. Natl. Acad. Sci. USA* **1962**, *48*, 2013.
226. Pinnavaia, T. J.; Marshall, C. L.; Mettler, C. M.; Fish, C. L.; Miles, H. T.; Becker, E. D. *J. Am. Chem. Soc.* **1978**, *100*, 3625.
227. Sen, D.; Gilbert, W. *Nature (London)* **1988**, *334*, 364.
228. Berman, H. M.; Young, P. R. *Ann. Rev. Biophys. Bioeng.* **1981**, *10*, 87.
229. Lavery, R.; Zakrewska, K.; Pullman, B. *J. Biomol. Struct. Dynamics* **1986**, *3*, 1155.
230. Mokul'skii, M. A.; Kapitonova, K. A.; Mokul'skaya, T. D. *Mol. Biol. (Moscow)* **1972**, *6*, 714.
231. Brothers, H. M., II; Kostić, N. M., Dept. of Chemistry, Iowa State University, Research in Progress.
232. Suh, M.; Kostić, N. M., Dept. of Chemistry, Iowa State University, Research in Progress.

APPENDIX: CRYSTALLOGRAPHIC STUDY OF [Pt(TRPY)Cl]Cl · H₂O

An equimolar reaction mixture of MeGua·HCl and [Pt(trpy)Cl]Cl·2H₂O with heating at 70 °C and pH 9.0 for 7 d produces the red complex {Pt(trpy)}₂MeGua⁴⁺ and some free methylguanidine as described in Section V. Some Pt(trpy)Cl⁺ remains in solution, perhaps unreacted or perhaps produced in the competitive reaction of the unstable yellow complex Pt(trpy)MeGua²⁺ with the excess Cl⁻ ligands and with another Pt(trpy)MeGua²⁺ forming in the former case the starting material Pt(trpy)Cl⁺ or in the latter case the thermodynamic product, {Pt(trpy)}₂MeGua⁴⁺.

In the course of the studies described in Section V, a small yellow crystal was obtained from such a reaction mixture. Hoping to get a crystal of the intermediate yellow complex Pt(trpy)MeGua²⁺, the yellow crystal of dimension 0.20- x 0.10- x 0.05-mm was mounted on a glass fiber in a random orientation. The technical details are summarized in Table A-1. The structure was solved by direct methods with an Enraf-Nonius CAD4 diffractometer and the standard programs. The position of the platinum atom was located on the mirror plane; the atoms in the coordination sphere were found by difference fourier map after isotropic refinement of the platinum position. However, the plane of the coordination sphere was found to be approximately perpendicular to the crystallographic mirror plane, so that the atom could only be described as two disordered overlapping sets related by the mirror plane. A difference map revealed two significant peaks which could be marginally refined as partially-occupied sites of H₂O.

X-ray data collection and structure solution were carried out at the Iowa State Molecular Structure Laboratory. The results are presented in Figure A-1 and Tables A-2 through A-4.

The crystallographic study of $[\text{Pt}(\text{trpy})\text{Cl}]\text{Cl}$ by itself has not been previously reported, although a communication¹⁶⁶ has appeared in which a crystal of the complex stacks with a dinucleotide has been achieved. Although the crystallographic study of the unprecedented guanidine complex was initially sought, the crystallographic data by itself of this versatile reagent is of merit. This study also confirms the instability of the $\text{Pt}(\text{trpy})\text{MeGua}^{2+}$ as discussed in Section V.

Table A-1. Crystallographic Data for [Pt(trpy)Cl]Cl · H₂O

formula: C ₁₅ H ₁₃ N ₃ OCl ₂ Pt	space group: C _{2/m} (No.12)
a = 14.623 (3) Å ⁰	T = -20±1 °C
b = 17.109 (4) Å ⁰	λ = 0.71073 Å ⁰
c = 6.913 (3) Å ⁰	ρ _{calcd} = 2.112 g cm ⁻³
β = 109.84 (2) °	μ = 90.5 cm ⁻¹
V = 1627 Å ⁰³	absorption correction factors:
	1.448-0.730
Z = 4	R(F _o or F _o ²) = 0.0647
FW = 517.29	R _w (F _o or F _o ²) = 0.0959

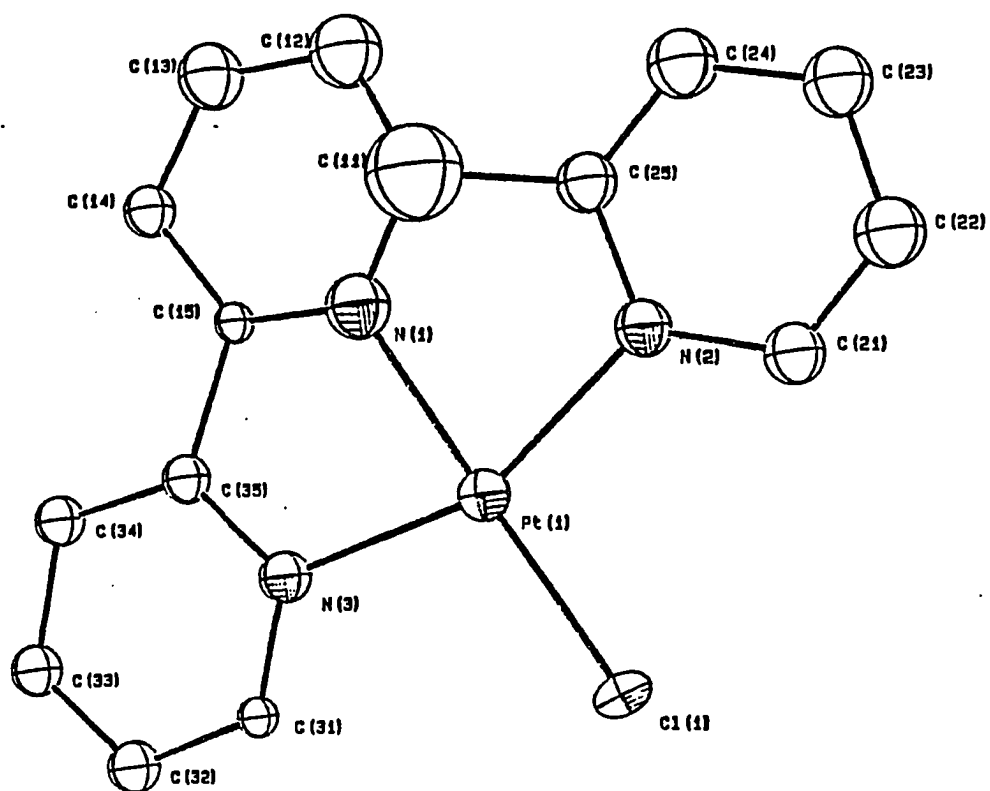


Figure A-1. ORTEP Plot of [Pt(trpy)Cl]Cl · H₂O

Table A-2. Coordinates of the Non-Hydrogen Atoms in [Pt(trpy)Cl]Cl · H₂O

atom	x	y	z	B _{eq} ^a A ⁰²
Pt(1)	0.06241(6)	0.000	0.3295(2)	1.68(3)
Cl(1)	0.1347(7)	0.1139(6)	0.425(2)	2.7(2)
Cl(2)	-0.1010(7)	0.2080(5)	0.174(2)	3.2(3)
N(1)	0.007(2)	-0.108(2)	0.218(6)	2.8(6) ^b
N(2)	0.180(2)	-0.075(2)	0.476(5)	2.1(5) ^b
N(3)	-0.072(2)	0.028(2)	0.144(5)	1.8(5) ^b
C(11)	0.066(4)	-0.171(4)	0.246(9)	6(1) ^b
C(12)	0.022(3)	-0.245(3)	0.226(8)	3.5(8) ^b
C(13)	-0.077(3)	-0.247(3)	0.125(7)	3.0(8) ^b
C(14)	-0.136(2)	-0.181(2)	0.071(6)	1.8(5) ^b
C(15)	-0.089(2)	-0.113(2)	0.138(6)	1.1(4) ^b
C(21)	0.273(2)	-0.049(2)	0.586(6)	2.4(6) ^b
C(22)	0.345(3)	-0.103(2)	0.657(7)	3.0(7) ^b
C(23)	0.330(3)	-0.183(2)	0.611(7)	3.0(7) ^b
C(24)	0.233(3)	-0.208(2)	0.511(7)	3.0(7) ^b
C(25)	0.159(3)	-0.155(3)	0.437(6)	2.4(7) ^b

^aAnisotropically refined atoms are given in the form of the isotropic equivalent displacement parameter defined as: $(4/3) * [a^2 * B(1,1) + b^2 * B(2,2) + c^2 * B(3,3) + ab(\cos \gamma) * B(1,2) + ac(\cos \beta) * B(1,3) + bc(\cos \alpha) * B(2,3)]$.

^bAtoms refined isotropically.

Table A-2 (Continued)

atom	x	y	z	$B_{eq}^a A^{O2}$
C(31)	-0.109(2)	0.100(2)	0.121(6)	1.1(4) ^b
C(32)	-0.203(2)	0.118(2)	0.010(6)	1.9(6) ^b
C(33)	-0.266(2)	0.058(2)	-0.059(5)	1.8(6) ^b
C(34)	-0.233(2)	-0.022(2)	-0.028(6)	1.7(6) ^b
C(35)	-0.134(2)	-0.032(2)	0.072(5)	1.6(5) ^b
O _w (1)	0.452(4)	-0.068(3)	0.912(9)	2(2) ^b
O _w (2)	0.50(2)	-0.066(7)	1.07(3)	8(5) ^b

Table A-3. Bond Distances (Å^o) in [Pt(trpy)Cl]Cl · H₂O

Pt(1) – Cl(1)	2.21(1)	C(12) – C(13)	1.38(5)
Pt(1) – N(1)	2.06(3)	C(13) – C(14)	1.40(5)
Pt(1) – N(2)	2.11(3)	C(14) – C(15)	1.36(5)
Pt(1) – N(3)	2.01(2)	C(15) – C(35)	1.53(4)
N(1) – C(11)	1.35(7)	C(21) – C(22)	1.36(5)
N(1) – C(15)	1.32(5)	C(22) – C(23)	1.40(6)
N(2) – C(21)	1.38(4)	C(23) – C(24)	1.43(5)
N(2) – C(25)	1.42(6)	C(24) – C(25)	1.37(6)
N(3) – C(31)	1.33(5)	C(31) – C(32)	1.36(4)
N(3) – C(35)	1.35(4)	C(32) – C(33)	1.36(5)
C(11) – C(12)	1.41(8)	C(33) – C(34)	1.43(5)
C(11) – C(25)	1.56(6)	C(34) – C(35)	1.40(4)

Table A-4. Bond Angles (deg) in [Pt(trpy)Cl]Cl · H₂O

Cl(1)–Pt(1)–N(1)	173(1)	N(1)–C(15)–C(35)	110(3)
Cl(1)–Pt(1)–N(2)	99.2(9)	C(14)–C(15)–C(35)	124(3)
Cl(1)–Pt(1)–N(3)	104.1(8)	N(2)–C(21)–C(22)	119(3)
N(1)–Pt(1)–N(2)	78(1)	C(21)–C(22)–C(23)	122(3)
N(1)–Pt(1)–N(3)	78(1)	C(22)–C(23)–C(24)	117(4)
N(2)–Pt(1)–N(3)	156(1)	C(23)–C(24)–C(25)	121(4)
C(11)–N(1)–C(15)	123(4)	N(2)–C(25)–C(11)	113(4)
C(21)–N(2)–C(25)	121(3)	N(2)–C(25)–C(11)	119(3)
C(31)–N(3)–C(35)	119(3)	C(11)–C(25)–C(24)	124(3)
N(1)–C(11)–C(12)	117(4)	N(3)–C(31)–C(32)	124(3)
N(1)–C(11)–C(25)	109(5)	C(31)–C(32)–C(33)	117(3)
C(12)–C(11)–C(25)	118(5)	C(32)–C(33)–C(34)	121(3)
C(11)–C(12)–C(13)	116(4)	C(33)–C(34)–C(35)	116(3)
C(12)–C(13)–C(14)	124(4)	N(3)–C(35)–C(15)	115(2)
C(13)–C(14)–C(15)	114(3)	N(3)–C(35)–C(34)	122(3)
N(1)–C(15)–C(14)	124(4)	C(15)–C(35)–C(34)	122(3)

ACKNOWLEDGEMENTS

This work was performed at Ames Laboratory under contract no. W-7405-eng-82 with the U. S. Department of Energy. The United States government has assigned the DOE Report number IS-T1453 to this thesis. Johnson Matthey, Inc. is thanked for the loan of K_2PtCl_4 and H_2PtCl_6 .

I would like to express my sincere thanks to Prof. Nenad Kostić, my mentor, for his patience, tolerance, and sensitivity during difficult times, his trust and belief in me and my abilities, and his support and guidance of my work.

I have been most fortunate to have such caring groupmates whose help and camaraderie I will always treasure. For those who contributed to the progress of this research: Herb Brothers, Kent Menzel, John Galbraith, Dave Gummin, Mr. Longgen Zhu, Mike Moxness, Brian Scott, Joni Johnson, and Mark Massa – my deepest appreciation. For those who were more than helpful and supportive: Linda, Amy, Ingrid, Venkatesh, and Elena – I am so touched and pleased to have worked with you.

It is a pleasure to acknowledge all those who were kind enough to lend a helping hand as I began my work here at ISU:

Dr. David Scott, Dr. Bob Domenick, Dr. Vinko Rutar, and Prof. Agustin Kintanar – for their

NMR expertise,

Prof. Richard Honzatko and Kyung Kim – for liberal use of the Evans and Sutherland

system, crystal growing techniques, and initial collaborative work on the crystals of the guanidine complexes and their readiness to help when asked,

Dr. Lee Daniels – for the crystallographic work of $[Pt(trpy)Cl]Cl \cdot H_2O$ and

$[(Pt(trpy))_2Can](ClO_4)_3 \cdot 5.5H_2O$, I had wished to share with him the fruit of a long wait after exhausting his list of techniques for growing crystals,

Judith Nocek, Linda Pearce, Ron Utecht, and Mark Brynildson – for EPR techniques,

Phil Anfinrud, Tim Causgrove, Sandy Bellefeuille, and Prof. Walter Struve – for collaborative spectroscopic work and discussions on laser spectroscopy,

Bill, Bruce, Shirley, and Prof. Graves – for know-how on HPLC, protein, and amino acid techniques; the idea of a lowered pK_a in Arg 91 arose from a topic discussed in our protein chemistry course,

Randy Holt, Vicki Schlegel, and Prof. Therese Cotton – for collaborative work using resonance Raman spectroscopy,

Arnold Guloy – for discussions and for help with computer problems,

My roomie, Clarissa – for her molecular biology know-how and for chauffeuring me during the wee hours,

Joni Johnson – for some DNA techniques,

Prof. Malcolm Rougvie and Prof. Gerry Small and his group – for helpful discussions on DNA and spectroscopy,

Feng Li and Prof. Herbert Fromm – for the use of the spectrofluorimeter,

Jan Beane and Steve Veysey – for FAB-MS work and helpful discussions on the topic,

Lee and Prof. Marit Nilsen-Hamilton – for the help and use of their lab facility,

and Eldon – for reliable fabrication of needed materials.

I thank my committee members: Prof. Nenad Kostić, Prof. Bob Angelici, Prof. James Espenson, Prof. Keith Woo, Prof. Gerry Small, and Prof. Don Graves.

My compatriots who have been with me in Ames and persons who've touched my life with their care and concern are deeply appreciated. They have made me feel at home where I was not.

Lastly, I wish to thank my mother, my siblings, my grandma, and my tita for their love, sacrifice, and unfailing support in all my decisions and my undertakings.